Journal of the OPTICAL SOCIETY *of* AMERICA

VOLUME 33
No. 3

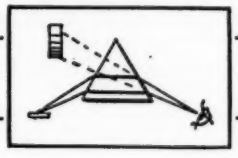

MARCH
1943

Development of the Microscope Objective . . . . . A. H. BENNETT 123

Theory of the Schmidt Telescope . . . . . J. L. SYNGE 129

Ophthalmic Lens Testing Instrument . . . . . KENNETH N. OGLE AND A. AMES, JR. 137

Improved Procedure for the Contact Printing Method of Measuring Photographic Density . . . . . MONROE H. SWEET 143

Impact of a Wave-Packet and a Reflecting Particle . . . . . HERBERT E. IVES 163

Study of the Applicability of the Pressed Pellet Electrode Method to the Spectrographic Analysis of Nickel Alloys . . . . . C. J. NEUHAUS 167

Dependence of Intrinsic Sensitivity on Grain Size . . . . . LUDWIK SILBERSTEIN 175

American Standards for Photography:

American Recommended Practice for Dimensions of Photographic Paper (Roll Leaders and Limit Signals)—Z38.1.4–1942 179
American Standard for Cameras (Tripod Connections for American Cameras)—Z38.4.1–1942 . . . 180
American Standard for Cameras (Tripod Connections for European Cameras with Adapter for American Tripods)—Z38.4.2–1942 181
American Standard for Distance Scales Marked in Feet—Z38.4.3–1942 182
American Standard for Focal Lengths of Lenses: Marking—Z38.4.4–1942 182
American Standard for Shutter Cable Release Tip and Socket with Taper Thread—Z38.4.5–1942 . 183
American Standard for Shutter Cable Release Tip and Socket with Straight Thread—Z38.4.6–1942 184

Letter to the Editor . . . . . ELLIOT Q. ADAMS 174

Published monthly
at Prince and Lemon Sts., Lancaster, Pa.
by the
AMERICAN INSTITUTE OF PHYSICS
Incorporated
175 Fifth Avenue, New York, N. Y.
FOR AND UNDER THE EDITORIAL SUPERVISION OF THE
OPTICAL SOCIETY OF AMERICA

THE OPTICAL SOCIETY OF AMERICA

Officers of the Society

A. G. WORTHING, *President*
University of Pittsburgh
Pittsburgh, Pennsylvania

A. H. PFUND, *Vice President*
Johns Hopkins University
Baltimore, Maryland

ARTHUR C. HARDY, *Secretary*
Massachusetts Institute of Technology
Cambridge, Massachusetts

W. W. GRAEPER, *Treasurer*
Bausch & Lomb Optical Company
Rochester, New York

The Board of Directors consists of the above officers; the Editor of the Journal; the Past President; and five directors-at-large.

K. S. GIBSON, *Past President*
National Bureau of Standards
Washington, D. C.

GEORGE R. HARRISON, *Editor*
Massachusetts Institute of Technology
Cambridge, Massachusetts

Directors-at-Large

J. W. BEAMS
University of Virginia
Charlottesville, Virginia

D. B. JUDD
National Bureau of Standards
Washington, D. C.

RUDOLF KINGSLAKE
Eastman Kodak Company
Rochester, New York

D. L. MACADAM
Eastman Kodak Company
Rochester, New York

R. A. SAWYER
University of Michigan
Ann Arbor, Michigan

Rochester, New York, Section

J. H. WEBB, *President*
G. H. AKLIN, *Vice President*
A. F. TURNER, *Secretary*
F. H. PERRIN, *Treasurer*

Councillors:

F. E. ALTMAN
J. W. FORREST
F. M. E. HOLMES
V. L. PARKS
R. B. HORSFALL (*ex officio*)

Patrons

AMERICAN OPTICAL COMPANY — BAUSCH & LOMB OPTICAL COMPANY
EASTMAN KODAK COMPANY

Corporation Members

AMERICAN CYSTOSCOPE MAKERS, INC., New York, New York
AMERICAN OPTICAL COMPANY, Southbridge, Massachusetts
BAUSCH & LOMB OPTICAL COMPANY, Rochester, New York
BELL & HOWELL COMPANY, Chicago, Illinois
BELL TELEPHONE LABORATORIES, INC., New York, New York
BENDIX AVIATION CORPORATION, New York, New York
CORNING GLASS WORKS, Corning, New York
E. I. DUPONT DE NEMOURS & COMPANY, INC., Chemical Department, Experimental Station, Wilmington, Delaware
EASTMAN KODAK COMPANY, Rochester, New York
FAIRCHILD AVIATION CORPORATION, Jamaica, New York
FISH-SCHURMAN CORPORATION, New York, New York
GAERTNER SCIENTIFIC CORPORATION, Chicago, Illinois
W. & L. E. GURLEY, Troy, New York
INTERCHEMICAL CORPORATION, New York, New York
KEUFFEL & ESSER COMPANY, Hoboken, New Jersey
NATIONAL CARBON COMPANY, Cleveland, Ohio
SIMPSON OPTICAL MANUFACTURING COMPANY, Chicago, Illinois
SPENCER LENS COMPANY, Buffalo, New York
ARTHUR H. THOMAS COMPANY, Philadelphia, Pennsylvania

THE OPTICAL SOCIETY OF AMERICA was organized in 1916 "*to increase and diffuse the knowledge of optics in all its branches, pure and applied, to promote the mutual interests of investigators of optical problems, of designers, manufacturers and users of optical instruments and apparatus of all kinds and to encourage cooperation among them.*" It aims to serve the interests of all who are engaged in any branch of optics from fundamental research to the manufacture of optical goods.

MEMBERSHIP

Regular Members: "Any person who has contributed materially to the advancement of optics is eligible for regular membership."

Associate Members: "Any person who is interested in optics is eligible for associate membership."

Corporate Members: "Any corporation desirous of encouraging the work of the Society is eligible for corporation membership."

Patrons: The payment, within any one year, of $1000 or more toward the expenses of the Society by any corporation or individual entitles such corporation or individual to the rank of patron.

The Society cordially invites to membership all who are interested in any branch of optics, either in research, in instruction, in optical or illuminating engineering, in the manufacture and distribution of optical goods of all kinds or in physiological and medical optics.

ANNUAL DUES

Regular members, $8.50; Associate members, $6.00; Corporate members, $50.00; Patrons, $1000.00. These dues include subscription to the Society's official journal, the *Journal of the Optical Society of America*.

CHANGES OF ADDRESS

All changes of address of members of the Optical Society of America should be communicated to the Secretary, Professor Arthur C. Hardy, Massachusetts Institute of Technology, Cambridge, Massachusetts.

Journal of the
OPTICAL SOCIETY
of AMERICA

VOLUME 33, NUMBER 3 MARCH, 1943

The Development of the Microscope Objective*

A. H. BENNETT
Spencer Lens Company, Buffalo, New York

THE compound microscope started from the simplest beginnings. It has evolved from its original form, which consisted of two single lenses, an eyepiece and an objective, into an optical system which may have as many as ten or more elements in the objective and frequently four elements in the eyepiece. This complexity of construction results from the necessity of correcting the errors or aberrations inherent in an optical system. The field of view of the microscope is comparatively small, but the quality of definition of high powered systems in an area near the center of the field is a prime necessity. Hence the successful design of such systems requires that the spherical and chromatic aberrations be well corrected, and it is desirable that coma, astigmatism, and curvature of field be reduced insofar as is possible. In the design of low powered systems greater stress is placed on good definition over a larger area of the field and here it is more important that good correction for coma, curvature of field, astigmatism, lateral color, and distortion be obtained.

THE INVENTION OF THE MICROSCOPE

The invention of the telescope and microscope are closely related. Prior to the beginning of the seventeenth century the Dutch spectacle lens makers were already famous. Credit for the invention of the compound microscope is given by most writers[1-5] on the subject to Hans Janssen and his son Zacharias between the years 1590 and 1609. This microscope contains the essential optical elements although the eyepiece has no field lens. The eyepiece and objective are both adjustable, so that the magnification could be changed. Of course, Janssen's microscope contained in a huge measure all of the aberrations which so absorb the interest of present-day optical designers, but it did represent a start and the principle of viewing a primary image formed by an objective, with an eyepiece, is still the basis of the modern microscope, including the electron microscope.

DEVELOPMENTS PRIOR TO ACHROMATISM

In 1665[1,4] about 60 years after Janssen, Hooke recognized the importance of increasing the aperture of the objective, but only to increase the amount of light entering the instrument. He seems to have had no idea of increasing the aperture in order to increase resolving power. This is to be expected as the excessive color and spherical aberration of his single lens objectives would not be conducive to any marked resolution. He complained of the quality of his objective lenses and hoped that these lenses could be made "elliptical" or "of a more true shape." Perhaps in a sense he anticipated aspheric surfaces. Hooke also suggested immersion lenses.

Reference to the first use of an objective more complicated than a single lens is given by Clay

* Paper presented at Symposium on Optical Instruments at Optical Society Meeting in New York City, October 30–31, 1942.

BOSTON UNIVERSITY
COLLEGE OF LIBERAL ARTS
LIBRARY

and Court in their *History of the Microscope*.[3] These authors state that Sturm in 1672 combined a pair of single converging lenses and obtained a magnification of forty-two diameters with this combination. He was led to this combination in a rather naïve way by observing that in his experiments he found a single lens that magnified more than a second one, but the latter gave an image of better quality, so he reasoned that if he combined the two he would retain the virtues

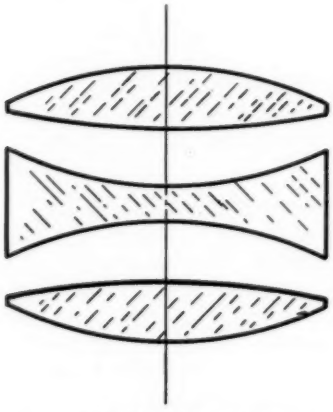

FIG. 1. Beeldsnyder's objective.

of both.[6] To be sure, the combination would have a shorter focal length and hence higher magnification than either of the elements, and it is likely that the increase in the number of refracting surfaces would reduce, to some extent, the spherical aberration and result in a better image.

A few years later, about 1687,[1, 6] Grindl devised an objective consisting of two plano-convex lenses with their convex surfaces facing each other.

The work of Sturm and Grindl[4] represents the first important accomplishment toward decreasing the spherical aberration of the microscope objective by increasing the number of refracting surfaces.

Going yet beyond the simple plano-convex objective, we find non-achromatic combinations of single lenses further developed in theory and practice by Wollaston, Brewster, Goring, Herschel, Tully, and Coddington from 1790 to 1830.[1, 4, 9] As the result of their efforts we find the familiar doublets, triplets, Coddington, and Stanhope forms which are still in use largely as hand magnifiers.

APPLICATION OF ACHROMATISM

The first achromatic microscope objective was made by Benjamin Martin in England,[1, 9] but he was not very enthusiastic about its performance. He compared an achromatic triplet with a reflecting objective and decided that the latter was much superior. When we consider the requirements of design, workmanship, and quality of optical glass in producing a good achromatic lens compared to those of a simple reflector it is of little wonder that the decision then was in favor of the reflector. At this time reflecting microscopes and high powered single lens magnifiers were serious competitors with the double or compound microscope.

Early in the nineteenth century Frauenhofer and Amici[1, 4, 9] experimented with the construction of achromatic objectives but because of the difficulty of manufacture they turned to reflecting microscopes.

In England, Cuthbert brought the reflecting microscope to a very high degree of excellence.[1] He constructed a combination achromatic and reflecting microscope.

APPLICATION OF THEORY

Toward the end of the eighteenth century and at the beginning of the nineteenth we find more intelligent efforts to utilize theoretical considerations in the design of achromatic microscope objectives. Euler,[1, 7, 10] the Swiss mathematician, about 1770, treated the theory of design of achromatic microscope objectives, and his student Nicolas Fuss gave detailed directions for the construction of an achromatic microscope objective.

In 1778 Klügel translated Fuss's instructions from the original French into German and later published a more comprehensive work on this subject.[8]

The work of Euler, Klügel, and Fuss had its first practical application in the achromatic objective of Beeldsnyder[1, 4, 9] in 1791. This objective, Fig. 1, consisted of an air-spaced triplet, a bi-concave flint between two bi-convex crown lenses, bringing to mind the present-day triplet construction.

Selligue[1,4,6,9] in 1824 proposed an objective consisting of a series of two, three, or four cemented doublets of equal power in order to increase the power and the aperture, Fig. 2.

Selligue's microscope was of such interest that the famous Fresnel was appointed by the French Royal Academy of Sciences to examine this microscope and make a report on it. Accordingly he compared it with one of the best available non-achromatic microscopes whose lenses Selligue had retouched and improved. Up to a magnification of 200 diameters the achromatic microscope was the better. Beyond this magnification no improvement could be noted in the definition of the achromatic over the non-achromatic objective. Fresnel preferred the non-achromatic objective for long observations because the achromatic instrument was provided with a diaphragm placed at a distance above the objective which reduced the field too much. For low power work the objective consisted of two doublets while for high powers two additional doublets were simply added.

Shortly after the construction of Selligue's objective it was found that better results could be obtained by turning the plane side of the doublet toward the object,[1] as shown in the two-doublet system of Fig. 2. It is evident that at this time the work was done mostly by trial and error.

INCREASE OF NUMERICAL APERTURE

In 1827 Amici[1,4,9] in Paris increased the apertures of his objectives by combining doublets and triplets. Such lenses had focal lengths as short as 1.25 mm, shorter than any regularly used at present.

At about the same time, Tully in England obtained objectives of increased aperture by using a small doublet front lens with larger triplets back of it.[1,9]

IMMERSION OBJECTIVES

An important advance was made in the theory of objectives when Lister[2,9] at this period discovered the application of aplanatic foci. This information, however, was not put into practice until a later date. In England, Hugh Powell is said to have produced the greatest advance in objectives. He worked entirely experimentally until Mayall[1] interested him in experimenting with immersion objectives in 1868. About 30 years previously Amici[1,9] made immersion objectives using certain oils as immersion fluids but it seems not to have occurred to him that the numerical aperture could be increased beyond that of the dry objective. He discontinued the use of oil as an immersion fluid in favor of water as the oil spoiled the slides of the microscopists of that time. Water immersion objectives became

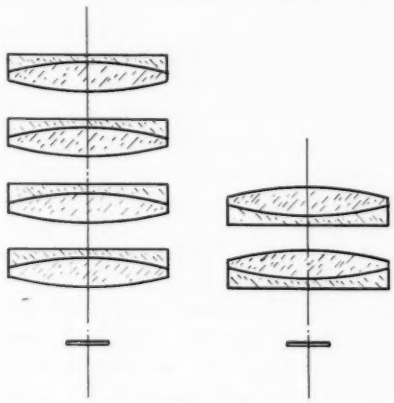

FIG. 2. Multiple doublet achromatic objectives.

very popular and were made in Paris by Nachet and Hartnack and in England by Powell and Lealand. In America as early as 1869 Wales and Spencer constructed high grade immersion objectives. A very important advance was made by the American, Robert Tolles (1872), when he produced apertures beyond those possible with dry objectives. Zeiss in his 1874 catalog advertised angular apertures of 104° to 108° in water which correspond to numerical apertures of 1.24 to 1.29.[1]

Today, when it is so well known that the maximum resolution of a microscope depends upon the numerical aperture, or angular aperture as it was formerly called, of the objective, it is difficult to realize the argument that took place between Tolles in America and Wenham in England which resulted in Tolles publishing computations relating to the numerical aperture of his objectives.[1,9,11]

In 1874, R. Keith[12] described the optical construction of one of Tolles' objectives having a focal length of 2.5 mm. In an accompanying

article in the same journal, Colonel J. J. Woodward of the Army Medical Museum in Washington, states that Keith had calculated the spherical aberration of this lens using Canada balsam as an immersion medium and found the spherical aberration practically eliminated. Then Woodward and Keith tested the objective with a diatom and found the definition definitely superior to that obtained with water immersion.[1]

Four years later in 1878 Zeiss produced oil immersion objectives under the direction of Professor Abbe.[1, 9] These were designated as homogeneous immersion objectives.

Abbe claimed to have obtained his original ideas from J. W. Stephenson of the Royal Microscopical Society. However, it is held by Mayall, writing only twelve years after Tolles' introduction of the oil immersion objective, that the original formula is due to Tolles rather than Abbe or Stephenson because of the priority of Tolles' publication.[1, 5, 9, 11]

About 1871 Abbe had started work on his famous and controversial diffraction theory of microscopic imagery; the formulation of the Sine Condition; and the trigonometrical calculation and design of objectives which was put to test by constructing and testing new forms of objectives made according to these designs.[1, 6, 9]

DEVELOPMENT OF APOCHROMATIC OBJECTIVES

Abbe and Schott[6, 9, 13, 15] became acquainted about eight years later and soon Abbe interested Schott in making experimental melts of optical glasses of new types. These new optical glasses had been prescribed by Abbe as a result of his calculations on the design of microscope objectives in which the secondary spectrum and spherical aberration were simultaneously corrected. These objectives known as apochromats were introduced in 1886 and were described in a catalog issued by Zeiss and entitled "New Microscope Objectives and Oculars of Special Glasses from the Laboratory for Glass Technology." The first model of these new lenses was made about three years prior to their general introduction. This lens had a focal length of one inch and a numerical aperture of 0.30 and with the eyepiece produced a total magnification of 250 diameters. It was said to give excellent definition and to have complete correction for every trace of chromatic aberration. It also showed equality of the spherical aberration for two different colors and to have the chromatic aberration corrected for three colors.

Abbe[13, 15] published in 1890 detailed information[14] on the use of the natural crystal fluorite in combination with the new Jena glasses. Previously, by a few years, Zeiss had produced various objectives having up to three fluorite lenses based on Abbe's formulations.

Semi-achromats or as they are called by some manufacturers, fluorites, are objectives having a correction between that of the apochromat and the achromat. These lenses were first produced at about the same time as the apochromats.

PROGRESS IN THE UNITED STATES

At this point I would like to mention the progress that had been made in America up to this period.[11, 16–19] In 1893 Dr. Henri van Heurck, Professor of Botany and Director of the Antwerp Botanical Gardens, published a book entitled *The Microscope*.[6] In regard to microscope objectives of 2″, $\frac{3}{4}$″ and $\frac{1}{12}$″ focus produced by the Bausch and Lomb Optical Company and examined by van Heurck he states: "These three objectives may be counted among the best that we have hitherto examined. The images are very clear, and chromatic correction is so well effected that practically no trace of color can be found. In this respect the objectives considerably surpass those of the most celebrated Continental firms."

Again concerning another American maker of microscopes, "The firm of Spencer has always maintained its old reputation. We are not acquainted with their stands but their objectives deserve all praise. At different times we have used excellent ones of their make, and we have in our possession one of their latest made about a year ago. This objective which enjoys an immense reputation in the United States is a $\frac{1}{12}$″ N.A. 1.37 . . . we consider this objective to be one of the best of the present date, and we have obtained some of our best photographs with it."

Some present day achromatic microscope objectives of the powers most commonly used are the 16-mm focus, N.A. 0.25-objective, consisting of two air-spaced cemented doublets; the 4-mm focus N.A. 0.66 having the addition of a hemispherical front lens, necessary in obtaining the

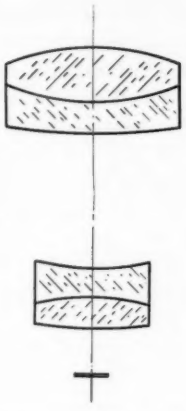

FIG. 3. Parfocal low powered achromatic objective.

larger N.A. with the required degree of correction; and the 1.8-mm focus, oil immersion objective having an N.A. of 1.25. This last illustrates the use of a hemispherical front lens combined with a meniscus shaped second front. The object is located at or in the near vicinity of the aplanatic point of the front lens. The second front introduces quite strong spherical aberration of the third, fifth, and seventh orders. The two rear doublets correct this aberration along with the chromatic aberration. The resulting spherical aberration is such that for a zone of the lens near the axis, undercorrection is found; for an intermediate zone a small amount of overcorrection is present; while for the marginal zone undercorrection again is present.

SPECIALIZED TYPES OF OBJECTIVES

Specialized types of objectives also have been designed and constructed. In this group may be included metallurgical objectives which are corrected for use without a cover glass as they are used in the study of metallographic specimens; also objectives for use in the polarizing microscope, especially free from traces of double refraction; and objectives having low magnifications, i.e., long focal lengths, but having their unit planes so placed that they can be parfocalized with objectives of the highest powers, thereby eliminating the necessity of much refocusing when changing from high power to low power. The construction of an objective of this type is shown in Fig. 3.

This construction is not in accord with the more conventional designs in that the front element has negative power. The N.A. is comparatively small which adds to the depth of focus, and high resolution is not necessary with such low magnification. Because the objective is used for the examination of gross objects flatness of field is of great importance in the design. In this construction it is possible to make the Petzval sum very small which leads to a flat field and consequently good coverage.

FLAT FIELD OBJECTIVES

H. Boegehold has described achromatic objectives especially designed for obtaining flatness of field and freedom from astigmatism while retaining sharpness of definition in the center of the field.[20,21] Ordinary achromatic microscope objectives, while having excellent correction in the vicinity of the center of the field, usually have some noticeable amounts of astigmatism or curvature of field towards the edge. By the introduction of thick meniscus lenses, Boegehold claims to have reduced the Petzval sum nearly to zero, which, in general, is a necessary although not sufficient condition for freedom from astigmatism and curvature. But since microscopes have comparatively small fields, the Petzval sum alone, i.e., the summation of the surface powers divided by their respective refractive indices, is a criterion for the curvature of field and astigmatism, and if this sum is made zero over such a limited field these aberrations practically vanish.

PHASE-CONTRAST

In general, images of microscopic specimens are the result of variations in the amplitude of the light waves emerging from different points in the object. In the point-for-point representation of the object, in the image space these variations in amplitudes result in corresponding variations in intensity in the image. Thus the image can give us a faithful representation of the object only insofar as the object has affected the amplitudes of the light waves incident on the objective. The object can affect these amplitudes in several ways, for example, by absorption, reflection, diffusion, refraction, and diffraction. But many microscopic objects possess these properties to a minor degree or not at all. Such objects may differ optically from their surrounding medium or within themselves only by slight

differences in refractive index. Such objects for practical purposes would affect only the phase of the incident waves of light. The eye is not sensitive to phase changes but only to changes of intensity or to the color characteristics of an object. In his rather recent work, Professor F. Zernike[22,23] attempted, and with considerable success developed, a method for converting point-by-point phase variations introduced by an object into corresponding variations in intensity in its image so that details of the microscopic object can be made visible. This was accomplished by the methods of physical rather than geometrical optics, but as the microscope objective is involved it seems proper to include mention of this method in a discussion of the development of the microscope objective.

In brief, instead of using the common extended source of illumination focused critically on the specimen, a narrow source is employed and this source is collimated so that light waves incident on the specimen are plane. Diffraction spectra of the source are formed by the microscopic object and since the source is at an infinite distance. images of these diffraction spectra are formed in the rear focal plane of the objective, often within the lens system. At this focal point is placed a small plate consisting of a film of isotropic material placed on a glass surface. This film is of such thickness that a retardation of $\frac{1}{4}$ wavelength takes place. Moreover the filmed area is of such size and shape that only the central maximum of the diffraction pattern of the source, i.e., the geometrical image of the source coincides exactly with the retarding film. Since the original light source is narrow its central and secondary maxima do not overlap to any great extent. Since the light passing through these maxima is coherent, by mathematical analysis Zernike was able to show that a change in phase of $\frac{1}{4}$ wave-length in the light of the central maximum can result in producing a difference in amplitude between light waves passing through the transparent details and their surrounding medium, respectively and thereby produce visibility of these details.

CONCLUSION

The importance of microscope objectives designed to have especially flat fields, obtained at the cost of more complex construction, and likewise the practical possibilities of the phase-contrast method have not yet been established by general use. The efforts of many optical designers are now to a large extent being employed in military efforts, but with the more recent optical glasses which will doubtlessly be available after the war, and with the greater interest, and larger number of workers in optical design we may well expect that more useful developments of the microscope objective will continue.

In conclusion, I wish to acknowledge with thanks the assistance of Mr. Allan L. Burton, Research Department, Spencer Lens Company in locating references, and preparing the bibliography for this article.

BIBLIOGRAPHY

(1) J. Mayall, Jr., "The microscope," J. Soc. Arts **34**, 987–1121 (1886).
(2) J. Hogg, *The Microscope* (London, 1871), eighth edition.
(3) R. S. Clay and T. H. Court, *The History of the Microscope* (London, 1932).
(4) P. Harting, *Das Mikroskop* (Braunschweig, 1866), vol. 3.
(5) S. H. Gage, *The Microscope* (Ithaca, 1932), 15th edition.
(6) H. van Heurck, *The Microscope* (London, 1893), English edition, trans. by W. E. Baxter.
(7) L. Euler, *Dioptrica*. (Petrop, 1771) 3 vols. From Mayall.
(8) Klügel, *Analytische Dioptrik* (Leipzig, 1778). From Mayall.
(9) W. B. Carpenter, *The Microscope and its Revelations* (London, 1901), eighth edition.
(10) J. Quekett, *Practical Treatise on the use of the Microscope* (London, 1852), second edition.
(11) J. D. Cox, "R. B. Tolles and the angular aperture question," Proc. Am. Soc. Microscopists, pp. 5–39, Seventh Annual Meeting (1884).
(12) R. Keith, Monthly Microscopical J. **10**, 124–5 (1874).
(13) M. von Rohr, *Abbe's Apochromats* (Leipzig, 1936).
(14) E. Abbe, Zeits. f. Instrumentenk. **10** (January, 1890).
(15) H. Hovestadt, *Jena Glass* (London, 1902).
(16) W. C. Krauss, "Debt of American microscopy to Spencer and Tolles," Trans. Am. Micros. Soc. **23**, 19 ff (1901).
(17) G. E. Blackham, "The evolution of the modern microscope," Proc. Am. Soc. Microscopists **4** (1882).
(18) H. L. Smith, "Memoir of C. A. Spencer," Proc. Am. Soc. Microscopists **4**, 49 ff (1882).
(19) H. R. Howland, "Memoir of H. R. Spencer," Trans. Am. Micros. Soc. pp. 252 ff (1899).
(20) H. Boegehold, "Die Verbesserung des Bildfeldes der Mikroskopobjektive," Zeits. f. wiss. Mikrosk. **55**, 17–25 (1938).
(21) Karl John, "Neue Fortschritte im Mikroskopbau. III." Zeits. f. Instrumentenk. **59**, 431–2 (1939).
(22) F. Zernike, "Das Phasenkontrastverfahren bei der mikroskopischen Beobachtung," Zeits. f. tech. Physik **16**, 454–457 (1935).
(23) A. Kohler and W. Loos, "Das Phasenkontrastverfahren und seine Anwendungen in der Mikroskopie," Naturwiss. **29**, 49 (1941).

The Theory of the Schmidt Telescope*

J. L. SYNGE
Department of Applied Mathematics, University of Toronto, Toronto, Canada

1. INTRODUCTION

IT is almost exactly a century since Hamilton (in 1843) designed a coma-free doublet.[5] His computations were based on his general method in optics, and the design is an example of the mathematician's procedure—to lay down a theory as general as possible and pass deductively from the general to the particular. Practical discoveries are rarely made in this way. The practical man prefers to work inductively; he likes to see the solution to a problem emerge as a refinement on a first rough idea—in this way his physical intuition carries him along step by step.

Schmidt[10] was an inventor at the opposite pole from Hamilton. His invention[9] of the telescope (or camera) that bears his name was a triumph of the mysterious intuition that skilled craftsmen sometimes possess. But to invent an instrument and to explain its operation are two different things, and Schmidt left it to the more mathematically-minded to expound the theory of his telescope. Mathematical treatments have been given by Stromgren[12] and Carathéodory,[4] and the aberrations up to the fifth order have been discussed by Baker.[1]

Nevertheless, I feel that something remains to be done—namely, to bring Hamilton and Schmidt together by discussing the Schmidt telescope in terms of the original theory of Hamilton. It is my firm belief that, in spite of the advances in geometrical optics in the last hundred years, the method of Hamilton must be regarded as the basic method in geometrical optics just as the method of Lagrange is basic in dynamics. Modifications of the Hamiltonian method are undoubtedly of great value for practical purposes, but they obscure the fundamental simplicity of the method. Therefore I shall go right back to the technique of Hamilton, adding nothing to this technique except a parametric expansion which proves very useful in the processes of elimination.

2. THE PROBLEM AND THE SCHMIDT TELESCOPE

Suppose we want to photograph a star. To do this we insert in the path of the rays a mirror or lens or a more complex system. The function of this optical system is to bend the rays so that they pass through a single point on the photographic plate. The more rays we can trap in this way, the brighter the image, and the more closely we can make them pass through a single point, the sharper the image.

It is very easy to bring rays from a single star to intersection at a point. We may use a paraboloidal mirror, pointing its axis of symmetry at the star. Then all reflected rays pass through the focus of the paraboloid.

But if we have to photograph a number of stars simultaneously, we cannot point the axis of the paraboloid simultaneously at all of them. For any position of the paraboloid, those stars near the axis will give sharp images, but the others will give blurred images (coma aberration). This is the great shortcoming of the paraboloidal mirror.

The trouble with the paraboloid is its axis of symmetry, which puts some stars in a privileged position. This trouble can be avoided by using a spherical mirror, but the cure is worse than the disease. Whereas the paraboloidal mirror treats some stars well and others badly, the spherical mirror treats all stars badly (spherical aberration). Can we correct this defect of the sphere without introducing the privileged axis of the paraboloid? Can we combine the specialized perfection of the paraboloid with the catholicity of the sphere?

It was here that Schmidt stepped in with his artful compromise. He applied to the sphere a compensating device which got rid of spherical aberration, but which was symmetric enough to avoid the coma-defect of the paraboloid.

The original Schmidt telescope consists of two simple parts—a spherical mirror S and a thin

* Paper presented at the Joint Symposium with the American Mathematical Society on Mathematics in the Field of Optics, at the Twenty-Seventh Annual Meeting of the Optical Society of America, New York, New York, October 30–31, 1942.

FIG. 1. Original Schmidt telescope.

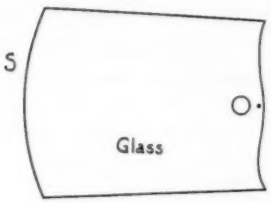

FIG. 2. The solid Schmidt.

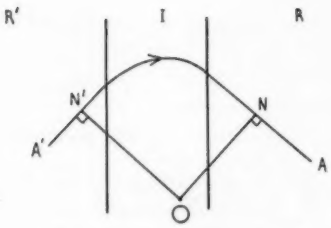

FIG. 3. T = optical length $N'N$.

glass plate P passing through the center O of the sphere (Fig. 1). The plate is figured in such a way as to eliminate spherical aberration for rays coming in a direction perpendicular to P. Thus the perfection of the paraboloid has been imparted to the sphere by means of this plate. It is not obvious whether the plate at the same time introduces the coma defect of the paraboloid for rays coming in an oblique direction. As a matter of fact, the coma defect does not appear, but the situation is one that calls for a mathematical argument.

The theory I am about to develop can be readily applied to the original Schmidt telescope. There is, however, a slight expository advantage in dealing with the "solid Schmidt." [1] This is very simple (Fig. 2), consisting of a block of glass, bounded on one side by a hemispherical silvered surface S and on the other by a face P, which is approximately a diametral plane of the hemisphere. The image in this case is formed inside the glass, which has to be made in two parts to allow the insertion of a photographic film. This does not affect the mathematical discussion.

3. HAMILTON'S ANGLE CHARACTERISTIC OR T FUNCTION

Hamilton's method is not as well known as it might be, and so I shall state the essentials briefly.[13, 14]

Rays start in an object space R' (Fig. 3), pass through an instrument I, and arrive at an image space R. O is an arbitrary origin and N', N the feet of the perpendiculars dropped from O on the parts of a ray which lie in R', R respectively. The *angle characteristic* or *T function* of the instrument is defined as the optical length $N'N$ expressed in terms of the directions of the two parts of the ray. It is most convenient to use the *components* of the rays. These are defined by

$$\begin{aligned} &\sigma' = n'\alpha', \quad \tau' = n'\beta', \quad \upsilon' = n'\gamma'; \\ &\sigma = n\alpha, \quad \tau = n\beta, \quad \upsilon = n\gamma, \end{aligned} \tag{3.1}$$

where n', n are the refractive indices of R', R, respectively, α', β', γ' the direction cosines of the incident ray and α, β, γ the direction cosines of the final ray. On account of the identities

$$\sigma'^2+\tau'^2+\upsilon'^2=n'^2, \quad \sigma^2+\tau^2+\upsilon^2=n^2, \tag{3.2}$$

T may be expressed in terms of four independent variables, and we write

$$T = T(\sigma', \tau', \sigma, \tau). \tag{3.3}$$

It is a consequence of Fermat's principle that the rays in R have the equations

$$x-z\frac{\sigma}{\upsilon} = -\frac{\partial T}{\partial \sigma}, \quad y-z\frac{\tau}{\upsilon} = -\frac{\partial T}{\partial \tau}. \tag{3.4}$$

Let us suppose that rays come from a star in R'. Then σ', τ' are constants and (3.4) are the equations of the congruence of rays in R; σ, τ are parameters changing from ray to ray. To deal with a different star, we give new values to σ', τ'.

This gives us a systematic way of discussing the patterns formed by rays from different stars. But we cannot make useful statements about the behavior of a given instrument until we know the T function for that instrument.

To find T, we must consider separately the reflecting or refracting surfaces that make up the instrument. We regard each such surface as an elementary instrument and find the T function for it. The T function for the complete instrument is given by adding these elementary T functions. This expression contains the intermediate components as well as the initial and

final components. The intermediate components have to be eliminated by means of stationary conditions, and it is this process of elimination that often makes T hard to calculate explicitly.

The rules for finding T for an elementary instrument are as follows. Let $z=f(x, y)$ be the equation of the reflecting or refracting surface. Then T is given by eliminating x, y, z, v', v from the six equations

$$T=(\sigma'-\sigma)x+(\tau'-\tau)y+(v'-v)z,$$
$$\frac{\partial z}{\partial x}=-\frac{\sigma'-\sigma}{v'-v}, \quad \frac{\partial z}{\partial y}=-\frac{\tau'-\tau}{v'-v}, \tag{3.5}$$
$$z=f(x, y),$$
$$v'^2=n'^2-\sigma'^2-\tau'^2, \quad v^2=n^2-\sigma^2-\tau^2.$$

If $T_1, T_2, \cdots T_N$ are the elementary T functions, the T function for the complete instrument is

$$T=T_1+T_2+\cdots+T_N. \tag{3.6}$$

From this expression the intermediate components are eliminated by the conditions that this expression shall have a stationary value with respect to each intermediate component.

4. THE T FUNCTION FOR THE SOLID SCHMIDT TELESCOPE, EXACT THEORY

Figure 4 shows the notation we shall use for the treatment of the solid Schmidt telescope. The components of the incident ray are σ_1, τ_1, after refraction at the figured surface S_1 the components are σ_2, τ_2, and after reflection at the hemisphere S_2 they are σ_3, τ_3. For the present we shall take S_1 to be any surface of revolution about Oz, with equation

$$z=\zeta(r), \quad r^2=x^2+y^2. \tag{4.1}$$

The solid Schmidt breaks into two elementary instruments with T functions

$$T_{12}=T_{12}(\sigma_1, \tau_1, \sigma_2, \tau_2),$$
$$T_{23}=T_{23}(\sigma_2, \tau_2, \sigma_3, \tau_3). \tag{4.2}$$

We shall write

$$\epsilon_1=\sigma_1^2+\tau_1^2, \qquad \epsilon_2=\sigma_2^2+\tau_2^2,$$
$$\epsilon_3=\sigma_3^2+\tau_3^2,$$
$$\epsilon_{12}=\sigma_1\sigma_2+\tau_1\tau_2, \quad \epsilon_{23}=\sigma_2\sigma_3+\tau_2\tau_3, \tag{4.3}$$
$$\epsilon_{13}=\sigma_1\sigma_3+\tau_1\tau_3.$$

Then direct application of (3.5) to S_1 gives

$$T_{12}=[(n^2-\epsilon_2)^{\frac{1}{2}}-(1-\epsilon_1)^{\frac{1}{2}}][\zeta(r)-r\zeta'(r)], \tag{4.4}$$

in which r is defined as a function of $\epsilon_1, \epsilon_{12}, \epsilon_2$ by

$$\zeta'(r)=\eta\cdot\frac{(\epsilon_1-2\epsilon_{12}+\epsilon_2)^{\frac{1}{2}}}{(n^2-\epsilon_2)^{\frac{1}{2}}-(1-\epsilon_1)^{\frac{1}{2}}}, \quad (\eta=\pm 1) \tag{4.5}$$

where n is the refractive index of the glass. By the same or another method[13] we get for S_2

$$T_{23}=R[(\sigma_2-\sigma_3)^2+(\tau_2-\tau_3)^2+(v_2-v_3)^2]^{\frac{1}{2}}$$
$$=R\sqrt{2}[n^2-\epsilon_{23}+(n^2-\epsilon_3)^{\frac{1}{2}}(n^2-\epsilon_2)^{\frac{1}{2}}]^{\frac{1}{2}}, \tag{4.6}$$

where R is the radius of the hemisphere. The T function for the complete instrument is then

$$T(\sigma_1, \tau_1, \sigma_3, \tau_3)=T_{12}(\sigma_1, \tau_1, \sigma_2, \tau_2)$$
$$+T_{23}(\sigma_2, \tau_2, \sigma_3, \tau_3), \tag{4.7}$$

from which the intermediate components σ_2, τ_2 are to be eliminated by the stationary conditions. These conditions are given by equating to zero the partial derivatives of the right-hand side of (4.7) with respect to σ_2, τ_2; they read

$$\frac{\eta r(\sigma_1-\sigma_2)}{(\epsilon_1-2\epsilon_{12}+\epsilon_2)^{\frac{1}{2}}}-\frac{\sigma_2\zeta(r)}{(n^2-\epsilon_2)^{\frac{1}{2}}}$$
$$-\frac{R}{\sqrt{2}}\cdot\frac{\sigma_3+\sigma_2[(n^2-\epsilon_3)/(n^2-\epsilon_2)]^{\frac{1}{2}}}{[n^2-\epsilon_{23}+(n^2-\epsilon_3)^{\frac{1}{2}}(n^2-\epsilon_2)^{\frac{1}{2}}]^{\frac{1}{2}}}=0, \tag{4.8}$$

and a similar equation with σ replaced by τ.

This result is completely general. It is not yet assumed that the rays are nearly parallel to the axis or that the face S_1 is nearly flat. But, of course, the elimination of the intermediate components presents a formidable difficulty.

5. THE PARAMETRIC METHOD AND THE APPROXIMATE T FUNCTION

Let us now assume that the inclinations of the rays to the axis Oz are small; this means that

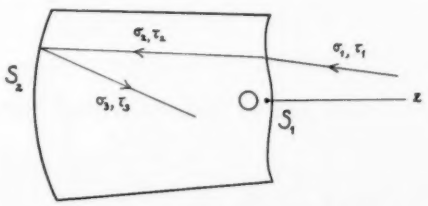

FIG. 4. Notation for the solid Schmidt.

σ_1, τ_1, σ_2, τ_2, σ_3, τ_3 are small. In most of the general theory of the instrument of revolution the smallness of the components is used as a basis of approximation. But in the Schmidt telescope there is another small quantity, namely the deviation of S_1 from a diametral plane. The systematic way to deal with such situations is to introduce a parameter λ and seek developments as power series in λ.

Accordingly we write

$$\sigma_1=\lambda s_1, \quad \tau_1=\lambda t_1, \quad \sigma_3=\lambda s_3, \quad \tau_3=\lambda t_3,$$
$$\epsilon_1=s_1^2+t_1^2, \quad \epsilon_{13}=s_1s_3+t_1t_3, \quad \epsilon_3=s_3^2+t_3^2. \tag{5.1}$$

We should realize that σ_1, τ_1, σ_3, τ_3 are the independent variables of the problem; r, σ_2, τ_2 are determined as functions of these independent variables by (4.5), (4.8). The transformation (5.1) introduces s_1, t_1, s_3, t_3 as new independent variables, which are to be regarded as finite. Our task is to solve (4.5), (4.8) for r, σ_2, τ_2 in terms of s_1, t_1, s_3, t_3, λ, in the form of series proceeding in powers of λ.

Instead of r we introduce the finite quantity ρ by the relation

$$r=\tfrac{1}{2}\lambda\rho R. \tag{5.2}$$

For the surface S_1 we take the equation

$$z=\zeta(r,\lambda)=R[\lambda^4 f(\rho)+\lambda^6 g(\rho)+\cdots]. \tag{5.3}$$

We regard the functions f, g, $\cdots$ as given.

The introduction of the parameter λ means essentially that we consider, not one instrument, but a sequence of instruments for the range $0<\lambda<\lambda_1$, where λ_1 is small. The smaller λ is, the nearer the rays lie to the axis by (5.1), and the more nearly S_1 approximates to a diametral plane by (5.3).

We seek power series in λ,

$$\rho=\rho^{(0)}+\lambda^2\rho^{(2)}+\cdots,$$
$$\sigma_2=\lambda s_2^{(1)}+\lambda^3 s_2^{(3)}+\cdots, \tag{5.4}$$
$$\tau_2=\lambda t_2^{(1)}+\lambda^3 t_2^{(3)}+\cdots.$$

The jumps of 2 in the powers of λ come from the axial symmetry of the instrument.

The plan is now to substitute from (5.4) in (4.5), (4.8), and treat the resulting equations as identities in λ.

From (4.5) we have

$$2\lambda^3 f'(\rho)=\eta\frac{(\epsilon_1-2\epsilon_{12}+\epsilon_2)^{\frac{1}{2}}}{(n^2-\epsilon_2)^{\frac{1}{2}}-(1-\epsilon_1)^{\frac{1}{2}}}, \quad (\eta=\pm 1). \tag{5.5}$$

The coefficient of λ on the right-hand side must vanish, and so

$$s_2^{(1)}=s_1, \quad t_2^{(1)}=t_1; \tag{5.6}$$

therefore

$$\epsilon_1-2\epsilon_{12}+\epsilon_2=\lambda^6 e_2^{(3)}+O(\lambda^8), \tag{5.7}$$

where

$$e_2^{(3)}=(s_2^{(3)})^2+(t_2^{(3)})^2. \tag{5.8}$$

We now equate the coefficients of λ^3 in (5.5) and get

$$2f'(\rho^{(0)})=\frac{\eta}{n-1}[e_2^{(3)}]^{\frac{1}{2}}. \tag{5.9}$$

Next we turn to (4.8), and its companion equation in τ, and consider the terms of the first degree in λ. We get

$$\eta\rho^{(0)}s_2^{(3)}=-[e_2^{(3)}]^{\frac{1}{2}}\frac{1}{n}(s_1+s_3),$$
$$\eta\rho^{(0)}t_2^{(3)}=-[e_2^{(3)}]^{\frac{1}{2}}\frac{1}{n}(t_1+t_3). \tag{5.10}$$

By squaring and adding we obtain

$$\rho^{(0)}=E, \tag{5.11}$$

where E is defined as

$$E=\frac{1}{n}(e_1+2e_{13}+e_3)^{\frac{1}{2}}. \tag{5.12}$$

Then by (5.9)

$$[e_2^{(3)}]^{\frac{1}{2}}=2\eta(n-1)f'(E), \tag{5.13}$$

and (5.10) gives

$$s_2^{(3)}=-2\left(1-\frac{1}{n}\right)\frac{1}{E}f'(E)(s_1+s_3),$$
$$t_2^{(3)}=-2\left(1-\frac{1}{n}\right)\frac{1}{E}f'(E)(s_1+s_3). \tag{5.14}$$

This completes the evaluation of σ_2, τ_2 to order λ^3 inclusive.

By (5.2), (5.11) we have

$$\rho=E+O(\lambda^2), \quad r=\tfrac{1}{2}\lambda RE+O(\lambda^3), \tag{5.15}$$

and by (5.3)

$$\zeta(r)=\lambda^4 Rf(E)+O(\lambda^6),$$
$$\zeta'(r)=2\lambda^3 f'(E)+O(\lambda^5), \tag{5.16}$$
$$\zeta(r)-r\zeta'(r)=\lambda^4 R[f(E)-Ef'(E)]+O(\lambda^6).$$

We now substitute in (4.4) and obtain

$$T_{12}=(n-1)\lambda^4 R[f(E)-Ef'(E)]+O(\lambda^6). \tag{5.17}$$

This expresses T_{12} in terms of the initial and final components.

Substitution of the power series (5.4) in (4.6) gives, after a little calculation involving binomial expansions,

$$T_{23}=2nR\left[1-\tfrac{1}{8}\lambda^2E^2+\tfrac{1}{2}\lambda^4\left(1-\frac{1}{n}\right)Ef'(E)\right.$$
$$\left.-\frac{\lambda^4(e_1-e_3)^2}{32n^4}-\frac{\lambda^4}{128}E^4\right]+O(\lambda^6). \tag{5.18}$$

To get the T function for the complete instrument, we add (5.17) and (5.18). This gives

$$T=T^{(0)}+\lambda^2T^{(2)}+\lambda^4T^{(4)}+O(\lambda^6), \tag{5.19}$$

where

$$T^{(0)}=2nR,$$
$$T^{(2)}=-\tfrac{1}{4}nRE^2,$$
$$T^{(4)}=R\left[(n-1)f(E)-\frac{1}{16n^3}(e_1-e_3)^2-\frac{n}{64}E^4\right], \tag{5.20}$$
$$E=\frac{1}{n}(e_1+2e_{13}+e_3)^{\frac{1}{2}}.$$

This expresses T, as required, in terms of the initial and final components to the order indicated. The accuracy is sufficient for the discussion of aberrations of the lowest order. But the method can of course be carried further without any difficulty.*

* $T^{(6)}=R\left[(n-1)g(E)+\frac{1}{2}\frac{n-1}{n}e_1f(E)-\frac{(n-1)^2}{n}[f'(E)]^2\right.$
$+\frac{n-1}{2n^4}(e_1-e_3)(e_1+e_{13})\frac{f'(E)}{E}+\frac{1}{8}(n-1)E^3f'(E)$
$\left.-\frac{1}{32n^8}(e_1-e_3)^2(e_1+e_3+\frac{1}{4}n^2E^2)-\frac{1}{512}nE^6\right].$

A feature of (5.19) is worth noting. Usually, in dealing with an instrument of revolution, the T function (or eikonal) is expanded in powers of the components. Now

$$\lambda^2T^{(2)}=-\frac{R}{4n}(\epsilon_1+2\epsilon_{13}+\epsilon_3), \tag{5.21}$$

and this is of the usual form for the second order part of T—a homogeneous expression of the second degree in the components. But

$$\lambda^4T^{(4)}=R\left[(n-1)\lambda^4f(E)-\frac{1}{16n^3}(\epsilon_1-\epsilon_3)^2\right.$$
$$\left.-\frac{1}{64n^3}(\epsilon_1+2\epsilon_{13}+\epsilon_3)^2\right]; \tag{5.22}$$

the last two terms are of conventional form—homogeneous of the fourth degree in the components—but the first term is something different. The function f is not necessarily algebraic. The term owes its smallness, not to the fact that the rays are nearly parallel to the axis, but rather to the fact that S_1 is very nearly the plane $z=0$.

The equations of the final rays are found from (3.4) and (5.19). They are

$$x-z\frac{\lambda s_3}{n}\left(1+\frac{1}{2}\frac{\lambda^2e_3}{n^2}\right)$$
$$=-\lambda\frac{\partial T^{(2)}}{\partial s_3}-\lambda^3\frac{\partial T^{(4)}}{\partial s_3}+O(\lambda^5), \tag{5.23}$$

and a similar equation with y, t substituted for x, s. From (5.20)

$$\frac{\partial T^{(2)}}{\partial s_3}=-\frac{1}{2}\frac{R}{n}(s_1+s_3),$$
$$\frac{\partial T^{(4)}}{\partial s_3}=\frac{R}{n}\left\{\left[\left(1-\frac{1}{n}\right)\frac{1}{E}f'(E)-\frac{1}{16}E^2\right](s_1+s_3)\right. \tag{5.24}$$
$$\left.+\frac{1}{4n^2}(e_1-e_3)s_3\right\}.$$

6. SPHERICAL ABERRATION

Consider a star on the axis of the telescope, and in particular rays of that color for which the refractive index is n. The incident rays are

parallel to the axis and so

$$s_1=t_1=e_1=e_{13}=0, \quad e_3=n^2E^2. \tag{6.1}$$

The equation (5.23) for a final ray becomes

$$x=s_3\left\{\frac{\lambda z}{n}(1+\tfrac{1}{2}\lambda^2E^2)+\tfrac{1}{2}\lambda\frac{R}{n}\right.$$

$$\left.-\lambda^3\frac{R}{n}\left[\left(1-\frac{1}{n}\right)\frac{1}{E}f'(E)-\frac{5}{16}E^2\right]\right\}+O(\lambda^5). \tag{6.2}$$

Consider the intersection of this ray with the plane

$$z=-\tfrac{1}{2}R(1+c\lambda^2), \tag{6.3}$$

where c is some finite constant. Substituting this value for z in (6.2), we find that $x=O(\lambda^5)$ provided that f satisfies the differential equation

$$\left(1-\frac{1}{n}\right)f'(E)=-\tfrac{1}{2}cE+\tfrac{1}{16}E^3. \tag{6.4}$$

Thus spherical aberration of the lowest order (for light having the index n) is avoided if the function f is of the form

$$f(X)=\frac{n}{n-1}\left(a-\frac{1}{4}cX^2+\frac{1}{64}X^4\right), \tag{6.5}$$

a and c being arbitrary constants. By (5.3) the corresponding shape of S_1 is

$$z=\zeta(r)=\frac{n}{n-1}R\left[\frac{1}{4}\left(\frac{r}{R}\right)^4-c\lambda^2\left(\frac{r}{R}\right)^2+a\lambda^4\right]. \tag{6.6}$$

7. CHROMATIC ABERRATION

So far we have considered light for which the index is n. All formulae hold equally well for light of a different color, corresponding to index $\bar{n}$, provided that symbols are marked with a bar. Of course, the radius R and the function f do not have to be so marked, and we shall use a common λ in all cases.

For light of index $\bar{n}$ we have, as in (5.20),

$$\bar{T}^{(2)}=-\tfrac{1}{4}\bar{n}R\bar{E}^2,$$

$$\bar{T}^{(4)}=R\left[(\bar{n}-1)f(\bar{E})\right.$$

$$\left.-\frac{1}{16\bar{n}^3}(\bar{e}_1-\bar{e}_3)^2-\frac{\bar{n}}{64}\bar{E}^4\right], \tag{7.1}$$

$$\bar{E}=\frac{1}{\bar{n}}(\bar{e}_1+2\bar{e}_{13}+\bar{e}_3)^{\frac{1}{2}}.$$

Let us suppose that f is as in (6.5), so that the telescope is corrected for spherical aberration for index n. Then

$$\bar{T}^{(4)}=R\left[\frac{\bar{n}-1}{n-1}\left(a-\frac{1}{4}c\bar{E}^2+\frac{1}{64}\bar{E}^4\right)\right.$$

$$\left.-\frac{1}{16\bar{n}^3}(\bar{e}_1-\bar{e}_3)^2-\frac{\bar{n}}{64}\bar{E}^4\right]. \tag{7.2}$$

Corresponding to oblique incident rays, the final rays are given by (5.23), with bars inserted. Let us, however, consider only incident rays of index $\bar{n}$ parallel to the axis. The intersection of a final ray with the plane (6.3) is then given by

$$x=\frac{\lambda^3R(\bar{n}-n)}{2\bar{n}^2(n-1)}\left(c\bar{s}_3-\frac{1}{8\bar{n}^2}\bar{s}_3^3\right)+O(\lambda^5), \tag{7.3}$$

and a similar equation for y. Even if we regard $(\bar{n}-n)$ as finite, x and y are only of order λ^3, whereas the chromatic aberration of an ordinary single lens is of order λ. Nevertheless (7.3) represents a significant chromatic aberration, which it is impossible to destroy for a finite range of the variable $\bar{s}_3$. The best we can do is to minimize it by suitable choice of the constant c. The same thing occurs in the original Schmidt (Fig. 1) as well as in the solid Schmidt (Fig. 2), which we are considering here.

To minimize the chromatic aberration we proceed as follows. Let r_0 be the radius of the aperture; then $\bar{\alpha}_3$ (the direction cosine of a final ray) lies approximately between the limits

$$-\frac{2r_0}{R}<\bar{\alpha}_3<\frac{2r_0}{R}. \tag{7.4}$$

So far we have not identified λ physically. Let us take

$$\lambda=2r_0/R. \tag{7.5}$$

Then

$$-1<\frac{\bar{\alpha}_3}{\lambda}=\frac{\bar{\sigma}_3}{\bar{n}\lambda}=\frac{\bar{s}_3}{\bar{n}}<1. \tag{7.6}$$

Let us put $\xi=\bar{s}_3/\bar{n}$, so that $-1<\xi<1$, and write (7.3) in the form

$$x=\frac{\lambda^3R(\bar{n}-n)}{2\bar{n}(n-1)}[c\xi-\tfrac{1}{8}\xi^3]. \tag{7.7}$$

For given c, the quantity $|c\xi-\frac{1}{8}\xi^3|$ takes its maximum value for the range $-1<\xi<1$ either at $\xi=1$ or at $\xi=(8c/3)^{\frac{1}{2}}$. (This is easily seen by considering the graph of the cubic curve $\eta=c\xi-\frac{1}{8}\xi^3$.) This maximum is made as small as possible by choosing c so that $c\xi-\frac{1}{8}\xi^3$ takes values at $\xi=1$ and $\xi=(8c/3)^{\frac{1}{2}}$ which are equal in magnitude but opposite in sign. Therefore we should choose c so that

$$c-\frac{1}{8}=-\frac{2}{3}c\left(\frac{8c}{3}\right)^{\frac{1}{2}}. \tag{7.8}$$

This is a cubic equation

$$\frac{32}{27}c^3=(c-\tfrac{1}{8})^2 \tag{7.9}$$

with roots $\frac{3}{8}$, $\frac{3}{8}$, $\frac{3}{32}$. The smallest root gives the smallest maximum, and so we take

$$c=\tfrac{3}{32}. \tag{7.10}$$

Accordingly, by (6.6), the form of S_1 is[1]

$$z=\zeta(r)=\frac{n}{n-1}R\left[\frac{1}{4}\left(\frac{r}{R}\right)^4-\frac{3}{32}\lambda^2\left(\frac{r}{R}\right)^2+a\lambda^4\right], \tag{7.11}$$

where λ has now the definite meaning (7.5). The constant a remains arbitrary; it represents a translation of S_1 parallel to the axis of the instrument. This means that S_1 may miss the center O of the sphere by a distance of order λ^4 without spoiling the above corrections.

8. THIRD-ORDER ABERRATIONS FOR OBLIQUE RAYS

The Eqs. (5.23), (5.24) give the final rays for index n, and (in barred form) the final rays for index $\bar{n}$. Let us take f as in (6.5), so that the telescope is corrected for spherical aberration for index n, but let us not make the special choice (7.10) for c.

Consider the intersections of the final rays with the plane

$$z=-\tfrac{1}{2}R(1+b\lambda^2), \tag{8.1}$$

where b is some constant. It is easily found that this intersection is

$$x=\bar{s}_1A+\bar{s}_3B+O(\lambda^5),\quad y=\bar{t}_1A+\bar{t}_3B+O(\lambda^5), \tag{8.2}$$

where

$$A=\tfrac{1}{2}\lambda\frac{R}{\bar{n}}-\lambda^3\frac{R}{\bar{n}}\left[\frac{n}{\bar{n}}\cdot\frac{\bar{n}-1}{n-1}(-\tfrac{1}{2}c+\tfrac{1}{16}\bar{E}^2)-\tfrac{1}{16}\bar{E}^2\right], \tag{8.3}$$

$$B=\lambda^3\frac{R}{\bar{n}}\left[-\frac{1}{2}\left(b+\frac{1}{2}\frac{e_3}{\bar{n}^2}\right)-\frac{n}{\bar{n}}\cdot\frac{\bar{n}-1}{n-1}(-\tfrac{1}{2}c+\tfrac{1}{16}\bar{E}^2)+\tfrac{1}{16}\bar{E}^2-\frac{1}{4\bar{n}^2}(\bar{e}_1-\bar{e}_3)\right].$$

For light of a given color coming from a given star, $\bar{s}_1$, $\bar{t}_1$, $\bar{e}_1$ are given constants, but $\bar{s}_3$, $\bar{t}_3$, $\bar{e}_3$, $\bar{E}$ are variables depending on the particular final ray considered. The general defect of the third order (commonly analyzed into coma and astigmatism) will be present unless x and y are independent of the variable elements up to the third order inclusive. It is clear from (8.2), (8.3) that they will not be so independent in general, and the coma-astigmatism defect will be present to an amount which can be calculated from these equations.

But if we consider light of index n (i.e., that light for which spherical aberration of the third order has been eliminated), we put $\bar{n}=n$ and get from (8.3)

$$A=\tfrac{1}{2}\lambda\frac{R}{n}+\tfrac{1}{2}\lambda^3c\frac{R}{n},\qquad B=\lambda^3\frac{R}{n}\left[-\tfrac{1}{2}b+\tfrac{1}{2}c-\frac{1}{4n^2}e_1\right]. \tag{8.4}$$

Choosing

$$b=c-\frac{1}{2n^2}e_1, \tag{8.5}$$

we make $B=0$, and then (8.2) read

$$x=As_1+O(\lambda^5),\quad y=At_1+O(\lambda^5). \tag{8.6}$$

These expressions are independent of the variable elements to order λ^3 inclusive, and so we get a stigmatic image to that order on the plane $z=-\frac{1}{2}R(1+b\lambda^2)$. Thus correction for spherical aberration automatically corrects for coma-astigmatism for the same index.

To treat chromatic aberrations systematically we should assign to $(\bar{n}-n)$ an order with respect to λ. The oblique chromatic aberrations given by (8.2) might be of order λ^4, and so more important than the fifth-order non-chromatic aberrations, or they might themselves be of the fifth or higher order. This will depend on the size of the aperture and the range of refractive indices which have to be considered.

But enough has been said to fulfil the primary purpose of this paper, which was to show how well Hamilton's method can be applied to the Schmidt telescope, and to open up the possibility of more elaborate developments rather than to give new practical results.

I take this opportunity to thank Dr. J. D. Williams for having suggested to me the application of Hamilton's method to the Schmidt telescope, and also to thank him and Dr. S. Chandrasekhar for orientation in the literature of the subject.

BIBLIOGRAPHY

(1) J. G. Baker, "The solid glass Schmidt camera and a new type of nebular spectrograph," Proc. Am. Phil. Soc. **82**, 323–338 (1940).
(2) J. G. Baker, "A family of flat field cameras, equivalent in performance to the Schmidt camera," Proc. Am. Phil. Soc. **82**, 339–349 (1940).
(3) C. Carathéodory, "Geometrische Optik," Ergeb. der Math. und ihrer Grenz. **5** (1937).
(4) C. Carathéodory, "Elementare Theorie des Spiegelteleskops von B. Schmidt," Hamburg Math. Einzelschr. **28** (1940).
(5) W. R. Hamilton, *Mathematical Papers* (Cambridge University Press, 1931), Vol. 1, pp. 383–386.
(6) D. O. Hendrix, "An extremely fast Schmidt camera," Pub. Astron. Soc. Pacific **51**, 158–159 (1939).
(7) D. O. Hendrix and W. H. Christie, "Some applications of the Schmidt principle in optical design," Sci. American **161**, 118–123 (1939).
(8) F. A. Lucy, "Exact and approximate computation of Schmidt cameras. I. The classical arrangement," J. Opt. Soc. Am. **30**, 251–254 (1940). "II. Some modified arrangements," *Ibid.* **31**, 358–361 (1941).
(9) B. Schmidt, "Ein lichtstarkes komafreies Spiegelsystem," Mitt. Hamburger Sternwarte in Bergedoff **7**, 15–17 (1932). Centralzeitung f. Optik u. Mechanik **52**, No. 2 (1931).
(10) R. Schorr, "Bernhard Schmidt" (obituary). Astron. Nach. **258**, 45–48 (1936).
(10a) R. Schorr, "Das B. Schmidtsche Verfahren bei der Herstellung der Korrektionsplatten für komafreie Spiegel," Zeits f. Instrumentenk. **56**, 336–338 (1936).
(11) C. Smiley, "The Schmidt camera," Pop. Astron. **44**, 415–421 (1936).
(12) B. Stromgren, "Das Schmidtsche Spiegelteleskop" Vierteljahrschrift Ast. Ges. **70**, 65–86 (1935).
(13) J. L. Synge, *Geometrical Optics*. Cambridge Tracts in Mathematics and Mathematical Physics, No. 37 (1937).
(14) J. L. Synge, "Hamilton's method in geometrical optics," J. Opt. Soc. Am. **27**, 75–82 (1937).
(15) Y. Väisäla, "Anastigmatisches Spiegelteleskop der Sternwarte der Universität Turku," Astron. Nach. **254**, 361–364 (1935).
(16) Y. Väisäla, Über Spiegelteleskope mit grossem Gesichtsfeld," Astron. Nach. **259**, 198–204 (1936).
(17) F. B. Wright, "An aplanatic reflector with a flat field related to the Schmidt telescope," Pub. Astron. Soc. Pacific **47**, 300–304 (1935).

Ophthalmic Lens Testing Instrument*

KENNETH N. OGLE AND A. AMES, JR.
Research Division, Dartmouth Eye Institute, Dartmouth Medical School, Hanover, New Hampshire

IN problems concerning the effect of the relative size and shape of the ocular images of the two eyes upon binocular vision and spatial localization, the particular optical properties of the ophthalmic lenses worn before the eyes are of utmost concern. These properties, which depend upon refractive power, flexure, thickness and position of lens before the eye, must be accurately known. While lenses can be designed by computation for accurately obtaining certain optical results, for example, by reducing aberrations, the complete optical properties of a given lens can really be ascertained only by measurement. A suitable lens testing instrument of greater flexibility than that found in the usual testing instruments became a necessity.

The principal optical properties to be determined are those which affect the image on the retina: Magnification, distortion, and power (blur or absence of blur). The problem of measuring these properties is complicated by the fact that the ophthalmic lens in general is an integral part of the whole ocular dioptric system, the primary purpose of the lens being to correct the existing refractive errors by focusing the image upon the retina. This complicating fact presents little difficulty so far as effective power and power aberrations are concerned, but it requires careful consideration when the effective magnification and distortion of the lens are measured. The instrument described in this article has been designed with these considerations especially in mind, although it was found to be quite useful for measuring other than ophthalmic lenses.

The practical method is to measure the angular magnification of the ophthalmic lens about some previously selected point of reference. This point may be variously chosen, depending upon the purpose of the measurements. In general, however, as is customary with optical instruments used in conjunction with the eye, especially where power errors may exist, the reference point should correspond to the center of the entrance pupil of the eye. Angular magnification will accordingly be defined as the ratio of the angle[1] subtended by the image of an extended object, to the angle subtended by the object itself, at the particular reference point; see Fig. 1.

Since the primary object of the lens testing instrument to be described is to determine magnification properties, the design centers about the measurements of those properties. The method consists essentially in measuring the angle subtended by two given points in an image field at a specified reference point, in comparison to the angle subtended at the same point by the corresponding given object points. In Fig. 2, for example, the space rectangle $ABCD$ is imaged in, say, the position $A'B'C'D'$ by the diverging prismatic spherical lens. The apparent angular displacement of the center F' of the image rectangle relative to the point F, the center of the object rectangle, is designated by δ; it is the prismatic deviation referred to the eye. The angular magnification of the lens for any space point P, referred again to the eye, is the ratio of the angular size $F'P'$ of the image, designated by α', to the angular size FP of the object, designated by α. The points $A'B'C'$, etc., may be astigmatic.

The scheme for measuring the angular magnification is indicated in Fig. 3. C is the center

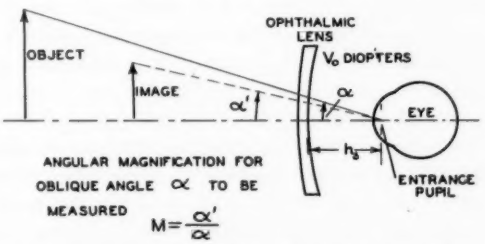

FIG. 1. Illustration of definition of angular magnification as used in this paper.

* Read before the October meeting of the Optical Society in Rochester, New York, October 11, 1940.

[1] More generally, the angular magnification refers to the ratio of the tangents of the image and object angles. The substitution of the angles for the tangents here simplifies the particular design of the instrument and introduces no appreciable errors.

point corresponding to the entrance pupil of the eye, about which a lens to be tested can be turned through fixed angles α. The distance, h, of the lens from C can be varied. A focusing telescope T is so mounted B that it can be turned about C and its position adjusted accurately by means of clamps and tangent screws. A point source of light S, fixed at a given distance from C, will be imaged by the lens in some position S' and this image may or may not be

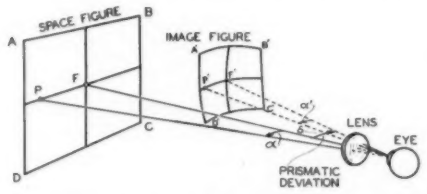

FIG. 2. Schematic drawing showing the relative dimensions of an object figure and its image formed by ophthalmic lens to be measured by the lens testing instrument.

astigmatic. The lens is first set up and centered in the instrument, and the telescope is focused upon the image of S and adjusted about C until the cross-hairs of the eyepiece are centered upon the image. When the lens is then turned about C through an angle α, and the telescope refocused upon the image S', the telescope will have to be turned through a small angle $\Delta\alpha$ (to a position T' in Fig. 3), if the image is again to be centered upon the cross-hairs. The small angle $\Delta\alpha$ is the increment of change in the angular distance α. The angle α will appear through the lens as $\alpha'=\alpha+\Delta\alpha$. The angular magnification, M, will be α'/α; and the percent angular magnification will be $100\times(\Delta\alpha/\alpha)$.

In general, however, if the telescope is focused and centered upon S before the lens is put in the instrument, and the lens is then mounted as it would be when placed before the eye, the telescope will have to be refocused and turned through an angle δ in order to center the cross-hairs upon the image S formed by the lens. This angle δ (cf. Fig. 4) is the prismatic deviation of the lens in that position, relative to the point C. When the lens is now turned through α, the angular magnification increment $\Delta\alpha$ is measured from the new position of the telescope.

The power of the lens for the peripheral angle α can be measured by means of an appropriate scale on the telescope focusing adjustment. If $\Delta\alpha$ and the power for a given lens are measured for each of a series of angles α, the magnifications, the distortion, power aberrations, etc., can be ascertained. One can, for example, plot $\alpha'=\alpha+\Delta\alpha$ against α, as shown in Fig. 5. This figure illustrates the direct measurements and shows the prismatic deviation of the lens. This representation is not so informative as one in which the angular magnification $M=\alpha'/\alpha$ is plotted, for example, against the oblique angle as shown in Fig. 6. In this graph the paraxial magnification can be interpolated. The distortion at any angle α will be, strictly speaking, $D=dM/d\alpha$. Usually, however, the average distortion of an ophthalmic lens is not great, and the distortion can be given by $D=(M_1-M_2)/(\alpha_1-\alpha_2)$ for the midpoint between α_1 and α_2 if the chosen values of α are not too large. Insofar as retinal image magnification is concerned, it must be remembered that this measurement of magnification is only relative to the particular reference point selected as, for example, the center of the entrance pupil of the eye.

If the magnification is to be measured for some oblique direction and the image is very astigmatic, it may be necessary to interpose a small diaphragm near the reference point C and to make the settings of the telescope on a blurred image, or to use a split lens device within the telescope with which both astigmatic images can be brought into focus simultaneously.

The essential features of the design are shown schematically in Fig. 7. The lens holder unit is mounted in a gimbal-like frame which permits the lens to be turned through fixed given angles about vertical and horizontal axes which pass through a central point C. This lens holder is so designed that a pair of spectacles can be held in the instrument. This mount is a complicated unit; it must permit variation of the distance of the lens holder from the point C, to allow for

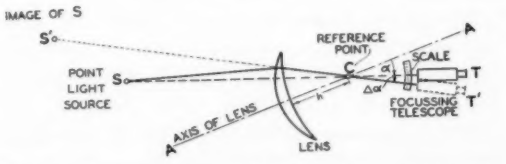

FIG. 3. Diagram of essential scheme for measuring the angular magnification of an aprismatic ophthalmic lens.

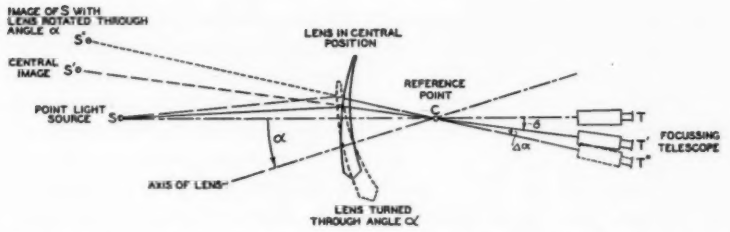

FIG. 4. Diagram of scheme for measuring angular magnification when the lens is prismatic.

different distances of the lenses from the reference point; there must be adjustments for height to allow for different sizes of lenses, for different inclinations, and for variously shaped lenses and frames; and the mount must provide a means for rotating the lens about its own axis so that the axes of astigmatic lenses can be aligned with the horizontal and vertical meridians of the instrument.

A point source of light, provided by a pin-hole behind a reversed microscope objective, is mounted independently at a distance of 40 cm from the central point. By interposing one of a battery of several lenses before the point light source, the vergence of the light can be changed to provide different object distances.

A bridge-like frame arrangement that supports the telescope also turns about horizontal and vertical axes through the same central point C. This frame can be turned and adjusted by clamps and tangent screws. The rotations of the lens mount described above and the telescope support are, of course, independent. The axis of the focusing telescope also passes through the central point C for all positions. This telescope can be focused from "beyond" infinity to a distance nearer than the central reference point C, and is provided with a scale calibrated to read image vergence power, i.e., the reciprocal of the distance (meters) of the image from C, in diopters. A battery of auxiliary lenses extends the range of the telescope.[2]

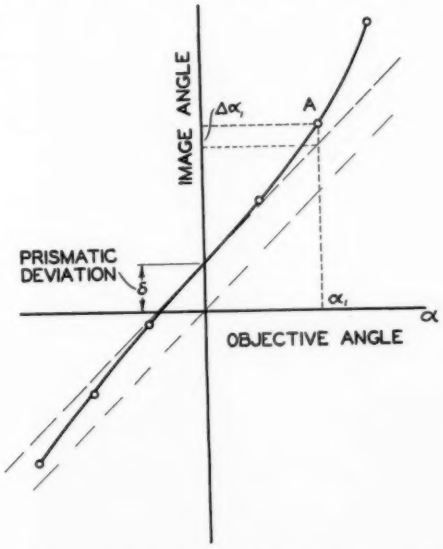

FIG. 5. Graphical representation of measured image angle compared to the object angle.

The small angles $\Delta\alpha$ are measured by means of a second telescope which, mounted rigidly on and above the focusing telescope, is focused upon a large chart at a distance of about 6 meters. By using millimeter divisions on that chart and a telescope of high magnifying power, angles of 0.002° can be estimated. An angle of this magnitude would correspond to about 0.02 percent magnification for an oblique angle of 10° through which the lens has been turned.

If very accurate centering of a lens is desired, a small shielded cystoscope lamp with a pin-hole aperture toward the lens is raised in front of the focusing telescope. The telescope can then be focused upon the images of that lamp as reflected from the surfaces of the lens. The latter, if not prismatic, can then be centered by adjusting it so that each of the reflected images falls upon the cross-hairs of the telescope eyepiece.

The instrument is mounted on a heavy cast iron pedestal, at such a height that it can be

[2] This method of determining the refractive power of a lens involves a scale with a non-linear calibration, but this has not proven a serious disadvantage.

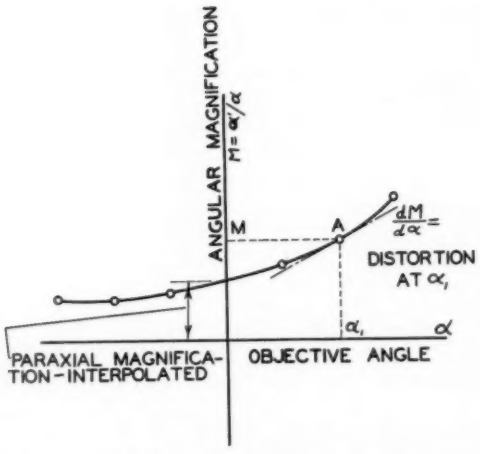

FIG. 6. Graphical representation of measured percent change in image angle compared to object angle, showing the determination of the paraxial magnification and distortion.

operated easily by a person who is seated. The telescope, lens supports, etc., are set in sturdy pieces, yet provided with adequate means of adjustment. The instrument is illustrated in Figs. 8 and 9.

When a prismatic lens is placed before the eye, the eye turns about its center of rotation to a new position so that it can perceive the image, and the entrance pupil, of course, will correspondingly take a new position. To duplicate this changed position of the entrance pupil exactly in the lens testing instrument would require a rather complicated construction and the gain in accuracy would be only slight. Hence, it has been considered within general accuracy to assume that the center of rotation coincides with the entrance pupil, as illustrated in Fig. 3. Since the prismatic deviation of the average ophthalmic lens does not exceed 8 prism diopters (4 arc degrees), the error is not appreciable, especially for increased object distances.[3]

In some circumstances it may be desirable to determine the differential eye movements which will occur when anisometropia (unequal refraction in the two eyes) is corrected, and the two eyes have to turn through different angles in order to fixate obliquely situated objects.[4] The complete measurements of the prismatic deviations for various oblique angles can be easily found with this instrument by assuming the

[3] Since the object distances range from 40 cm to 6 meters, the difference between the prismatic deviation as measured about the entrance pupil and that measured about the center of rotation (true prism power) could be practically compensated for by a displacement and a slight rotation of the lens. The displacement, however, is of the order of 0.1 mm per prism diopter, which is too small to be taken into account. This is also true of the slight rotation of the lens. The difference between the true prism power Δ and the prismatic deviation δ, as measured about the entrance pupil, is $\Delta = \delta p/(p+d)$ when p is the object distance from the entrance pupil and d is the average distance of the entrance pupil from the center of rotation of the eye. The instrument described here does have a second center of rotation so that this deviation for prisms of high power can be compensated for.

[4] The general problem of the differential eye movements caused by lenses of different refractive power has received considerable attention, and these different movements have been suggested as a cause of ocular discomfort. Cf. especially, M. v. Rohr, *Die Brille als optisches Instrument* (J. Springer, Berlin, 1921), p. 197 ff; H. Erggelet, Zeits. f. Psych. u. Physiol. d. Simnesorg. **49**, 326–364 (1916); E. Weiss, Ber. d. 43. Vers. d. Dtsch. Ophthalm. Gesellsch. Jena, 101–106, 1922; and J. S. Friedenwald, Arch. of Ophthalm. [2] **15**, 283–307 (1936).

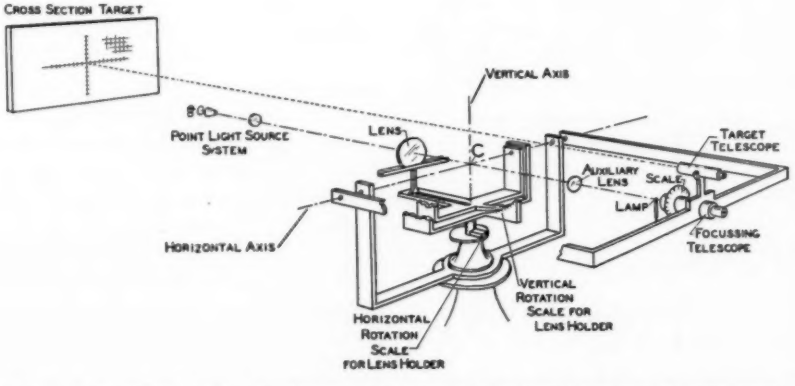

FIG. 7. Perspective drawing showing essential parts of ophthalmic lens testing instrument.

central point of the instrument to correspond to the center of rotation of the eye. The differences in the apparent angles measured for the same obliquely seen object in each of the lenses of a given pair of spectacles indicate the differential eye movement involved in those spectacles.

By attaching filters before the objective of the telescope, a rough measure of chromatic aberration can be obtained.

The exact nature of the retinal image in a corrected ametropic eye, that is, an eye having refractive errors as compared with that of a normal eye, cannot be ascertained. This follows because the size of the image on the retina of the corrected ametropic eye depends upon the cause of the defect, namely, whether the ametropia is due to dioptric factors within the eye, or to an anomaly of the axial length of the eyeball.

While the magnification of the retinal image of a corrected ametropic eye is not determinable, this magnification is modified by the particular physical dimensions of the actual ophthalmic lens used and its position before the eye. In measuring the effective magnification of a given ophthalmic lens, therefore, the basic magnification cannot be measured; only the modifications in that basic magnification (which modifications are due to various types and positions of ophthalmic lenses) become the important quantities to be measured. Clearly, these modifications can be measured only when referred to some elementary and convenient standard correcting lens.[5] This standard may be a hypothetical infinitely thin lens specified at a particular distance from the eye, or it may be a standard trial case test lens or a combination of test lenses

FIG. 9. Photograph of ophthalmic lens testing instrument.

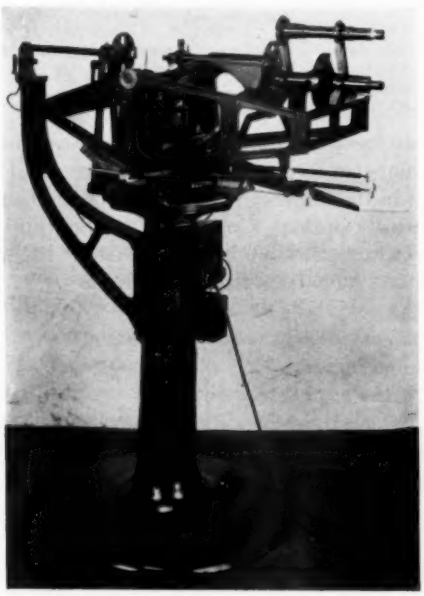

FIG. 8. Photograph of instrument.

used at specified distances from the eyes and all having the same corrective refractive power. In the following example, where the measured optical properties of a pair of iseikonic spectacles are described, the latter standard was used.

The initial prescription for this pair was R.E.: $+2.00\ S-0.75\ C$ axis 90°; L.E.: $+2.25\ S-1.25\ C$ axis 90°; combined with one percent over-all with two percent meridional axis 90°,magnification. This refers to eikonic measurements made with trial case lenses. Eyewire distance is to be 12 mm. This prescription was manufactured as follows (see Fig. 10): The right eye lens was a single toric lens—front surface (toric) $= +4.50\ S +0.75\ C$ axis 180°; thickness = 3.5 mm; ocular surface $= -3.25$ sphere. The left eye lens was an air spaced doublet cemented at the edges. First component: Front surface (toric) $= +9.50\ S +3.50\ C$ axis 90°, thickness = 2.0 mm, back surface $= -9.00\ S$. Air space = 2.5 mm. Ocular

[5] K. N. Ogle, J. Opt. Soc. Am. **26**, 324–337 (1936).

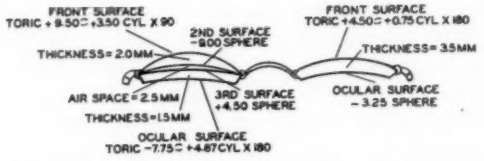

FIG. 10. A spectacle design to obtain special magnification properties in addition to the correction of refraction errors of the eyes.

component: Front surface $= +4.50\ S$, thickness $= 1.5$ mm, and back surface (toric) $= -7.75\ S + 4.37\ C$ axis 180°.

The measured characteristics of the two lenses, namely, the effective power and the effective magnification for the vertical and horizontal meridians, for an object distance of 40 cm, are shown in Fig. 11. The abscissae of this graph are the peripheral angles in degrees, positive to the right for the horizontal meridian and upward for the vertical meridian. The central ordinate axis is the magnification axis, the units being percent. The effective power axis is at the left of the graph, the units being diopters. The points showing magnification data are joined with solid lines, while the points showing the power data are joined by dashed lines. The measured results gave: R.E. $+1.84 - 0.71$ axis 90°; L.E. $+2.08 - 1.25$ axis 90°; combined with 1.07 percent over-all with 1.90 percent axis 90°.

An inspection of the graph shows that the aberrations, insofar as power and magnification are concerned, are small.[6] There is an indication of pin-cushion distortion, in which respect the doublet (L.E.) lens is no worse than the single (R.E.) lens. The power aberrations are greater in the doublet lens, but in this respect it is interesting to note the difference in the various meridians. These spectacle lenses showed negligible prism power (less than $\frac{1}{8}$ diopter).

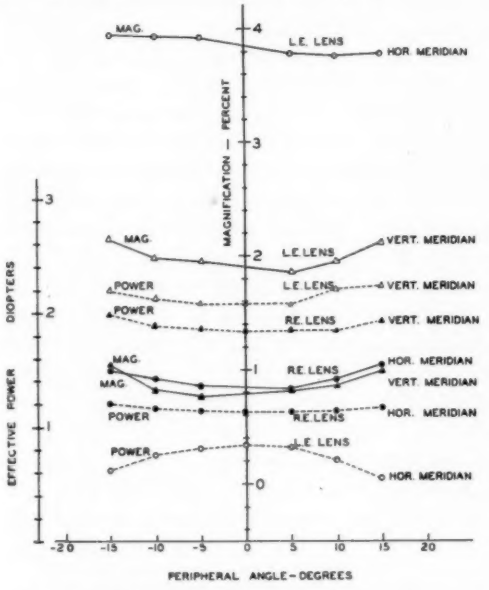

FIG. 11. Graphical representation of measurements of a typical pair of spectacles having an aniseikonic correction incorporated.

Two instruments (also referred to as Dioptoeikonometers), the one at Hanover and the other in the aniseikonic Lens Department of the Americal Optical Company, in Southbridge, Massachusetts, have been in constant use since 1934 and have been found satisfactory.

[6] In this connection it is apparent that the remarks of H. Hartinger [Klin. Monatsbl. f. Augenh. **100**, 278–280 (1938)] in which he attributes large peripheral aberrations to lenses in this general type of prescription, are not applicable here.

An Improved Procedure for the Contact Printing Method of Measuring Photographic Density

MONROE H. SWEET
Physics Division, Research Laboratories, Agfa Ansco, Binghamton, New York
(Received January 9, 1943)

OUTLINE

I. Introduction and Statement of Purpose
II. Historical Background of Density Measurement
III. Preliminary Considerations
  A. Effect of Ultraviolet Radiation
  B. Validity of General Procedure
IV. The Improved Procedure
  A. General Plan
  B. Description of Apparatus
    1. Light Source
    2. Printing Frames
    3. Baffles
    4. Electrical System
    5. Printing Media
  C. Procedure
    1. Measurement of Distances Involved
    2. Handling of Print Material
    3. Selection of Position of Test Frame
    4. Processing of the Prints
    5. Computations
    6. Null Point Check
    7. Special Precautions
    8. Sources of Error
V. Results
  A. Effect of Print Material on C.P.D.
  B. Comparison of Results Obtained by Other Criteria
  C. Density Defined
VI. Summary
VII. Appendix

I. INTRODUCTION AND STATEMENT OF PURPOSE

IN making an analysis of modern sensitometric procedures, it became clear that the common definition of density is inadequate for photographic purposes. Since photographic sensitometry is dependent upon the measurement of density* physically or visually, this aspect of the subject was considered important enough to justify a survey of the possible methods of density measurement with the view of establishing a more meaningful criterion than any currently adopted. Appraisal of the pertinent data indicated that contact printing density (C.P.D.) offered a number of advantages found in no other definition.

The basic procedure for determining contact printing density consists of exposing adjacent areas of a sensitized photographic material, one directly to a point source of radiation at a definite distance and the other to the same source for the same length of time but at some position nearer the light source and *in contact with the transmission sample of unknown density*. The C.P.D. of the specimen is then calculated from the reflection or transmission coefficients of the exposed and subsequently processed photographic material. .

In order to propose a specific technique as a standard for determining photographic density, sufficient evidence must be provided by theoretical analysis and by detailed practical trial to demonstrate that the procedure gives accurate results irrespective of the laboratory in which they are derived. With such evidence, the adoption of C.P.D. as a criterion for photographic density measurement may be rationalized. The first paper, therefore, aims to present a simplified and otherwise improved procedure for determining C.P.D. and to give the necessary data to allow study and verification by those concerned with the establishment of a standard method for density measurement. It is believed that the procedure described here presents definite advantages, in respect to both accuracy and facility of operation, and eliminates or liberalizes many of the restrictions associated with other techniques.

The second paper† deals in part with the exposition of a basic densitometer which measures with precision a variety of types of specimens according to the C.P.D. specification. (It is a recognized fact that existing densitometers, both physical and visual, could be recalibrated in terms of C.P.D. and, thereafter, be used to read C.P.D. with satisfactory accuracy for many kinds of materials.)

* Directly or by comparison.

† To be published in a later issue of this journal.

II. HISTORICAL BACKGROUND OF DENSITY MEASUREMENT

Hurter and Driffield are credited with establishing the first general definition of density late in the nineteenth century.

$$D = \log 0,$$

where 0 is the opacity of the material and equals the reciprocal of the transmission.

This expression has been widely adopted for use in several branches of optics. If unmodified, when this definition is applied to the photometry of photographic transmission specimens a number of complications arise. Photographic layers are generally somewhat spectrally selective in their absorption and consequently the numerical value of density may vary according to the spectral attributes of the light source-filter-receiver combination involved. Of equal importance are the effects of scattering by the silver grains. Thus, if the geometry of the photometric system is such that all of the transmitted light is received by the detector, the apparent density will be lower than if only the normal emergent beam is considered (in both of the latter cases, it is assumed that the incident beam is collimated). The inter-reflection of rays by the various surfaces involved also plays a part in the result.

Efforts to reach agreement on some generally acceptable specification for photographic density have made their appearance in the literature from time to time commencing with the activities of Toy, Renwick, and Ferguson,[1–4] in the 1920's. Toy supported a form of C.P.D., whereas Renwick vigorously attacked Toy's approach and attempted to prove that C.P.D. would make an unsatisfactory standard. Renwick's criticism centered chiefly around the fact that in the C.P.D. method the inter-reflection (and, hence, the result) will vary when different papers are used as print materials. While Renwick's arguments are substantially correct, in practice the effects with which he is concerned are certainly not of sufficient practical importance to justify exclusion of the C.P.D. method from consideration as a standard.

[1] F. C. Toy, Phot. J. **49**, 164 (April, 1925).
[2] F. Renwick, Phot. J. **49**, 293 (June, 1925).
[3] F. C. Toy, Phot. J. **49**, 294 (June, 1925).
[4] W. B. Ferguson, Phot. J. **50**, 294 (June, 1926).

Ferguson supported Toy's opinions with independent experimental data and concluded "My data confirm the correctness of Toy's formula $D_p = D_{\text{diffuse}} \times R$. This work indicates that the search for a perfect primary instrument is unnecessary."

As a counter proposal, a form of visual diffuse density (V.D.D.) was offered. However, the objections to such a proposal seem to be more numerous than to C.P.D. and hence it was not adopted. The activities mentioned above took place in Europe.

In this country, Koerner and Tuttle[5] proposed to standardize the integrating sphere using the eye as a receiver. This has been objected to primarily because of the expense of integrating sphere instruments but also the apparent availability of simpler, more direct, and sufficiently precise criteria in which cost is not a factor.

Any satisfactory treatment of the merits of different proposed specifications for standard density measurement will involve an extended discussion and space limitations prevent a proper handling of this topic in the present manuscript. Readers are directed to reference 6 for a more complete resume of the general subject of density measurement.[6]

Certain fundamental experimental work dealing with the C.P.D. method has been described by the present author in the recent literature.[7]

III. PRELIMINARY CONSIDERATIONS

A. Effect of Ultraviolet Radiation

So-called neutral-density photographic deposits are usually characterized by a different contact printing density (C.P.D.) and visual diffuse density (V.D.D.) under the conditions described in reference 7. The cause of this difference has been satisfactorily explained by a spectrophotometric investigation of the ultraviolet transmission of photographic layers.[8] It has been shown that there is a narrow absorption gap in the region of 320 mμ. This characteristic is of sufficient magnitude to cause a C.P.D.-V.D.D.

[5] C. Tuttle and A. Koerner, J. Soc. Mot. Pic. Eng. **29**, 622 (Dec. 1937).
[6] C. Mees, *Theory of the Photographic Process* (Macmillan, New York, 1942), Chapter 16, p. 638.
[7] M. H. Sweet, J.P.S.A. **7**, 126 (Oct. 1941).
[8] M. H. Sweet, J. Opt. Soc. Am. **32**, 324 (1942).

difference of 0.2 at a V.D.D. level of 2.5 when an unfiltered tungsten radiator is used in conjunction with a chloride printing paper.

Accordingly, the elimination of ultraviolet radiation is suggested in order to avoid the disturbing results caused by the selective transmission in the 320-mμ region. The elimination of the ultraviolet simplifies the specification of density and makes it unnecessary to give tolerances for the ultraviolet transmission of lamp envelopes and glass in printing frames or the ultraviolet sensitivity of the printing materials.

This modification seems further justified in view of the large assortment of optics used in contact printers and the corresponding range of percentage of ultraviolet radiation present. In many cases, practically no ultraviolet radiation reaches the print material.

B. Validity of General Procedure

In a discussion of "Photographic Radiometry,"[9] L. A. Jones has enumerated conditions to be fulfilled if errors in the photographic procedure are to be reduced to a minimum:

1. Both exposures must be given non-intermittently, thus eliminating any error which might arise from failure of the photographic material to integrate correctly an intermittent exposure.
2. Exposures must be simultaneous, thereby avoiding error due to growth or decay of the latent image which might occur during the time between the termination of exposure and development.
3. The condition of equal print densities

$$d_{(\text{reference})} = d_{(\text{test})}$$

when the exposure times are the same is the criterion of equal radiant energy. This eliminates errors arising from failure of the reciprocity law.
4. Radiant energy of the same spectral composition must be used for both exposures.
5. The two areas of the print material to be exposed, must be small and adjacent to each other. The total area involved must be very small. Placing the two areas side by side in processing practically eliminates errors which might arise from differential development, and simplifies the requirements for processing.*
6. Errors due to differences in temperature and moisture content of the photographic material that might arise from differences in handling are practically eliminated when the exposures are made simultaneously on small areas of photographic material immediately adjacent to each other.

Jones' requirements seemed valid and were adopted by the author. Our original procedure failed to satisfy all of these requirements because:

a. Exposures were not made simultaneously.
b. Computations were not made from equal print densities but depended on the difference in densities produced by the test exposure and the reference exposure.
c. Simultaneous exposures were not specified; therefore, the light source had to be maintained at constant intensity. This represents the most serious objection to the method, for it is difficult to provide a light source of uniform intensity in modestly equipped laboratories.

To overcome the difficulties caused by separate exposures, it was suggested that radiation from a common source be used to expose both the reference strip and the test strip simultaneously. If, however, the radiation perpendicular to the primary beam were used to expose the reference strips, there would remain the possibility of disproportionate variations in effective light intensity arising from individual variations in the characteristics of the lamp and the optical system. If a semi-transparent mirror were used to split the primary beam, polarization would result. Both of these means have a further common disadvantage. In practice, the reference strips would ordinarily be exposed relatively close to the effective light source, and small disturbances

[9] W. E. Forsythe, Editor, *Measurement of Radiant Energy* (McGraw-Hill, New York, 1937) Chapter VIII, L. A. Jones, p. 269.

* Dr. A. C. Hardy has called the writer's attention to the fact that Jones apparently had in mind the use of two areas on the same piece of film during exposure and processing. Nevertheless, we feel that condition (5) as we have interpreted it, is sufficiently rigorous under normal circumstances to avoid error of the type which the requirement is designed to eliminate.

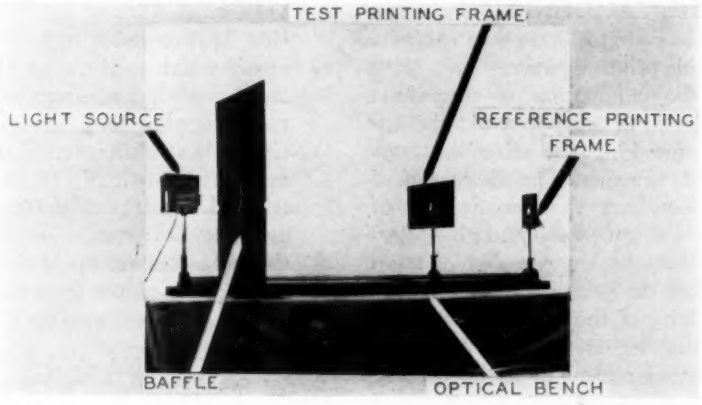

FIG. 1. General arrangement of optical parts used for the improved technique of measuring contact printing density.

in the optical distance would cause serious errors in the results. Despite these difficulties, the use of a single light source seemed to present so many advantages that work along these lines was continued, and an arrangement ultimately was devised in which these objections are avoided.

IV. THE IMPROVED PROCEDURE

A. General Plan

Two views of the general arrangement of the optical components are shown in Figs. 1 and 2. Figure 3 is a diagram of the system.

A light source screened by a sharp-cutting, ultraviolet absorbing filter is mounted rigidly at one end of the optical bench. An ordinary photographic printing frame is mounted at the other end of the bench, and the sensitized material for all reference exposures is held in this frame. The distance between the light source and material for reference exposures is constant.

A second printing frame is mounted between the source and the reference frame. This second frame is constructed so that the density sample and the sensitized material are held in contact, but only the upper part of the beam is intercepted. The direct part of the beam passes through an aperture in the glass and pressure plate of this frame and proceeds unobstructed (regardless of the relative distances of the two frames from the light source) until it reaches the sensitive material in the reference printing frame.

For every possible position of the test frame on the bench (between the light source and the reference frame) there is a corresponding transmission density of the sample which will absorb that fraction of light required to equalize exposures for the test and reference materials, and consequently produce equal print densities when developed. Hence, the bench may be graduated in "equivalent transmission density" divisions instead of units of length. When a sample whose density is presumed to be, say 0.23, is submitted for measurement, trial exposures are made with the test frame at "equivalent density" positions of 0.20, 0.25, and 0.30. From an interpretation of the resulting reference and test print densities, it is a simple matter to predict the position (the null point) of the test frame which should give identical test and reference densities. Exposures are then made with the test frame at this position. By making several trial exposures with the test frame at the "null point," it is possible to determine the true C.P.D. with a high order of accuracy. Clearly, the "null point" technique satisfies the requirements for precision photographic photometry, as enumerated by Jones.*

* An exception arises when spectrally selective samples are to be measured. In such cases the spectral composition of the light incident on the reference print may be dissimilar to that on the test print. Nevertheless, practical trials show that the maximum error introduced by the effects of selective absorption of common density specimens is negligible.

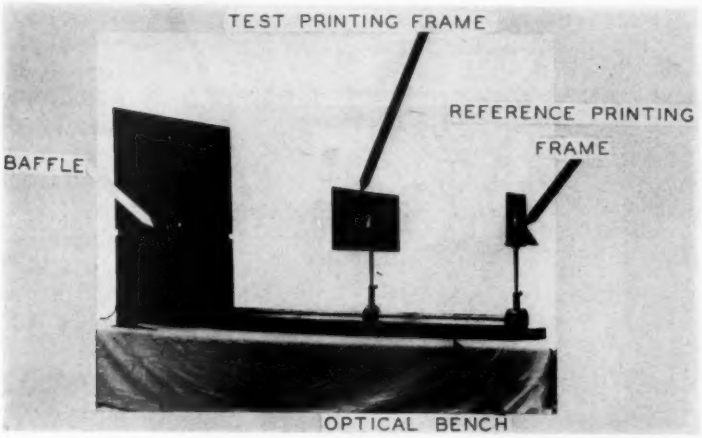

FIG. 2 .C.P.D. measuring system showing rear of test and reference printing frames.

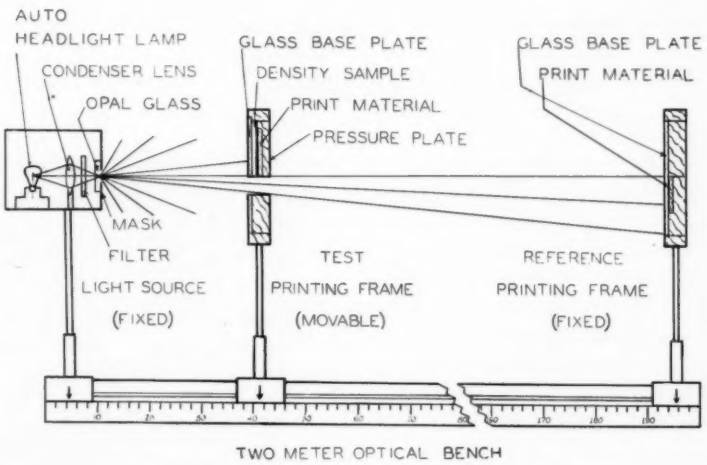

FIG. 3. Optical system used in the measurement of C.P.D. (Baffle not shown.)

B. Description of the Apparatus

1. Light Source

In our original experiments, a bare tungsten coil filament lamp served as the light source. This was not satisfactory because of bulb defects and the coil type of filament construction. When a lamp of small filament dimensions is used, the focusing effects of mould wrinkles is pronounced. Furthermore, bright ghost images of the filament are likely to occur. In all applications of inverse square law photometry, perfectly uniform angular distribution of radiation is ordinarily assumed and any departures from this condition may give rise to errors. The orientation of coils in the filament is frequently a source of error because the total area of the coils to which the sensitive material is exposed, varies with the source-frame-distance.

The uniformity of flux distribution can be readily estimated by holding a white card approximately one meter from the source and observing the brightness distribution and the presence of any "hot spots." Coil shadows

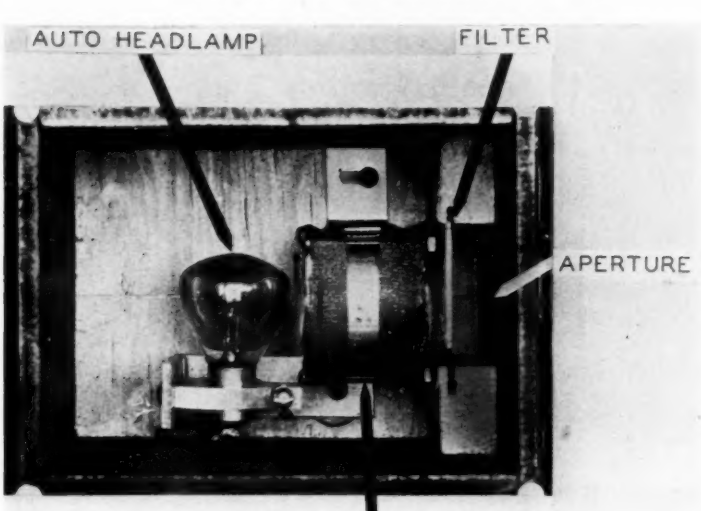

FIG. 4. Component parts of light source (with exception of opal glass which is not visible in this view).

usually appear as dark striations, whereas ghost images and bulb defects give rise to alternate bright and dark spots.

By substituting for the bare tungsten lamp an intensely illuminated opal glass of small area, uniformity of flux distribution over the angular range of interest is assured. No ghost images are present and by this arrangement errors attributable to light reflected from surfaces behind the source are entirely eliminated. Such an arrangement is practical only because of the exclusion of ultraviolet radiation from the system. Commercial opal glass of sensibly neutral density over the spectral range of concern, in the present case (360–500 mμ), is readily obtainable.

A satisfactory construction is illustrated in Figs. 3 and 4. Light from a 50-c.p. auto headlamp is concentrated on an opal glass which is masked so that only a circle 5 mm in diameter is exposed. A Corning No. 738 ultraviolet absorbing solid glass filter is mounted between the condensing lens and the opal glass.*

* A Wratten No. 1 filter might have been equally suitable but apparently its stability to heat and light is not equal to that of the solid glass filter.

2. *Printing Frames*

a. Reference frame.—The reference printing frame is provided with a mask on the inside surface of the glass so that only the area desired for actual exposure is left uncovered. By using black velvet to cover the front and sides of both frames and the base, reflections are minimized. Like the other components, the reference frame is

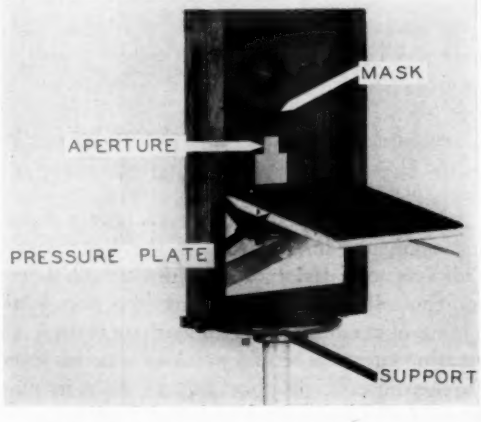

FIG. 5. Rear view of reference printing frame.

securely mounted on the optical bench. Figure 5 is a rear view of the reference printing frame, showing constructional details.

b. Test frame.—Figure 6 is a photograph showing the details of the test printing frame. Features of its construction will be clear from study of Fig. 7 which is a cross-section diagram of the frame. An inverted *L*-shaped metal strip, with the longer side horizontally disposed, serves to position the glass base plate, density sample, and the sensitive material in the test printing frame. The ledge formed by the perpendicular section of the strip serves as a mask to absorb or reflect light which might otherwise be reflected by the under side of the horizontal section and thus fog material in the reference frame. Reflections are further reduced by painting the strip with matte black lacquer.

The pressure plate is hinged at the top of the frame so that the lower edge of the plate just clears the metal strip. The test frame as a whole is adjusted, vertically, so the lower edge of the metal strip is slightly higher than the top of the

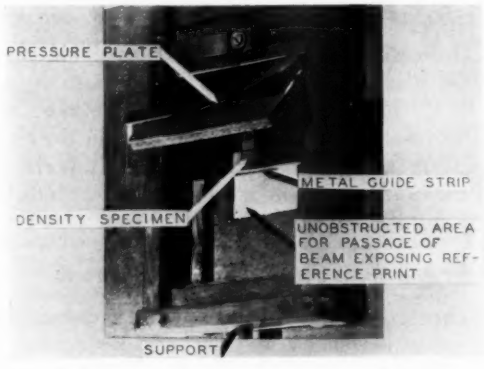

FIG. 6. Rear view of test printing frame.

5-mm circle of illuminated opal glass. With this alignment no part of the beam directed at the reference frame will be obstructed by the test frame.

3. *Baffles*

The light source was so designed that stray radiation was practically eliminated. The large baffle shown in Fig. 1 further reduces stray radiation. To make the absorption of stray light even

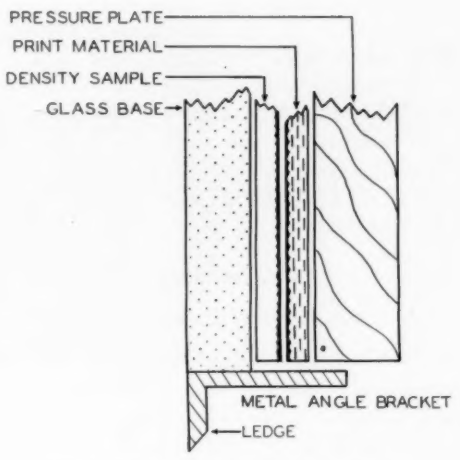

FIG. 7. Construction of test printing frame.

more complete, a heavy black cloth was draped over the baffle and light source when the apparatus was in use.

Early in the development of the present technique, it was discovered that some light was reaching those portions of the step wedge which extended beyond the frame itself. A portion of the light scattered by the exposed sections of the wedge served to fog the reference sensitized material. Therefore, a small baffle was attached to the front of the test frame to prevent light from striking portions of the step wedge extending beyond the exposure aperture.

4. *Electrical System*

An important advantage of the present procedure lies in the fact that constant light-source intensity is not required, although reasonable uniformity is obviously desirable. It is only necessary to make certain that exposures are always of a magnitude such that resulting densities will lie approximately on the portion of the D *vs.* log E curve of the print material where the slope is nearly constant. For convenience, a magnetic type of voltage stabilizer was used. The complete electrical and timing circuit is shown in Fig. 8a. Figure 8b shows an alternative arrangement suggested for laboratories where a voltage regulator and time switch are not available.

5. *Printing Media*

After an extensive investigation of the pertinent characteristics of sensitive materials, it was concluded that a high contrast, glossy surface, double weight, bromide enlarging paper was satisfactory. For routine measurements, Agfa Brovira, double weight white stock "hard" grade, was used.

C. Procedure

1. *Measurement of Distances Involved*

In practice, one of the factors often limiting the accuracy of results obtained by the inverse square method of photometry, is measurement of the distances involved. It is helpful to compile a table listing the calculated positions of the test printing frame which give equal test-reference material densities for specific sample density increments of 0.05. In addition, a graphical plot of "C.P.D." *vs.* the corresponding scale setting of the test frame holder is of assistance. Such a plot facilitates the location of the test frame when the null point checks are undertaken.

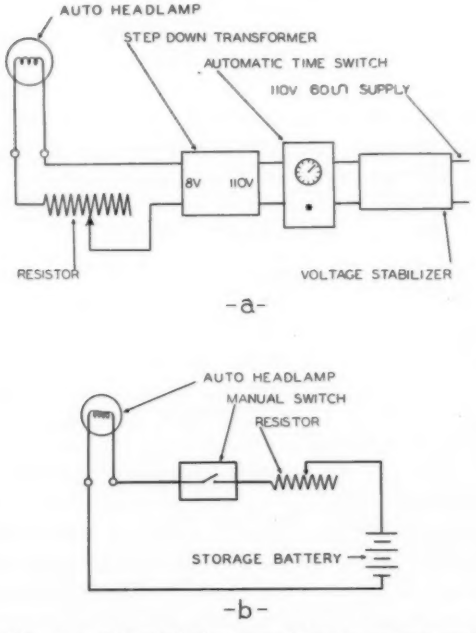

FIG. 8. a. Electrical circuit used for the present work. b. Alternative circuit for use where a voltage regulator is not available.

Table A, in the Appendix, will aid in the calculation of the required distances for specified density values when using an optical bench of any particular length. In Table A, column (3) gives the factor by which the distance between the light source and the reference printing frame should be multiplied in order to obtain the correct light source—test frame distance for the corresponding equivalent density. The values in column (2) are the logarithms of the multiplying factors.

If the ultraviolet absorbing filter is located between the source and the printing frames, a correction should be made in the position of the light source. (See formula (1) in Appendix.) However, this position for the ultraviolet absorbing filter cannot be recommended.

It is helpful to know the effect of an error of given magnitude, say 1 mm, in the test printing frame-light source distance setting. The formula for determining this factor is included in the Appendix (6). The errors introduced at different density levels by a variation of 1 mm, for a base distance of 200 cm, are given in Table B.

2. *Handling of Print Material*

Ordinarily, the sensitive photographic material is cut from 8″ by 10″ sheets into strips 1″×3″. These strips are paired and marked, so as to insure their proper orientation in the two printing frames; thus, their optical juxtaposition at the time of exposure will correspond with their physical configuration before cutting.

3. *Selection of Position of Test Frame*

Three positions of the test frame, corresponding to equivalent densities that are, respectively, lower, equal to, and greater than the C.P.D. of the sample are selected, after a preliminary density measurement with an ordinary transmission densitometer. For instance, if the predicted C.P.D. were 1.03, exposures would be made at equivalent density positions of 1.00, 1.05, and 1.10. Hence, for each *set* of exposures there are three reference prints and three matched test prints.

4. *Processing of the Prints*

It is convenient to develop three sets of prints together by tray development. Rubber bands are

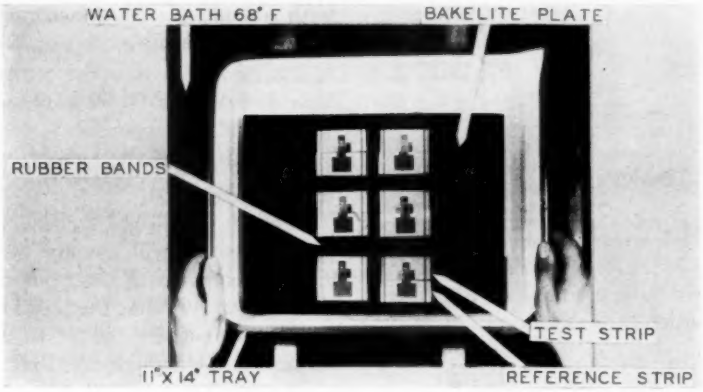

FIG. 9. Method of developing reference and test strips.

used to retain the strips in position, as illustrated in Fig. 9. A Bakelite plate, approximately 10″×12″ forms a satisfactory support as it is not easily broken and is impervious to the processing solutions. The exposed materials must remain side by side in pairs, oriented as during exposure (see Fig. 9). This is a precaution which avoids unequal treatment of the individual strips of a given pair.

Tray development in any suitable metol-hydroquinone formula has been found satisfactory for purposes of routine investigation, with agitation provided by rocking in four directions at 35 rocks per minute. After drying the strips in air, the densities of the test and reference materials are compared by any convenient means. The type of densitometer used is of no consequence as long as the measurements of density differences between each reference strip and its mated test strip are reliable. Later, it will be shown that it is only necessary to detect mismatches in the test and reference densities to obtain accurate results.

TABLE I.

(1) Equivalent densities	(2) Measured reference print densities	(3) Measured test print d	(4) Adjusted R.P.D.	(5) Adjusted T.P.D.	Δ
1.00	.78	.69		.71	.15
1.05	.77	.83	.80	.86	
1.10	.80	1.01		1.01	.15
Av. trial print density (adjusted)				.86	

5. *Computations*

Assuming that in the example selected, the predicted C.P.D. was within +0.06, −0.02 of the true value, the test print from the first set of exposures would be less dense than the reference strip, the test print from the second set would have a density about equal to that of the second reference strip, and the test print of the third set would be more dense than the third reference print. Obviously, any valid quantitative treatment of the data would enable one to find the precise C.P.D. of the sample.

After tabulating the print densities, the numerical values required to bring each of the two lower reference densities to equal the highest of the three reference densities can be added to the corresponding test print density values. (See Table I.) From the adjusted values in column four and five, the C.P.D. may be calculated in a number of ways. The following treatment was used in our tests:

$$\text{C.P.D.} \equiv D_{(\text{eq.})} + (d_{(R)} - d_{(T)}) \cdot \frac{0.05}{\text{Av. } \Delta}, \quad (10_a)$$

d_T = Av. of all trial print densities (adjusted),
d_R = Av. reference print density (adjusted),
$d_{eq.}$ = Middle equivalent density,
Av. Δ = Av. print density difference in successive trial print densities corresponding to log E increments of 0.05. This is proportional to the gradient of the print material.

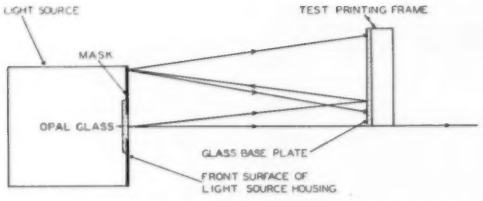

FIG. 10. Geometry of reflections existing when the test printing frame is near the light source.

For the specific data used in the illustrative case, the substitutions are as follows:

$$\text{C.P.D.} = 1.05 + \frac{.80 - .86}{.15} \times .05,$$

$$= 1.03.$$

6. *Null Point Check*

The position at which the test frame should be placed in order to give identical test and reference print densities may be found directly from the above treatment. The proper distance may be read from the graph relating Eq. D to the test frame position. The "null point check" is simply the exposure of pairs of strips when the test frame is at the "null point" position. If the original C.P.D. determination were correct and free from photographic errors, each pair of strips would yield identical print densities. However, if a small error were present, for example, 0.003, in the original computation of the C.P.D., the density difference between the average reference strip and the average test strip densities would be

$$\Delta d_{(\text{Av. print})} = \epsilon_d \times \gamma, \tag{8}$$

where ϵ_d is the error in estimating the equivalent density of the sample and γ is the D *vs.* $\log E$ gradient of the print material in the density region corresponding to the density of the prints. γ can be determined by conventional sensitometric methods or, more accurately, from the data obtained in the first phase of the procedure

$$\gamma = \text{Av. } \Delta / 0.05. \tag{9}$$

The Av. Δ is defined above.

Similarly, when the average difference in test print *vs.* reference print densities is known, the true C.P.D. of the sample may be estimated with a high degree of accuracy from the following relationship:

$$\text{True C.P.D.} = \text{Eq. } D + \frac{d_{(R)} - d_{(T)}}{\gamma}. \tag{10}$$

The print material used in our tests had a γ value of about 3.0.

In the first null point check, the average test print densities will usually be within density 0.03 agreement with their reference print densities. This proves that the position chosen for the test frame is easily correct to within 0.010 Eq. density, and, furthermore, that the true C.P.D. can be calculated to still closer limits.

Unless some mistake in technique occurs, it is seldom necessary to repeat the null point check. Statistical treatment of data shows that density determinations by this method have a repeatability approximating ± 0.002 in the average case. To illustrate the form customarily followed in notation of these data, the complete experimental results and computations for routine calibration of an ordinary wedge are included in the Appendix (Tables C and D).

7. *Special Precautions*

The simplicity of the present procedure, especially that of the null point check, renders unnecessary a number of the precautions that are essential for accurate results with other techniques and the corresponding errors that

TABLE II.

Negative	Printing medium	Printing D
Ilford special rapid	Ilford process plate	1.14
	Ilford bromide lantern plate	1.14
	Illingworth bromide paper (platino-matt)	1.14
	Illingworth bromide paper (glossy)	1.14
	Kodak Velox, soft art (chloride paper)	1.13*
	Wellington cream crayon (extra rough)	1.16
Ilford process plate	Ilford process plate	0.59
	Illingworth bromide paper (platino-matt)	0.59
	Illingworth bromide paper (glossy)	0.59
	Wellington cream crayon (extra rough)	0.60

* Toy was evidently unacquainted with the 320 mμ effect (reference 8), and the lower C.P.D. value obtained with Velox may be the result of greater relative ultraviolet sensitivity of this material.

may arise if these precautions are not observed. The few points of special interest that characterize the improved procedure are listed below:

a. Distance measurements.—The accurate positioning of the test printing frame is very important when measuring high density values. The magnitude of errors due to incorrect distances have been reviewed in an earlier section of this paper.

In our apparatus, a two-meter stick was fastened to the bench, in a manner such that the operator could sight the scale markings across the edge of riders supporting the optical fixtures. A metal rod, precisely cut to a given length, was used for calibration of the scale. This rod was held against the light source, and the test printing frame was moved toward the source until it engaged the end of the rod. The length of the rod, plus $\frac{2}{3}$ the thickness of the glass plate in the printing frame determined the optical distance for that position of the test frame.* From this information, the relationship between optical distance and scale readings was accurately established.

b. Stray light.—Stray light reaching either of the printing frames may cause serious errors.

TABLE III.

Density sample	Print material	C.P.D.
Process film (normal development)	Agfa Brovira, hard, d.w., glossy white	1.487
	Eastman Kodak Kodabrome F-4, hard, s.w., glossy white	1.487
	Defender Velour Black M., hard, blue white, s.w., glossy	1.484
	Agfa Cykora No. 3, s.w., glossy white	1.486
	Eastman P.M.C. Bromide No. 9 extra contrast white	1.484
	Haloid Halobrome F-Y, hard, s.w., glossy white	1.489
	Agfa Speedex No. 4, s.w., glossy (dye sensitized), white	1.475

* The author is indebted to Mr. Clifton Tuttle, of the Kodak Research Laboratories, for calling to the writer's attention an oversight in the original manuscript, i.e., the fact that $\frac{2}{3}$ the thickness should be added rather than the total thickness.

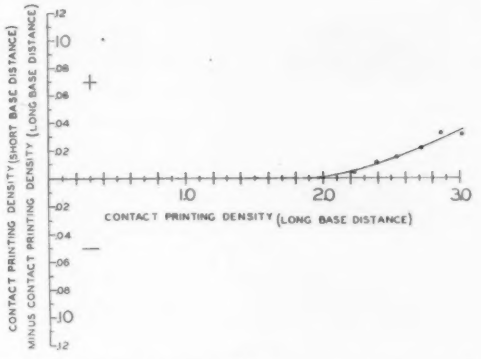

FIG. 11. Comparison of C.P.D. measurements made using a base distance of 2 meters and those made using a base distance of approximately 8 meters.

In general, it is convenient to determine whether or not stray light is present by mounting a small photo-cell in the position to be occupied by the sensitive material. If the masking is then altered, it is possible to calculate the changes to be expected in subsequent density measurements from the percentage change in photo-cell output.

For positions of the test printing frame which are very close to the light source in one case, or to the reference frame in another case, reflections are most likely to be troublesome. Figure 10 shows the geometrical path of light when high densities are to be measured with small base distances. Although this difficulty could be avoided by use of baffles, limitations of space would make such construction inconvenient. For this reason, the reflecting surfaces were covered with black velvet, and thereafter null point checks on a previously measured sample density of 1.83 showed a change of 0.006.

c. Humidity control.—There are indications that the densities of photographic silver deposits, in developed gelatin emulsion coated on acetate or nitrate film bases, vary with humidity. It is known that there is a large change in density between wet and dry films.[10] This problem is the subject of continued study, and it will be discussed in a later paper. During the course of work reported in the present paper, relative humidity was held between 50 percent and 65 percent.

[10] R. G. Hopkinson, Brit. J. Phot. **86**, 234 (April 14, 1939).

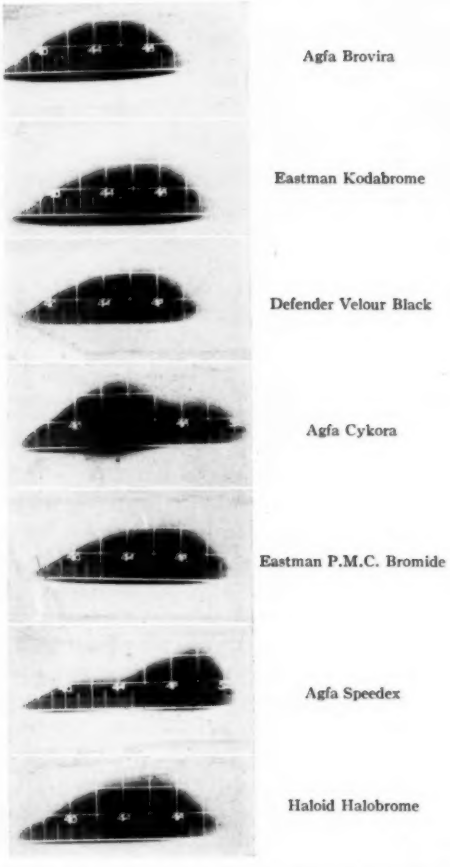

FIG. 12. Wedge spectrograms of the photographic papers tested as print materials for determining C.P.D. (Wavelength values are millimicrons $\times 10^{-1}$.)

8. *Sources of Error*

a. Basically, it is necessary to know only the ratio of the distances between the test printing frame and the reference frame which satisfy the null condition, in order to calculate the C.P.D. of a sample. Therefore, these distances must be measured with a degree of accuracy commensurate with the precision required of the density determinations. From formula (7) it will be understood that when making determinations at a density level of 1.0, using an optical bench 2 meters long, a mistake of 1 mm in the test frame setting introduces an error of 0.0014 in the C.P.D. calculation of the sample.

b. If the remaining requirements for precise photographic photometry are observed, an over-all *photographic error* of about ± 0.002 in the calculated C.P.D. is to be expected.

The chief advantages of the improved procedure of C.P.D. measurement result from elimination of errors associated with earlier techniques. The remaining sources of error may be listed as follows:

i. Errors due to variation in the specific sensitivity of the emulsion. A large number of print materials have been tested with respect to the uniformity of print density from point to point on sheets given uniform over-all exposure. It was found that different batches of paper vary considerably in this property.

ii. When reflection print densities are read on conventional visual densitometers, the errors may be about ± 0.02 for individual readings. *The higher the gradient of the print material, the less a given error in print density reading will influence the* C.P.D. *determination.* The print material used in our tests had a gradient of approximately 3, therefore, individual mistakes in density readings of 0.02 amounted to less than ± 0.007 in equivalent C.P.D.

iii. For each null point check three pairs of strips are used. This results in a corresponding statistical reduction in photometric error. By the use of a suitable photoelectric reflection densitometer, or better, a photoelectric density comparator, this source of error can be eliminated.

c. Stray light can usually be reduced to such an extent that its effect is negligible.

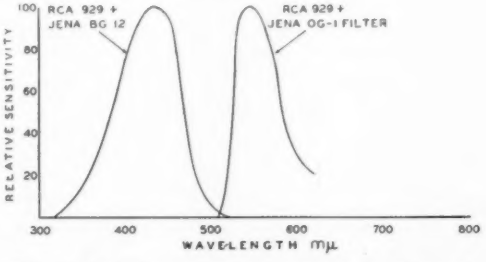

FIG. 13. Relative spectral response of the photo-tube-filter combinations used in the E.R.P.I. model R.A. 1100 densitometer. The OG-1 filter is used where visual density is desired, the BG-12 filter for measuring printing density. Redrawn from data by Frayne (reference 14).

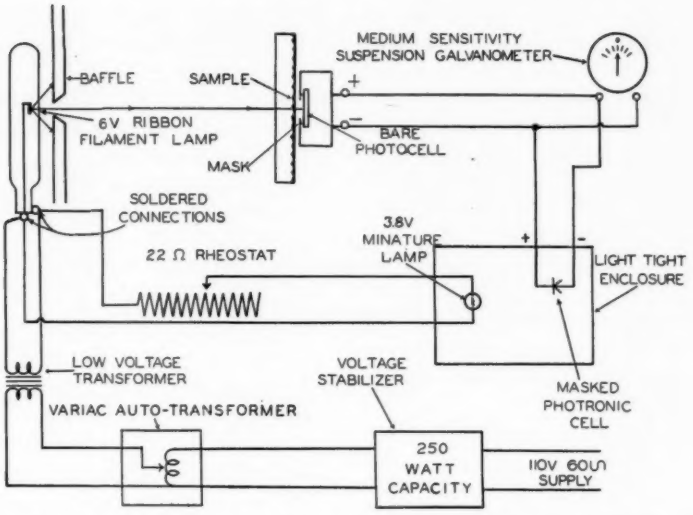

FIG. 14. Modified Hiatt and Tuttle plan for photoelectric measurement of diffuse density.

d. Another source of error is failure of the inverse square law at very short distances, because the test printing frame is not on the optic axis.

Contributing factors are:

i. Influence of oblique rays on the effective density of the sample.
ii. Non-uniform sensitivity of photographic materials at varying angles of incidence.*
iii. Difference in effective area of the light source as the test printing frame (not centered on the optical axis) approaches the source.

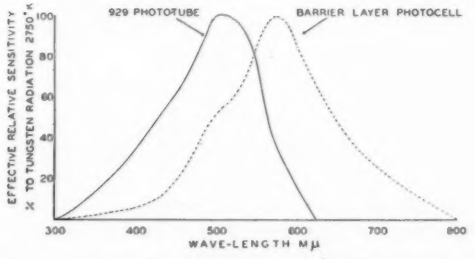

FIG. 15. Spectral response of RCA 929 photo-tube (used in E.R.P.I. and Ansco Model 11 densitometers) and the barrier layer photo-cell used in an experimental method of density measurement (manufacturer's data).

* This factor has been investigated previously and is reported on page 129 of reference 7.

iv. Difference in the length of the optical path between the real case and the ideal case.
v. The finite area of the source and the finite area of the receiver.

All five of these factors are treated mathematically in the appendix.

e. In any experimental work of this nature, the possibility of undiscovered systematic errors is nearly always a source of concern. In the present case, an obvious check would be the measurement of identical samples in other laboratories. However, *by increasing the base distance appreciably and repeating the measurements, one is afforded benefits practically equivalent to those gained by independent verification of the work.* Furthermore, this procedure provides a simple experimental means for quantitatively determining the effect of integrated errors which may occur at short base distances.

In some of the work described in this paper, a base distance of 776 cm was used, and measurements were compared with those obtained with the normal base distance of 2 meters. Figure 11 shows C.P.D. measured at the longer base distance, plotted against the difference between C.P.D. (short base distance, uncorrected) and C.P.D. (long base distance).

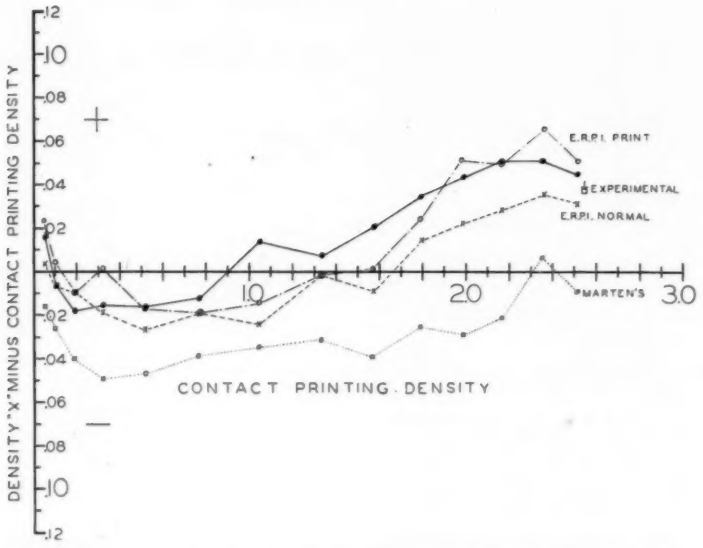

FIG. 16. Results of density measurements by various primary methods of Wedge *E* (a photographic wedge). □·····—Visual diffuse density (Martens); ○– – – – —E.R.P.I. printing density; ●——— —Experimental; x– – – —E.R.P.I. visual.

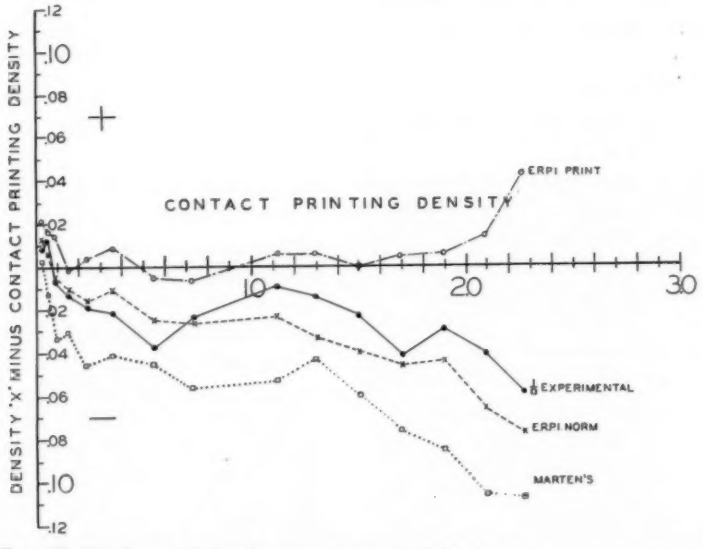

FIG. 17. Fundamental density measurements of Wedge *F* (process emulsion, underdeveloped).

V. RESULTS

A. Effect of Print Material on C.P.D.

C.P.D. could not be seriously considered for standardization unless reasonable latitude were permissible in the selection of sensitized materials. Toy's results[1] showed that variations in the measured C.P.D. resulting from the use of widely different print materials were negligible. Table II is a summary of his pertinent data.

Toy's print materials vary both in the nature of the paper surface and in the spectral sensitivity of the emulsion.

Tests in our laboratories tend to confirm the results listed in Table II. However, our search for print materials most suitable for C.P.D. standardization led to the use of bromide and chloro-bromo-iodide projection printing papers. Wedge spectrograms for six materials that received special study are shown in Fig. 12. Using these print materials, null point exposures were made at a fixed density level. Table III gives the results. From this evidence, it is reasonable to conclude that a number of commercially available sensitive materials will assure C.P.D. values which may be considered identical within practical limits.* The use of materials characterized by a large point-to-point variation in specific sensitivity simply increases the probable error in the determination of density. By repeated null point exposures, errors of this kind may be reduced to any desired low level.

B. Comparison of Results Obtained by Other Criteria

A number of different photographic wedges have been measured by the C.P.D. procedure, by other techniques that have been proposed for standardization, and with densitometers of the primary type. Photographic wedges designated "*E*," "*F*," and "*G*" (See Tables E, F, and G in the Appendix) have been measured with a Martens polarization photometer[11] (visual), the E.R.P.I. Model R.A. 1100 densitometer (integrating sphere, photo-tube),[12] and a laboratory photo-cell system, as well as by the C.P.D. method.

The Martens photometer is old and well known. It is calibrated according to the law of Malus, and is, therefore, a primary instrument. It is designed to measure diffuse density. In the E.R.P.I. densitometer, light transmitted by the sample is totalized in a sphere by a photo-tube-filter combination and the photo-current is measured by a high gain linear amplifier. It is intended by its manufacturers to serve as a prime standard and is calibrated by electronic methods and checked by means of bench photometry. Ordinarily, the 929 photo-tube is used in conjunction with a Jena OG-1 filter to simulate visual response. The 929 photo-tube is sometimes used in combination with a Jena BG-12 to measure printing density. The spectral response curves of these combinations are shown in Fig. 13, redrawn from data by Frayne.[13]

The laboratory photo-cell technique employed in this investigation is similar to that described by Hiatt and Tuttle.[14] These workers concluded that when a barrier layer photo-cell is used as a radiation receiver, diffuse transmission density measurements are most closely approached by eliminating the glass plate covering the cell and placing the sample practically in contact with the cell surface.

The optical and electrical arrangement for the laboratory photo-cell system is shown in Fig. 14. A circular photo-cell of $\frac{3}{4}''$ diameter served as the receiver. The spectral response curve of this cell is given in Fig. 15. The photo-cell output was bucked by current from another photo-cell, activated by flux from a separate incandescent lamp. Lamps for both photo-cells were operated from a common (voltage stabilized) supply. This arrangement was unusually stable with respect to drift and sensitivity to disturbances in the voltage supply.

Density specimens were placed practically in contact with the photo-cell (approximately 1-mm separation), and the area of the specimen measured was approximately 5 mm in diameter. The photo-cell-specimen combination was mounted on an optical bench. The intensity of light from the comparison lamp was adjusted so that the bucking photo-cell balanced the measuring cell output when the sample was entirely removed and the measuring cell was at maximum distance from the lamp. Upon interposing the sample, the photo-cell was moved toward the lamp until electrical equilibrium was restored. A medium sensitivity L. & N. suspension galvanometer was used to detect balance.

* Speedex paper was included to show the effect of a dye-sensitized material on the result.

[11] Martens, Phot. Korr **39**, 528 (1901).

[12] J. G. Frayne and G. R. Crane, J. Soc. Mot. Pic. Eng. **25**, 184 (Aug. 1940).

[13] J. C. Frayne, J. Soc. Mot. Pic. Eng. **36**, 622 (June, 1941).

[14] B. C. Hiatt, J. Soc. Mot. Pic. Eng. **26**, 195 (Feb. 1936).

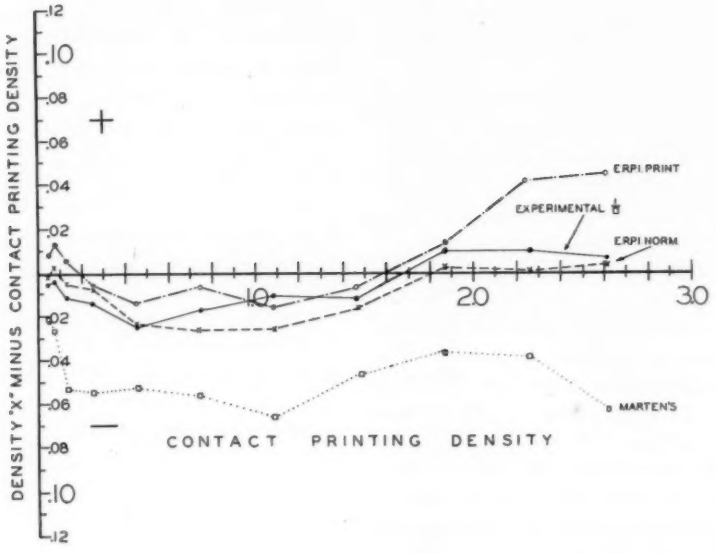

FIG. 18. Fundamental density measurements of Wedge *G*. (A photographic wedge processed under normal conditions.)

By using a ribbon filament lamp, difficulties due to ghost images, coil shadows, and low intensity were avoided. The influence of bulb wrinkles was minimized by the relatively large solid area presented by the ribbon. The chief objection to this light source for the present application is the difficulty in determining the effective position of the ribbon with sufficient accuracy.

The photo-cell arrangement was unusually sensitive and repeated determinations showed agreement of the order of $\pm 10^{-3}$ density. Measurements of densities greater than 1.2 were made by using a bucking current which balanced that obtained from the measuring cell when a density of 1.12 was interposed, and with the photo-cell at a maximum distance from the source. The nominal density value obtained thus was added to 1.12 for determining the actual density. This procedure dispensed with the need for extremely accurate measurements of photo-cell scale settings.

In Figs. 16–18, the C.P.D. values are plotted as abscissae. The comparison density values minus C.P.D. serve as ordinates. Figures 16 and 18 represent readings of Wedges *E* and *G* which are typical photographic emulsions. Figure 17 for Wedge *F* shows the curves obtained from readings of underdeveloped process film.

The trends in normal emulsions (Wedges *E* and *G*) are similar, with the possible exception of the curve for visual density values. The curves for Wedge *F* show that all densitometer values were lower than normal, except the curve for E.R.P.I. printing density which has approximately the same shape in the case of all three emulsions.

The specific factors which must be considered to account for the individual shapes of curves for particular specimens are quite numerous. The premium on space will not justify a discussion of these factors but an idea of the relative influence of a number of them can be obtained from a review of reference 15. However, it is considered important to demonstrate that a simple physical densitometer may be constructed which will read C.P.D. for various types of materials with good precision. Such an instrument is described in the following paper.

[15] A. M. Koerner and C. Tuttle, J. Opt. Soc. Am. **27**, 274 (1934).

The curves shown in Figs. 16–18 are of course plotted on a greatly exaggerated vertical scale. The difference between the corresponding D *vs.* log E curves for any of the sets of sensitometer values would appear to be relatively small.

C. Density Defined

In the introduction it was explained that the Hurter and Driffield expression of density, e.g., $D=\log(1/T)$ is too indefinite, and is inadequate for photographic purposes. In the light of the present discussion, it seems desirable to modify the original definition in a manner that specifies density values of practical photographic significance.

Let contact printing density be defined as

$$D_p=\log F_0/F_1, \qquad (2)$$

where F_0 represents unit value of actinic flux from a tungsten radiator at 2848°K so screened as to eliminate spectral energy of wave-lengths shorter than 360 millimicrons, incident normally on the density specimen, and

F_1 is the value of actinic flux transmitted to a sensitized material consisting of a white paper support coated with a gelatino-silver bromide glossy surface emulsion held in contact with the density specimen.

This definition has purposely been made more explicit than necessary for ordinary work so that stained specimens may be measured with satisfactory accuracy.

VI. SUMMARY

The contents of the present paper describe a simplified procedure for obtaining precise measurements which conform with a specific criterion for evaluating photographic density. It has been shown that a number of commercially available sensitized materials can be used without influencing the accuracy of the results for ordinary density specimens.

Sources of error have been investigated. Reproducibility of results was shown to be satisfactory, and a technique has been described for obtaining advantages practically equivalent to an independent check. Contact printing density values obtained for three photographic wedges have been compared with those obtained by other primary methods.

On the basis of this investigation, an explicit definition of photographic printing density has been proposed.

VII. APPENDIX

TABLE A. Auxiliary table for computing test frame—light source distances for any base distances. Multiply the base distance by $X^{(col.\ (3))}$ to find the test frame—light source distance for a given equivalent density.

(1) Equivalent density	(2) log (X)	(3) (X)	(1) Equivalent density	(2) log (X)	(3) (X)
0.05	$\bar{1}$.975	0.9441	1.55	$\bar{1}$.225	0.1679
0.10	.950	.8913	1.60	.200	.1585
0.15	.925	.8414	1.65	.175	.1496
0.20	.900	.7944	1.70	.150	.1413
0.25	.875	.7499	1.75	.125	.1334
0.30	.850	.7080	1.80	.100	.1259
0.35	.825	.6683	1.85	.075	.1189
0.40	.800	.6310	1.90	.050	.1122
0.45	.775	.5957	1.95	.025	.1060
0.50	.750	.5624	2.00	.000	.1000
0.55	.725	.5309	2.05	$\bar{2}$.975	.0944
0.60	.700	.5012	2.10	.950	.0891
0.65	.675	.4732	2.15	.925	.0841
0.70	.650	.4467	2.20	.900	.0794
0.75	.625	.4217	2.25	.875	.0749
0.80	.600	.3981	2.30	.850	.0708
0.85	.575	.3759	2.35	.825	.0668
0.90	.550	.3548	2.40	.800	.0631
0.95	.525	.3350	2.45	.775	.0595
1.00	.500	.3163	2.50	.750	.0562
1.05	.475	.2986	2.55	.725	.0530
1.10	.450	.2819	2.60	.700	.0501
1.15	.425	.2661	2.65	.675	.0473
1.20	.400	.2512	2.70	.650	.0446
1.25	.375	.2371	2.75	.625	.0421
1.30	.350	.2239	2.80	.600	.0398
1.35	.325	.2114	2.85	.575	.0376
1.40	.300	.1995	2.90	.550	.0355
1.45	.275	.1884	2.95	.525	.0335
1.50	.250	.1778	3.00	.500	.0316

TABLE B. Density errors due to a mistake in positioning test frame. From Eq. (6) the density errors ϵ introduced by a mistake of 1 mm in positioning the test frame for a base distance of 200 cm have been calculated.

Density level	1.0	1.5	2.0	2.5	3.0
ϵ	±0.0014	±0.0025	±0.0043	±0.0078	±0.0140

Correction in Optical Distance Necessitated by Introduction of Filters

If a filter (planes parallel) of thickness t and index of refraction n is introduced between the source and the receiver, a correction should be made for the reduced effective optical distance according to the first-order for-

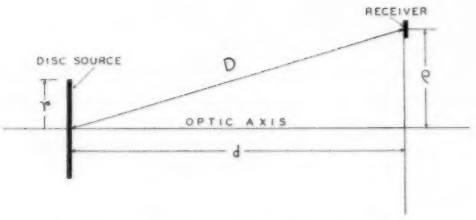

FIG. 19. Diagram showing the configuration assumed by the disk source and receiver in the present optical system.

mula (for paraxial rays).

$$x = t(1 - 1/n), \tag{1}$$

where x is the value to be subtracted from the actual measurements.

Effect of Errors in Distance Measurements

Given

$$D_p = \log F_0/F, \tag{2}$$

where D_p = contact printing density,
F_0 = intensity incident on test frame
F = intensity incident on reference frame (constant).

From inverse square law

$$F_0/F = (X_1/X_0)^2, \tag{3}$$

where X_1 = distance between reference frame and light source,
X_0 = distance between test frame and light source.

From (2) and (3)

$$D_p = 2 \log X_1 - 2 \log X_0 \tag{4}$$

and

$$dD_p = 2(\log e)(dX_1/X_1 - dX_0/X_0). \tag{5}$$

Since X_1 is a constant

$$dD_p = -2(\log e)dX_0/X_0; \tag{6}$$

from (4)

$$dD_p = -.8686\left(\frac{dX_0}{\text{antilog } (\log X_1 - D_p/2)}\right). \tag{7}$$

Relation Between Errors in Estimated C.P.D. and Print Density Difference

In a null point check, an error in equivalent density setting of ϵ_D will produce a density difference Δd in test-reference print densities as follows:

$$\Delta d_{(\text{Av. print})} = \epsilon_D \cdot \gamma. \tag{8}$$

Determination of γ

γ may be determined by averaging the difference in successive test print minus reference print densities for a set of three consecutive exposures in the first phase of the procedure.

$$\gamma = \text{Av. } \Delta/0.05. \tag{9}$$

Determination of C.P.D. from Results of Null Point Check

$$\text{True C.P.D.} = \text{Eq. } D - \left(\frac{d_{(T)} - d_{(R)}}{\gamma}\right). \tag{10}$$

Eq. D = equivalent density setting of the sample,
$d_{(T)}$ = average test print density, and
$d_{(R)}$ = average reference print density.

Errors Due to Failure of Inverse Square Law

Because the source is of finite area, and the receiver is located off the optic axis, use of the nominal source-receiver distance as the effective optical distance will give erroneous results.

Figures 19 and 20 illustrate the geometry of the problem. The uncorrected expression for the effective flux is

$$F_u = Bbr^2/d^2, \tag{11}$$

where B is the brightness of the disk,
r is the radius of the disk,
b is the area of the receiver,
d is the nominal source-receiver distance.

The corrected expression will then be

$$F_c = 2\pi Bbd^2 \int_{x=\rho-r}^{x=\rho+r} \int_{y=0}^{y=[r^2-(x-\rho)^2]^{\frac{1}{2}}} \times \frac{1}{(d^2-x^2-y^2)^2} dydx. \tag{12}$$

The notation corresponds to that used in Fig. 20. Walsh's solution[16] gives

$$F_c = \tfrac{1}{2}\pi bB\left[1 - \frac{c}{c^2+r^2}\right], \tag{13}$$

where

$$c \equiv \frac{(d^2-r^2-\rho^2)}{2d}.$$

Therefore the correction factor becomes

$$\log\left(\frac{F_u}{F_c}\right) \tag{14}$$

which should be subtracted from the apparent C.P.D. determined without correction.

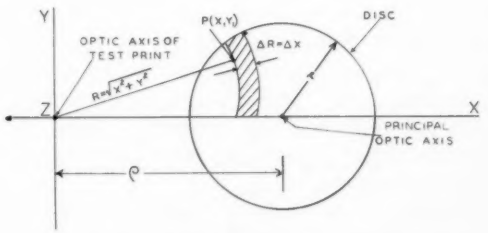

FIG. 20. Diagram illustrating the notation used in the mathematical treatment.

[16] J. W. T. Walsh, *Photometry* (Constable & Co., Ltd., 1929), Chapter IV, p. 102.

TABLE C. Test density data for wedge *H*.

(1) Step	(2) Predicted C.P.D. (on the basis of Ansco Model 11 densitometer with W. 49 filter)	(3) Reference print density	(4) Equivalent density setting	(5) Test print density	(6) Reference print density	(7) Equivalent density setting	(8) Test print density	(9) Reference print density	(10) Equivalent density setting	(11) Test print density	(12) $d_T - d_R$	(13) C.P.D.
		0.84		0.70	0.86		0.86	0.85		1.05		
1	0.045	0.86	0	0.72	0.86	0.05	0.86	0.86	0.10	1.06	+0.06	0.044
		0.82		0.74	0.81		0.90	0.84		1.10		
2	0.075	0.84	0.05	0.76	0.84	0.10	0.93	0.84	0.15	1.10	+0.27	0.074
		0.81		0.54	0.80		0.70	0.81		0.86		
3	0.125	0.81	0.05	0.54	0.81	0.10	0.71	0.81	0.15	0.86	−0.32	0.135
		0.85		0.72	0.88		0.90	0.83		1.06		
4	0.245	0.88	0.20	0.75	0.88	0.25	0.90	0.88	0.30	1.11	+0.12	0.239
		0.80		0.56	0.89		0.75	0.82		0.88		
5	0.435	0.89	0.35	0.65	0.89	0.40	0.75	0.89	0.45	0.95	−0.32	0.436
		0.82		0.64	0.81		0.75	0.79		0.92		
6	0.700	0.82	0.65	0.64	0.82	0.70	0.76	0.82	0.75	0.95	−0.11	0.713
		0.82		0.58	0.87		0.81	0.84		0.98		
7	1.046	0.87	1.00	0.63	0.87	1.05	0.81	0.87	1.10	1.01	−0.16	1.063
		0.90		0.61	1.03		0.87	1.02		1.06		
8	1.425	1.03	1.35	0.74	1.03	1.40	0.87	1.03	1.45	1.07	−0.41	1.443
		0.98		0.68	1.04		0.87	1.01		1.02		
9	1.810	1.04	1.75	0.74	1.04	1.80	0.87	1.04	1.85	1.05	−0.46	1.847
		1.24		1.08	1.23		1.22	1.23		1.44		
10	2.195	1.24	2.15	1.08	1.24	2.20	1.23	1.24	2.25	1.45	+0.04	2.197
		1.37		1.03	1.26		1.18	1.32		1.39		
11	2.535	1.37	2.45	1.03	1.37	2.50	1.29	1.37	2.55	1.44	−0.35	2.530
		1.27		0.96	1.32		1.22	1.38		1.45		
12	2.825	1.38	2.75	1.07	1.38	2.80	1.28	1.38	2.85	1.45	−0.34	2.829

TABLE D. Null point check data for wedge *H*.

(1) Step	(2) Predicted density (from test exposure)	(3) Scale setting of test frame	(4) Reference (1-)	(5) Trial (1-)	(6) Reference (2-)	(7) Trial (2-)	(8) Reference (3-)	(9) Trial (3-)	(10) Average	(11) C.P.D.
1	0.044	191.2	1.45	1.45	1.46	1.46	1.47	1.46	−0.003	0.045
2	0.074	185.3	1.48	1.50	1.50	1.48	1.49	1.48	− .003	0.075
3	0.135	173.0	1.54	1.54	1.54	1.54	1.51	1.50	− .003	0.136
4	0.239	154.6	1.57	1.55	1.57	1.54	1.56	1.55	− .020	0.245
5	0.436	125.2	1.60	1.61	1.57	1.58	1.60	1.60	+ .006	0.434
6	0.713	93.7	1.60	1.62	1.59	1.59	1.61	1.62	+ .010	0.710
7	1.063	65.9	1.00	1.04	0.97	1.02	0.97	1.04	+ .050	1.046
8	1.443	46.0	0.97	1.03	0.97	1.03	0.99	1.05	+ .060	1.423
9	1.847	32.6	1.06	1.15	1.04	1.14	1.02	1.18	+ .110	1.81
10	2.197	25.0	1.69	1.70	1.71	1.70	1.67	1.69	+ .006	2.195
11	2.530	20.15	1.02	1.01	1.00	0.98	1.00	1.03	± .000	2.530
12	2.829	17.15	1.02	1.03	1.00	1.04	1.06	1.05	+ .013	2.825
					1st repeat					
4	0.245	153.8	0.96	0.97	1.00	0.99	0.95	0.96	+0.003	0.244
7	1.046	67.0	1.33	1.31	1.30	1.28	1.23	1.24	− .010	1.049
8	1.423	46.9	1.25	1.21	1.23	1.24	1.25	1.24	− .013	1.427
9	1.81	33.55	1.27	1.22	1.23	1.20	1.20	1.18	− .033	1.821
					2nd repeat					
9	1.821	33.25	1.09	1.09	1.13	1.12	1.12	1.11	−0.006	1.823

TABLE E. Density values for wedge *E*.

(1) Step	(2) C.P.D. (Brovira)	(3) Martens	(4) $\frac{1}{\square}$ Photoelectric	(5) E.R.P.I. (normal)	(6) E.R.P.I. (printing)	(7) Ansco Model 11 density (white light)	(8) Ansco Model 11 density (blue)	(9) Ansco Model 11 density (green)	(10) Ansco Model 11 density (red)
1	0.057	0.04	0.0742	0.06	0.08	0.06	0.06	0.05	0.05
2	0.106	0.08	0.0990	0.10	0.11	0.08	0.09	0.08	0.08
3	0.190	0.15	0.1728	0.18	0.18	0.17	0.16	0.15	0.15
4	0.319	0.27	0.3040	0.30	0.32	0.27	0.275	0.27	0.28
5	0.517	0.47	0.5014	0.49	0.50	0.455	0.455	0.45	0.475
6	0.769	0.73	0.7570	0.75	0.75	0.70	0.70	0.70	0.73
7	1.044	1.01	1.0584	1.02	1.03	1.00	0.98	0.99	1.025
8	1.321	1.29	1.3292	1.32	1.32	1.26	1.25	1.26	1.30
9	1.579	1.54	1.6002	1.57	1.58	1.52	1.51	1.52	1.56
10	1.795	1.77	1.8308	1.81	1.82	1.73	1.72	1.73	1.79
11	1.988	1.96	2.0326	2.01	2.04	1.92	1.92	1.94	1.99
12	2.171	2.15	2.2224	2.20	2.22	2.12	2.12	2.13	2.18
13	2.353	2.36	2.4040	2.39	2.42	2.30	2.28	2.30	2.35
14	2.519	2.51	2.5656	2.55	2.57	2.46	2.44	2.46	2.52
15		2.63	2.6938	2.70	2.70	2.60	2.58	2.59	2.645
16						2.73	2.72	2.72	2.78
17						2.82	2.82	2.82	2.87

TABLE F. Density values for wedge *F*.

(1) Step	(2) C.P.D. (Brovira)	(3) Martens	(4) $\frac{1}{\square}$ Photoelectric	(5) E.R.P.I. (normal)	(6) E.R.P.I. (printing)	(7) Ansco Model 11 density (white light)	(8) Ansco Model 11 density (blue)	(9) Ansco Model 11 density (green)	(10) Ansco Model 11 density (red)
1	0.038	0.04	0.0462	0.05	0.06	0.04	0.04	0.04	0.03
2	0.053	0.04	0.0542	0.06	0.07	0.045	0.05	0.045	0.04
3	0.085	0.05	0.0788	0.08	0.10	0.06	0.07	0.06	0.055
4	0.141	0.11	0.1282	0.13	0.14	0.10	0.11	0.10	0.10
5	0.236	0.19	0.2174	0.22	0.24	0.19	0.19	0.18	0.18
6	0.371	0.33	0.3504	0.36	0.38	0 30	0.31	0.30	0.30
7	0.545	0.50	0.5178	0.52	0.54	0.47	0.475	0.46	0.47
8	0.726	0.67	0.7026	0.70	0.72	0.65	0.65	0.64	0.67
9									
10	1.103	1.05	1.0934	1.08	1.11	1.03	1.03	1.01	1.03
11	1.293	1.25	1.2792	1.26	1.30	1.21	1.22	1.19	1.21
12	1.500	1.44	1.4772	1.46	1.50	1.40	1.42	1.39	1.41
13	1.695	1.62	1.6540	1.65	1.70	1.58	1.60	1.56	1.57
14	1.884	1.80	1.8540	1.84	1.89	1.77	1.80	1.75	1.76
15	2.086	1.98	2.0452	2.02	2.10	1.97	2.00	1.94	1.95
16	2.257	2.15	2.1982	2.18	2.30	2.13	2.16	2.10	2.10
17		2.30	2.3530	2.34	2.47	2.27	2.32	2.22	2.22

TABLE G. Density values for wedge *G*.

(1) Step	(2) C.P.D. (Brovira)	(3) Martens	(4) $\frac{1}{\square}$ Photoelectric	(5) E.R.P.I. (normal)	(6) E.R.P.I. (printing)	(7) Ansco Model 11 density (white light)	(8) Ansco Model 11 density (blue)	(9) Ansco Model 11 density (green)	(10) Ansco Model 11 density (red)
1	0.051	0.03	0.0472	0.05	0.06	0.05	0.045	0.04	0.045
2	0.077	0.05	0.0742	0.08	0.09	0.07	0.07	0.07	0.065
3	0.144	0.09	0.1320	0.14	0.15	0.125	0.12	0.12	0.115
4	0.265	0.21	0.2528	0.26	0.26	0.235	0.23	0.23	0.23
5	0.474	0.42	0.4506	0.45	0.46	0.42	0.41	0.41	0.42
6	0.747	0.69	0.7290	0.72	0.74	0.70	0.68	0.68	0.70
7	1.097	1.03	1.0852	1.07	1.08	1.04	1.025	1.03	1.05
8	1.487	1.44	1.4742	1.47	1.48	1.42	1.40	1.40	1.435
9	1.877	1.84	1.8862	1.88	1.89	1.80	1.795	1.79	1.83
10	2.259	2.22	2.2688	2.26	2.30	2.17	2.17	2.16	2.20
11	2.615	2.55	2.6210	2.62	2.66	2.52	2.515	2.505	2.55
12	2.916	2.91		2.92	2.96	2.80	2.80	2.795	2.82

Another important source of error arises from the fact that the flux passing through the density sample does so at various angles and Beers' law of absorption may be used to evaluate the correction since the optical path through the sample is greater than for normal incidence.*

The expression for calculating the total error becomes

$$\log\left(\frac{Fc\left(\frac{1}{\text{antilog } D_L}\right)}{2\pi Bb\int_{\rho-r}^{\rho+r}\int_0^{\sqrt{[r^2-(x-\rho)^2]}}\frac{1}{D^2}\cdot\cos^2\phi\,\frac{1}{\text{antilog }\frac{D\cdot n}{(n^2-\sin^2\phi)^{\frac{1}{2}}}}\,dydx}\right), \quad (15)$$

where D_L is the nominal density level of the sample, n is the index of refraction of the emulsion and support, and the remaining symbols are the same as used above. This equation has not yet been shown capable of solution.

The difficulties in treating these errors do not seriously detract from the simplicity of the method since their integrated effect may be evaluated directly by simply changing the base distance and comparing results.

* Correction for this phenomenon is further complicated by the scattering power of the silver grains.

JOURNAL OF THE OPTICAL SOCIETY OF AMERICA VOLUME 33, NUMBER 3 MARCH, 1943

Impact of a Wave-Packet and a Reflecting Particle

HERBERT E. IVES
Bell Telephone Laboratories, New York, New York

(Received January 4, 1943)

INTRODUCTION

THE impact of a wave-packet and a particle has been studied by A. H. Compton, for the special case of a light quantum striking an electron. The frequency of the reflected or "scattered" radiation was deduced by Compton along relativistic lines by invoking the laws of conservation of momentum and energy, and introducing the known values of h and m. A general study of the impact of wave trains of definite length, or "packets," on reflecting particles, using classical wave theory, does not appear to have been made. In the investigation which follows this is done, with the interesting result that a derivation of the *variation of mass with velocity* is obtained, using only the principles of conservation of mass, momentum, and energy.

PROBLEM AND SOLUTION

We start with the definition of a wave-packet as a train of waves of energy density E, emitted in time Δt; its total energy content is $E(c\Delta t)$. Our problem is to study the impact of such a packet on an initially stationary reflecting particle. The result of such an impact will be the reflection of the packet, with a change of energy content, and the recoil of the particle at a velocity dependent on its mass.

We attack the solution of the problem by finding the energy content of the reflected wave-packet, and the pressure which causes the recoil of the particle.[1]

Consider first the energy content of a wave-packet reflected from a *uniformly* moving mirror whose velocity is v in the direction of wave propagation. The frequency of the reflected wave system is

$$\nu=\nu_0\left(\frac{c-v}{c+v}\right), \quad (1)$$

where c is the velocity of propagation of the waves; its energy density

$$E=E_0\left(\frac{c-v}{c+v}\right)^2, \quad (2)$$

[1] For the following energy, pressure, and mass relations see H. E. Ives, J. Opt. Soc. Am. **32**, 32 (1942).

the length of the packet after reflection

$$l=l_0\left(\frac{c+v}{c-v}\right)=c\Delta t\left(\frac{c+v}{c-v}\right), \tag{3}$$

where the subscript 0 indicates in each case the value for a stationary mirror; the energy content is therefore

$$El=E_0(c\Delta t)\left(\frac{c-v}{c+v}\right). \tag{4}$$

To transform this result over to the case of a mirror initially stationary, but which under the impact of the wave-packet acquires the velocity v, we require the average value of the velocity of the mirror. This will be somewhere between 0 and v; call it for the present $f(v)$. The energy content of the reflected packet is then

$$E(c\Delta t)\left[\frac{c-f(v)}{c+f(v)}\right]. \tag{5}$$

Proceeding now to the pressure, we equate the net flow of energy into the mirror per unit time with the work done by moving the mirror against the pressure. Calling P the average pressure we have

$$E[c-f(v)]-E\left[\frac{c-f(v)}{c+f(v)}\right]^2[c+f(v)]=Pf(v) \tag{6}$$

from which

$$P=2E\left[\frac{c-f(v)}{c+f(v)}\right]. \tag{7}$$

The existence of a pressure due to the incidence of a train of waves furnishes the wave-packet with an attribute characteristic of a moving mass—the reflecting particle in other words will be affected as though struck by another moving particle. We can utilize this fact for the solution of our problem by determining the *mass equivalent* of the wave-packet. We do this by using a definition of pressure made in terms of mass, namely,

$$\text{Pressure}=\frac{\text{change of momentum}}{\text{time}}$$

$$=\frac{\text{change of (mass}\times\text{velocity)}}{\text{time}}. \tag{8}$$

Noting that the duration of the impact of wave-packet and particle is $c\Delta t/[c-f(v)]$ we set up the impulse equation, which is stated in (8), as follows, designating the mass equivalent coefficient by m:

$$2E\left[\frac{c-f(v)}{c+f(v)}\right]\frac{c\Delta t}{c-f(v)}=mE(c\Delta t)c$$

$$+mE(c\Delta t)\left[\frac{c-f(v)}{c+f(v)}\right]c \tag{9}$$

from which

$$m=\frac{1}{c^2}. \tag{10}$$

The mass equivalent of the incident wave-packet is thus

$$E\frac{(c\Delta t)}{c^2} \tag{11}$$

of the reflected wave-packet

$$E\frac{(c\Delta t)}{c^2}\left[\frac{c-f(v)}{c+f(v)}\right]. \tag{12}$$

Since the velocity of the wave-packet is c, we can, from the definition of momentum as mass $\times$velocity, ascribe to the wave-packet before and after reflection the momenta

$$E\frac{(c\Delta t)}{c^2}c=E\frac{(c\Delta t)}{c} \tag{13}$$

and

$$E\frac{(c\Delta t)}{c^2}\left[\frac{c-f(v)}{c+f(v)}\right]c=E\frac{(c\Delta t)}{c}\left[\frac{c-f(v)}{c+f(v)}\right]. \tag{14}$$

Having thus assigned a mass equivalent and a momentum to the wave-packet we make use of these through the *assumption* that the principles of conservation of mass and of momentum are applicable to all the masses and mass equivalents, and to all the momenta involved in the impact of packet and particle; that is, that "mass equivalent" and particle mass are constant in sum, and that the momentum of the particle and the momentum of the packet due to its mass equivalent are also constant in sum.

For the conservation of mass we then have, designating the mass of the particle by M,

before impact

$$E\frac{(c\Delta t)}{c^2}+M, \tag{15}$$

after impact

$$E\frac{(c\Delta t)}{c^2}\left[\frac{c-f(v)}{c+f(v)}\right]+M. \tag{16}$$

It is at once evident that the conservation of mass+mass equivalent, which we are assuming, cannot hold unless the mass of the particle after impact is greater than before the impact. Calling the new mass of the particle after impact Mg we then set up the equations for conservation of mass and momentum as follows:

$$E\frac{(c\Delta t)}{c^2}+M=E\frac{(c\Delta t)}{c^2}\left[\frac{c-f(v)}{c+f(v)}\right]+Mg, \tag{17}$$

$$E\frac{(c\Delta t)}{c}=-E\frac{(c\Delta t)}{c}\left[\frac{c-f(v)}{c+f(v)}\right]+Mgv. \tag{18}$$

In these equations are two unknowns, $f(v)$ and g. Solving first for $f(v)$ we find

$$f(v)=\frac{c^2(g-1)}{gv}. \tag{19}$$

Now we know that $f(v)$ must be between 0, the initial velocity of the particle, and v, its final velocity. For a very short wave-packet $f(v)$ will approximate to $v/2$. Putting this value in (19) we obtain

$$g=\frac{1}{1-(v^2/2c^2)}. \tag{20}$$

By the use of successive approximations[2] it may be shown that the complete expression for g approaches asymptotically the value

$$g=\frac{1}{1-(v^2/2c^2)-\frac{1}{8}(v^4/c^4-)\cdots} \tag{21}$$

or

$$g=\frac{1}{[1-(v^2/c^2)]^{\frac{1}{2}}}, \tag{22}$$

which is the Lorentz value for the coefficient of variation of mass with velocity of an electrically charged particle.

DISCUSSION

The first point to demand discussion is the principal assumption made in this study, namely, that the "mass equivalent" of radiation—ascribed to radiation because radiation, like moving matter, exerts a pressure—is to participate like real mass in the conservation of mass in impact of radiation and particle. The assumption finds its justification in a survey of the final result. Having arrived at

$$\frac{M_0v}{[1-(v^2/c^2)]^{\frac{1}{2}}}$$

as the momentum of a reflecting particle of mass M_0 traveling with the velocity v, we note that the kinetic energy of the particle, by a well-known process of differentiation and integration[3] is

$$Mc^2\left[\frac{1}{\left(1-\frac{v^2}{c^2}\right)^{\frac{1}{2}}}-1\right].$$

This kinetic energy is to be equated to the net rate of flow of radiant energy toward the particle (no energy is dissipated by absorption or other process) or to

$$E(c\Delta t)\left[1-\frac{(c-f(v))}{(c+f(v))}\right]$$

giving

$$E(c\Delta t)\left[1-\frac{c-f(v)}{c+f(v)}\right]$$

$$=Mc^2\left[\frac{1}{\left(1-\frac{v^2}{c^2}\right)^{\frac{1}{2}}}-1\right]=Mc^2[g-1].$$

[2] The formula for any interval between two velocities v_1 and v_2, derived by the same reasoning as above is

$$f(v_1, v_2)=[c^2(g_2-g_1)]/(v_2g_2-v_1g_1).$$

If we put $f(v_1v_2)=v_1+[(v_2-v_1)/2]$, and put $v_1=v_2/2$, we have for g_1, in term of v_2,

$$g_1=1/[1-(v_2^2/8c^2)].$$

Putting this in the above expression and solving for g_2, we get

$$g_2=1/[1-\tfrac{1}{2}(v_2^2/c^2)-\tfrac{3}{32}(v_2^4/c^4)].$$

Repeating this process for successive equal increments we get values for the coefficient of v^4/c^4, of $\frac{1}{8}$, 15/128, 3/25, etc., which asymptotically approach the value $\frac{1}{8}$; and values for the coefficient of v^6/c^6 which similarly approach $\frac{1}{16}$.

[3] See F. K. Richtmyer, *Introduction to Modern Physics* (McGraw-Hill, New York, 1934), second edition, p. 723.

This by rearrangement gives

$$E\frac{(c\Delta t)}{c^2}+M_0=E\frac{(c\Delta t)}{c^2}\left[\frac{c-f(v)}{c+f(v)}\right]+M_0g$$

which is our assumption, which is thus shown to express *the conservation of energy.*[4]

A second point to be noted is that while we have used the pressure of a wave system in our development there is nothing in the final result which restricts the pressure to being so produced. The equation for the conservation of momentum (18) can in fact be re-expressed in the simple form:

Change of momentum of the particle = pressure × time. The pressure may equally well be exerted by another particle.

Our method of derivation of the factor $1/[1-(v^2/c^2)]^{\frac{1}{2}}$ through the use of a wave system brings in the factor c^2, c being the velocity of wave propagation in the medium, which would, in an attempt to solve the problem from purely mechanical considerations, be unlikely to be suspected.

The derivation of the variation of mass with velocity here given is to be contrasted with that from the *Theory of Relativity*. In that derivation, as given for instance by Eddington[5] *the necessity of the variation only appears when the platform carrying the impacting system is set in motion, or is viewed by a moving observer,* ("let the observer witness this collision as he flies over in an airplane"[6]), and the occurrence of the factor c^2 comes about through the Fitzgerald contraction of the rods and the variation of rate of the clocks[7] used in making the observations of velocity under these artificial conditions. In the present derivation the theory of relativity does not enter, the observer needs no airplane, the result follows from the classical properties of wave systems and the Newtonian conservation principles.

---

[4] If we assume, contrary to our result, the M is invariant with velocity we would have for the conservation of momentum

$$E\frac{(c\Delta t)}{c^2}c+E(c\Delta t)m'\left[\frac{c-f(v)}{c+f(v)}\right]c=Mv$$

where m' is a new (variable) coefficient of mass equivalence of radiation. The conservation of mass would then be expressed by

$$E\frac{(c\Delta t)}{c^2}+M=E(c\Delta t)m'\left[\frac{c-f(n)}{c+f(v)}\right]+M,$$

giving

$$m'=\frac{1}{c^2\left[\frac{c-f(v)}{c+f(v)}\right]}$$

so that

$$Mv=2\frac{E(c\Delta t)}{c^2}c.$$

The kinetic energy of the particle corresponding to momentum Mv is $\frac{1}{2}Mv^2$, giving

$$\tfrac{1}{2}Mv^2=E(c\Delta t)\frac{v}{c},$$

which obviously is not equal to $E(c\Delta t)\left[1-\frac{c-f(v)}{c+f(v)}\right]$; so that conservation of energy and momentum would not hold, in the impact process here studied, for an invariant M.

[5] A. S. Eddington, *Mathematical Theory of Relativity* (Cambridge University Press, London, 1937), second edition, p. 31.

[6] F. K. Richtmyer, reference 3, p. 719.

[7] Of interest in this general connection is an article by P. S. Epstein [Am. J. Phys. **10**, 1 (1942)] in which it is pointed out that, given the variation of mass with velocity here deduced, the variation of clock rate may be derived. It thus appears probable that all the behaviors characteristic of the restricted theory of relativity may be obtained from earlier principles.

A Study of the Applicability of the Pressed Pellet Electrode Method to the Spectrographic Analysis of Nickel Alloys*

C. J. NEUHAUS
The International Nickel Company, Inc., Huntington, West Virginia

THE fact that millings and filings as well as small cuttings and particles from which pellet electrodes may be pressed can readily be prepared from most any material characterizes the pellet electrode method as a more or less universally applicable one. This as well as the feasibility of employing proper sampling methods in selecting the sample material seemed of sufficient importance to warrant an investigation as to the pellet method's usefulness in the spectrographic analysis of nickel.

It is contemplated to explore the pellet method using various modes of excitation such as the spark, a.c. arc, and d.c. arc. Since the spark excitation seems to enjoy the reputation of being associated with high precision this mode was examined first, and it is described in this paper.

In contradistinction to methods proposed by other workers[1] in which both electrodes are of the pellet type, the procedure described employs only one pellet, the sample electrode, and a graphite auxiliary electrode. This permits the analysis of a sample of 1 gram or less.

For the purpose of this investigation, iron, magnesium, and manganese were chosen as test elements: the first one because its quantitative determination in nickel is desired frequently by consumers; the concentration of the second one is important to the producer; and the third one, manganese, serves as a standard for precision, since it seems least affected by experimental variations. The dimensions of the pellets were $\frac{1}{4}''$ diameter, approximately $\frac{5}{32}''$ length, weight approximately 1 gram, face angle of the sparking surface 8°.

The pellet electrodes were prepared by compressing either millings or small cuttings in a suitable die. Whenever possible, millings were produced by machining the sample. If this was not feasible as with thin sheets or small tubing, small cuttings were made.

The millings used in these experiments were of such size as to pass through a No. 20 mesh which has openings of approximately $\frac{1}{32}''$. Assembling four circular saw cutters of $2\frac{3}{4}''$ diam. and $\frac{3}{32}''$ thickness, having approximately 58 teeth, on an arbor and using this aggregate as milling cutter provides a means for the production of suitable millings. The r.p.m. of this cutter was around 165, the feed 8" per minute, and the depth of cut approximately 0.005". No lubricant was used.

When preparing cuttings from thin sheets, tubing, and foil the following was found to require consideration if the pellets were to be ground. Thin flat cuttings will arrange themselves in strata in the die during the shaking down operation. Upon grinding such a pellet, layers tend to flake off; it was impossible to produce a clean ground face. Fairly good results were obtained by preparing the sample material as follows: After dividing the gram sample in strips approximately $\frac{1}{16}''$ wide, several, say 6, small spirals were formed; gripping one end of a strip about $\frac{1}{2}''$ long in tweezers and winding the other end around the tweezer's point was found to facilitate this. The remainder of the gram sample was cut in small diamond-shaped pieces.

In filling the die, several spirals were placed on the bottom and some of the diamond-shaped particles filled in. After shaking down, the remaining spirals were placed, and the rest of the particles filled in. This method, especially if followed by sintering at 1800°F for 5 hours in a H_2 atmosphere, insured compact pellets.

The pressing operation was performed on a tensile testing machine. However, if time is of concern, a press especially designed for this purpose is available on the market. A Carboloy die was found to be almost indispensable since dies made of steel are apt to gall necessitating frequent polishing. The punches, however, may be made of a suitable steel, for instance, a 0.5

* Presented at the Tenth Summer Conference on Spectroscopy and its Applications held at the Massachusetts Institute of Technology, Cambridge, Massachusetts, July 20–22, 1942.

[1] H. W. Dietert, J. Opt. Soc. Am. **31**, 693 (1941).

percent chromium—1.0 percent carbon steel. The pressing procedure was to fill the 1 gram sample in the die as described above and to apply 16,000 lb. for 30 seconds. This pressure corresponds to 327,000 psi. A comparative density determination showed the density of the pressed pellet to be approximately 16 percent less than that of the solid metal. Following pressing, the sparking surface of all pellets was uniformized by grinding to a face angle of 8

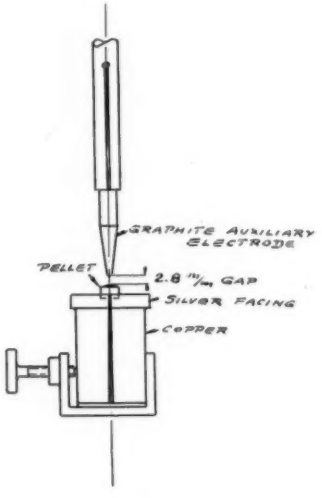

FIG. 1.

degrees. A small jig designed to hold the pellet and at the same time permit its rotation facilitated this operation. A grinding wheel of the following specification was found to be convenient. Grinding wheel: cupped type, Aloxite, 6″ outside diam., 5″ inside diam., 1″ height of cup, $\frac{1}{2}$″ thickness of cup bottom, 180 grit, silicate bond; motor $\frac{1}{2}$ hp, 1750 r.p.m.

The surface of the ground pellet appears satisfactory; still better results might be produced by increasing the r.p.m. from 1750 to 3600.

Occasionally a sufficient amount of sample material may not be available to produce a pellet of standard length. In this case the pressing die may be filled up with millings of either nickel or copper depending on the composition of the alloy under examination after the sample material has been placed first. Care, of course, must be taken in shaking down to prevent millings of the fill-up material to penetrate too far into the sample proper. Another method suggested is the backing of sub-standard length pellets with molten metal of low melting point in a small mold. Tin, cadmium, or solder may serve. This method, naturally, is practicable only if the temperature of the pellet remains sufficiently far below the melting point of the backing-up metal during the sparking period.

The pellet was held by screw pressure in solid copper jaws faced with silver. (See Fig. 1.)

The auxiliary electrode consisted of a high purity graphite rod of $\frac{1}{4}$″ diam.,[2] pointed to 2 m/m diam. It was held in a partially slit Monel tube. The auxiliary electrode was freshly pointed after each exposure.

The gap between the pellet-sample-electrode and the graphite auxiliary electrode was normally kept at 2.8 m/m.

Excitation was from a generator of the controlled spark type designed to permit the following settings: 2/3, 4/3, and 2 kva in connection with capacities of 0.007, 0.014, and 0.021 μf, respectively. Each one of these settings could be modified by the addition of inductances of 0.04, 0.08, 0.16, and 0.32 mh in the secondary circuit. Also a non-inductive damping resistance of 0.83 ohm was available for insertion in the secondary circuit.[3]

The image of the spark was focused on the collimating lens of the large Littrow type spectograph by a two-lens condensing system. In order to control the exposure of certain parts of the spectrum, a mask was available which could be swung in front of the photographic plate for a fraction of the exposure time. This mask was found to be convenient to prevent overexposure of the magnesium and nickel line pair.

Development of the Eastman Analysis No. 1 plates was in a developing machine permitting development under constant temperature and rate of stirring. The developer used was of the Eastman formula D8, developing time was 60 seconds, and the temperature was 70°F. Following development, the plate was immersed in a

[2] H. V. Churchill and J. R. Churchill, J. Opt. Soc. Am. **31**, 611 (1941).

[3] H. Kaiser, "Problems of Light Excitation in Spark Sources," Proceedings of Seventh Summer Conference on Spectroscopy, Cambridge, Massachusetts.

Chrome Alum hardening bath of the Eastman formula SB2 for 30 seconds, and fixed in a fixing bath prepared from Eastman x-ray fixing powder. After this, the plate was rinsed for five minutes in running water, swabbed with cotton and immersed in distilled water for a few seconds. Removal of the surplus water by means of a viscose sponge followed. The plates were dried in a hot air stream.

The analysis lines and their respective control lines selected, are as follows:

Fe II 2599.396 Mn 2701.700	Ni II 2670.328
Mg II 2790.787	Ni II 2825.236

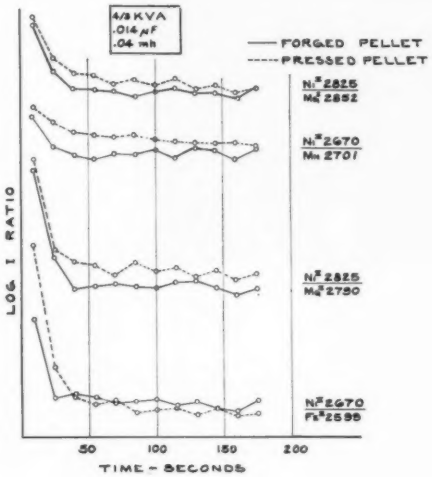

FIG. 2. Effect of sparking time on log *I* ratio.

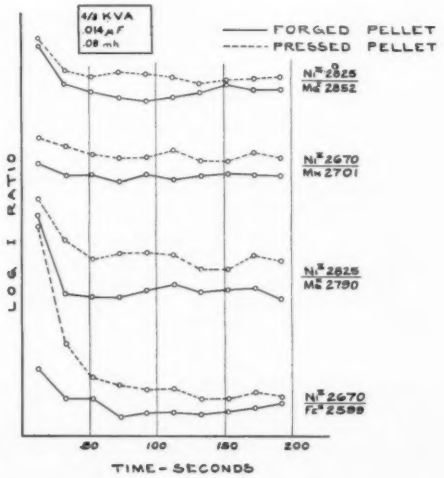

FIG. 3. Effect of sparking time on log *I* ratio.

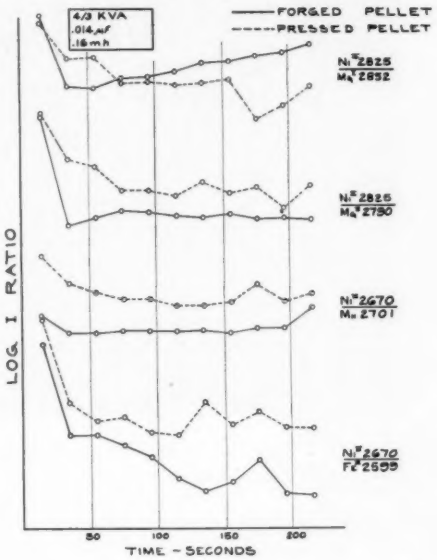

FIG. 4. Effect of sparking time on log *I* ratio.

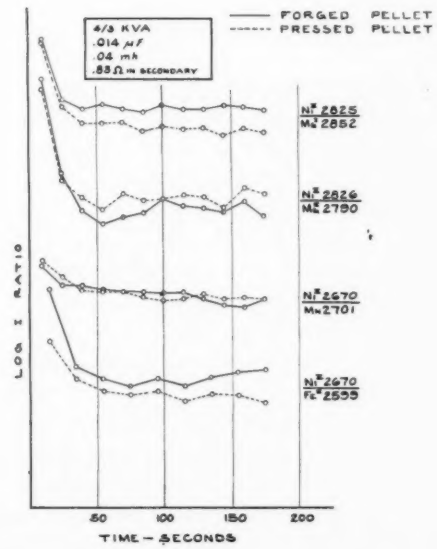

FIG. 5. Effect of sparking time on log *I* ratio.

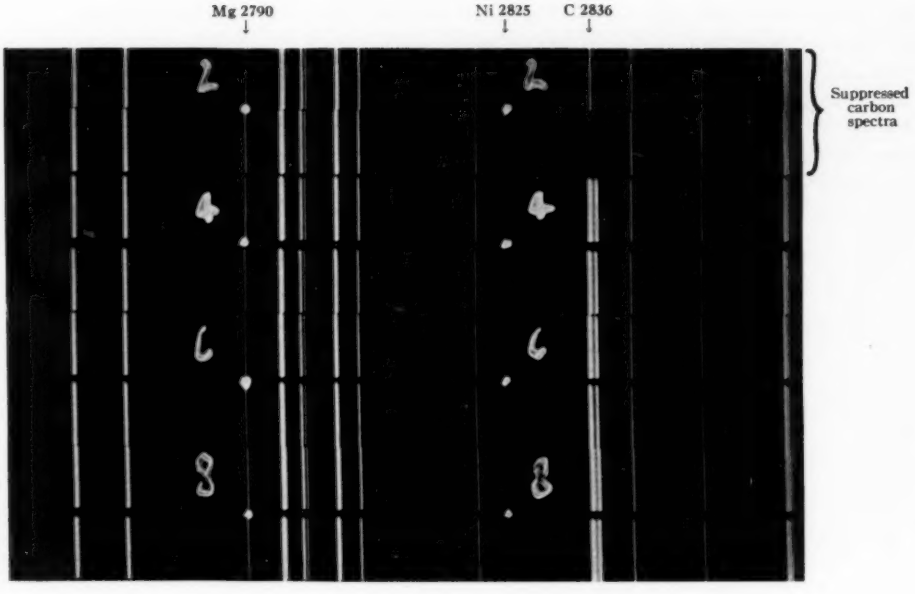

FIG. 6. Variation of carbon spectrum.

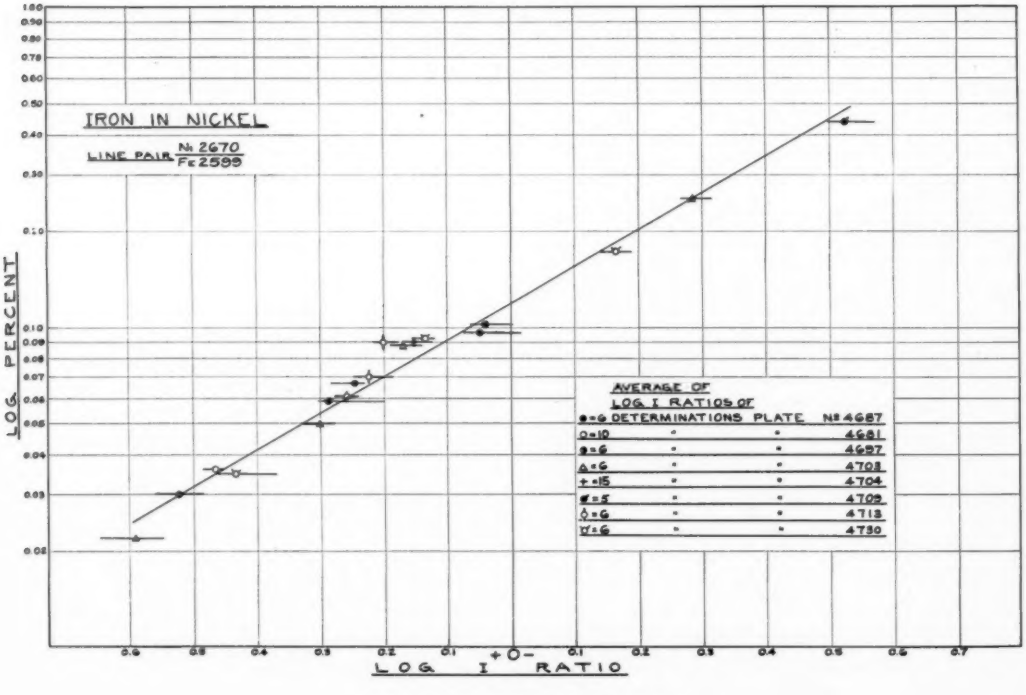
IRON IN NICKEL
LINE PAIR Ni 2670 / Fe 2599
LOG PERCENT
LOG I RATIO
AVERAGE OF LOG I RATIOS OF
●=6 DETERMINATIONS PLATE No 4687
○=10 " " 4681
▣=6 " " 4697
△=6 " " 4708
+=15 " " 4704
✱=5 " " 4709
◇=6 " " 4713
▽=6 " " 4730

FIG. 7. Analytical curve—iron in nickel.

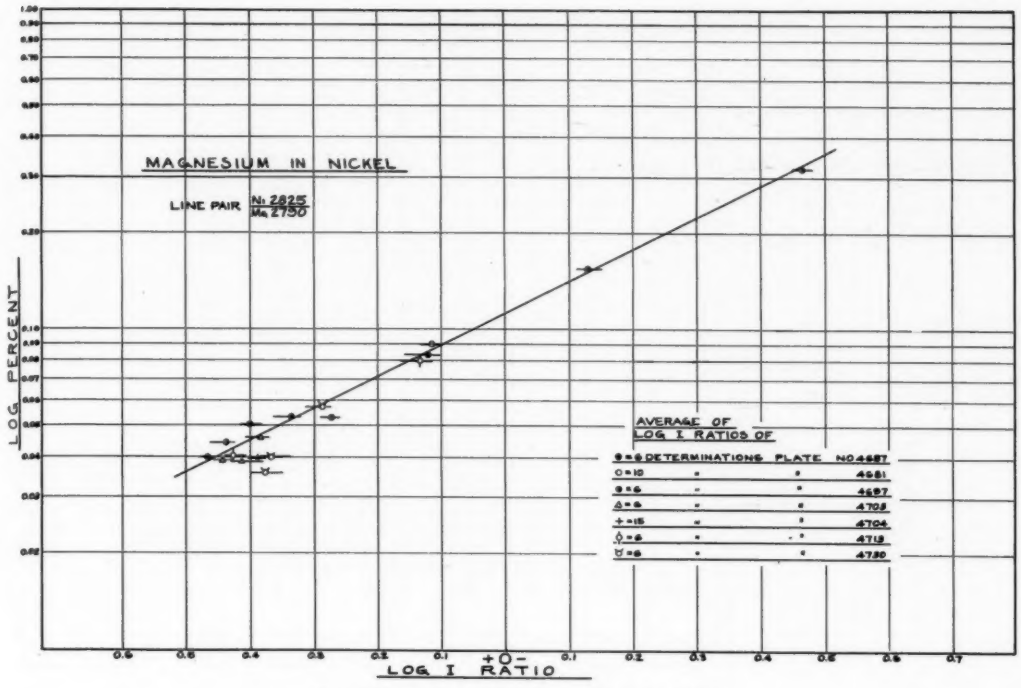

FIG. 8. Analytical curve—magnesium in nickel.

Calibration of each plate was effected by impressing a density pattern by means of a rotating sector.

Using chemically analyzed standards, analytical curves correlating log I intensity and log percentage were drawn from which rulers to be operated in conjunction with a calculating board may be prepared.[4]

By means of a densitometer, the transmissions of the analysis and control lines as well as of the 7 steps of the calibration pattern were determined.

After drawing the calibration curve, relating log transmission and log intensity, the percentage concentration of the unknown was found by applying the prepared ruler in known fashion on the calculating board.

Analytical curves were prepared for the following ranges:

Iron	from 0.030 percent to 0.50 percent,
Magnesium	from 0.040 percent to 0.30 percent,
Manganese	from 0.050 percent to 0.90 percent.

See Figs. 7–9.

[4] J. S. Owens, Metals and Alloys (January, 1938).

The surface structure of pellets produced from millings can hardly be expected to be identical to that of pellets pressed from cuttings. Hence it was thought important to discover sparking conditions unaffected by differences in pellet surface structure. To this end, pellets were produced from one standard by forging and subsequent machining as well as by compressing millings. A series of successive spectra under different sparking conditions were taken from both the forged and the pressed pellets.

Graphs showing the relationship between log I ratio and the sparking time with different conditions of excitation are shown in Figs. 2–5.

Close proximity of the graphs for the forged and pressed pellets should indicate insensitivity of that particular sparking condition to differences in surface structure.

From these curves it may be deduced that with the least inductance a fair degree of insensitivity to differences in surface structure can be expected. It is also evident from these

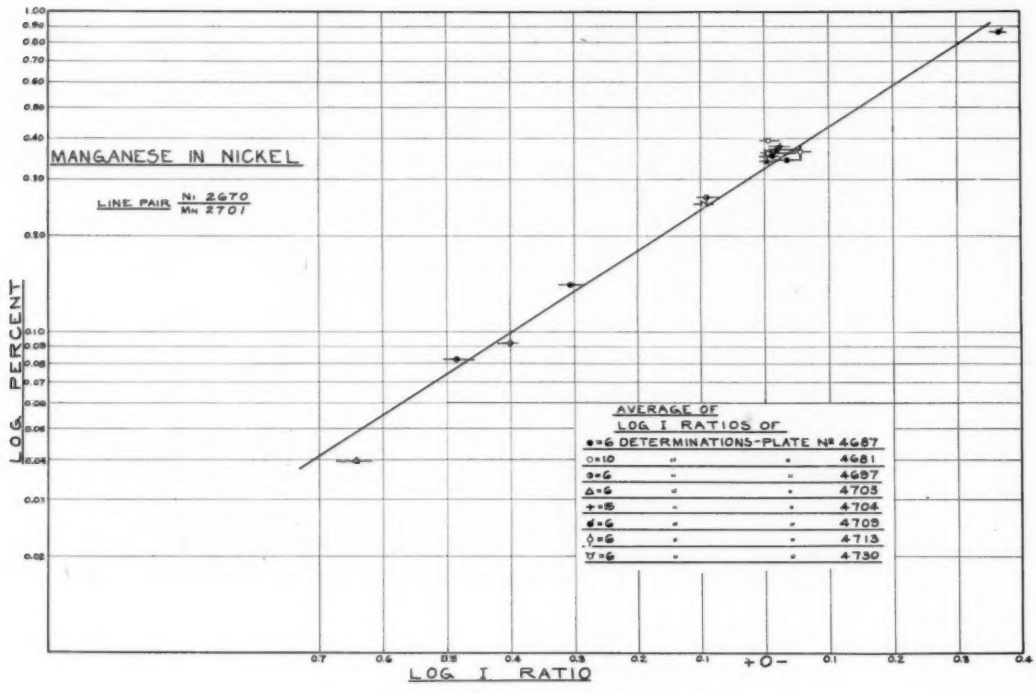

FIG. 9. Analytical curve—manganese in nickel.

curves that a presparking period of 50 seconds is desirable.

Further experiments showed that $\frac{2}{3}$-kva input required an exposure of more than 2 minutes which was considered too long. Using the 2-kva input resulted in lower reproducibility.

On the basis of the above the following operating conditions were chosen: 4/3-kva input with a capacitance of 0.014 μf, 0.04-mh inductance, primary voltage 105 volts, voltage drop across transformer 40 volts, damping resistance 0.83 ohm in secondary, spark gap: 2.8 m/m, exposure time 70 seconds preceded by a presparking period of 50 seconds.

Since the magnesium line and its nickel control line became too black with an exposure of 70 seconds, the photographic plate was shielded from the radiation of these two lines for the first 40 seconds of the total exposure time of 70 seconds.

The following variations in operating conditions were examined and found to be of no significant influence on the log I ratio.

(1) Variations of the diameter of the auxiliary electrode point from 1 to 3 m/m.
(2) Variations of the length of the auxiliary electrode from 50 m/m to 150 m/m.
(3) Variations of the length of the spark gap from 2.4 to 3.3 m/m.
(4) Varying the input voltage from 105 volts to 110 volts.
(5) Voids left at the periphery of the sparking area of the pellet due to tearing out of particles during the grinding operation.
(6) Variations of the pellet face angle from 0° to 8°.
(7) Pickling of millings in diluted hydrochloric acid before pressing.

Generally the log I ratios for iron show a greater spread than those of the other two elements. This might be owing to contamination of the millings during the milling operation. To study this possibility a batch of millings was pickled in dilute hydrochloric acid, washed in

TABLE I. All determinations from the same plate.

Spectrum	Percentage determined from analytical curves			Average percentage			Deviation from mean			% Deviation from mean		
	Mn	Fe	Mg	Mn	Fe	Mg	Mn	Fe	Mg	Mn	Fe	Mg
1	0.340	0.078	0.045	0.350	0.080	0.046	0.01	0.002	0.001	2.9	2.5	2.2
2	0.350	0.076	0.047				0.00	0.004	0.001	0.0	5.0	2.2
3	0.350	0.076	0.045				0.00	0.004	0.001	0.0	5.0	2.2
4	0.360	0.078	0.045				0.01	0.002	0.001	2.9	2.5	2.2
5	0.350	0.078	0.046				0.00	0.002	0.000	0.0	2.5	0.0
6	0.330	0.079	*				0.02	0.001	*	5.7	1.3	
7	0.360	0.076	0.045				0.01	0.004	0.001	2.9	5.0	2.2
8	0.360	0.081	0.042				0.01	0.001	0.004	2.9	1.3	8.7
9	0.360	0.081	0.048				0.01	0.001	0.002	2.9	1.3	4.4
10	0.350	0.081	0.047				0.00	0.001	0.001	0.0	1.3	2.2
11	0.330	0.082	0.047				0.02	0.002	0.001	5.7	2.5	2.2
12	0.340	0.081	0.048				0.01	0.001	0.002	2.9	1.3	4.4
13	0.350	0.085	0.046				0.00	0.005	0.000	0.0	6.3	0.0
14	0.330	0.081	0.045				0.02	0.001	0.001	5.7	1.3	2.2
15	0.350	0.081	0.050				0.00	0.001	0.000	0.0	1.3	8.7

* Line damaged.

TABLE II. Each determination from a different plate.

Plate No.	Percentage determined from analytical curve			Average percentage from Table I			Deviation			Percent deviation		
	Mn	Fe	Mg	Mn	Fe	Mg	Mn	Fe	Mg	Mn	Fe	Mg
4703	0.350	0.076	0.041	0.350	0.080	0.046	0.00	0.004	0.005	0.0	5.0	11.0
4704	0.350	0.079	0.046				0.00	0.001	0.000	0.0	1.3	0.0
4709	0.340	0.085	0.040				0.01	0.005	0.006	2.9	6.3	13.0
4730	0.350	0.079	0.048				0.00	0.001	0.002	0.0	1.3	4.4
4741	0.340	0.085	0.047				0.01	0.005	0.001	2.9	6.3	2.2
4742	0.340	0.083	0.044				0.01	0.003	0.002	2.9	3.8	4.4
4747	0.340	0.083	0.047				0.01	0.003	0.001	2.9	3.8	2.2
4791	0.340	0.082	0.045				0.01	0.002	0.001	2.9	2.5	2.2

hot distilled water, and dried in a drying oven.[5] This treatment seems to have been beneficial as far as iron is concerned. The log I ratio points for iron for the pellets from pickled millings do not seem to scatter quite as much as those of pellets made from not pickled millings.

Annealing the pellets does seem to be of influence on the log I ratio, at least as far as iron and manganese are concerned.

Varying the interrupter setting, voltage drop across the transformer input, within plus or minus 5 volts, appears to be of some influence on the log I ratio values.

From time to time a spectrum will occur in which the carbon spectrum is suppressed to a larger or smaller degree. See Fig. 6.

The occasional variations in the carbon spectrum do not seem to affect the analysis results.

Analytical curves prepared for the elements and concentration ranges mentioned above are shown in Figs. 7–9.

The horizontal lines extending to either side of the points on the analytical curves indicate the range of the log I ratios from which the average was calculated for the particular standard.

The fact that a number of points do not fall on a straight line is an indication that a re-check of the chemical analysis of these particular standards is advisable.

The range of magnesium can easily be extended to approximately 0.005 percent by omitting the masking operation and plotting a separate analytical curve for the lower range of say 0.005 percent to 0.05 percent.

Also, the manganese range can easily be extended downward by choosing a stronger line.

With iron, however, a more sensitive method of excitation, for instance the a.c. arc, or even, perhaps, the d.c. arc will be found necessary.

The precision attainable with the method

[5] B. F. Scribner, Research Paper, No. R. P. 1451, National Bureau of Standards.

described may be judged from Tables I and II. Table I shows the results of 15 repeat analyses of the same standard on one plate, while in Table II data are given for 8 determinations of the same standard on 8 different plates.

The higher deviations for iron, probably, are chargeable to contamination incurred during the milling operation. Pickling the millings before pressing, probably, will improve the reproducibility, as mentioned in a previous paragraph.

The higher deviations from the mean for magnesium are, probably, owing to the fact that the magnesium percentage is close to the lower end of the analytical curve and the magnesium line density is low. In this case, changing to a method for a lower percentage range is indicated.

As to the analysis time, it may be mentioned that with twenty-four samples and a calibration pattern placed on a 4″×10″ plate, the working time per element amounts to approximately 4.5 minutes.

Letter to the Editor

In a recent article,[1] "Mercury Arc Lamps: Effect of Energy Distribution," it is stated: "It was generally considered that if two lamps had approximately the same physical structure, the same vapor pressure, the same electrical input, and equal total radiant energy emission, and if the quartz glass of the envelope was of equal quality, then the spectral energy distribution of the radiations from the two lamps would be very similar," and "Both lamps were filled with equal quantities of mercury vapor and argon gas."

Since the over-all voltages of the lamps were equal (within one volt) and the cathode falls unequal, the gradients in the lamps were not equal. From the results of Elenbaas,[2] it therefore seems clear that the amounts of mercury *left* in the two lamps were not equal; in which case there is nothing surprising in the observed differences in spectral distribution as reported by Dr. Anderson.

"In Table II are given the corrected relative distributions, for the Lamps *A* and *B*, as measured by monochromator and thermopile, of some of the principal bands of the mercury spectrum." These "bands" are designated by the wave-lengths of various mercury lines, the last of which is λ2537. At the operating pressure of these lamps, neither would emit any considerable amount of energy (flux) in the *line* 2537; the lamp with the higher mercury pressure would emit more energy (flux) in the region passed by a wide monochromator slit.

The final conclusion: "Activated electrodes with low work function decrease the rate of lamp depreciation," seems a rather sweeping generalization to be based on observations of one lamp with a (not too well designed) tungsten electrode.

ELLIOT Q. ADAMS
Lamp Development Laboratory,
General Electric Company,
Nela Park, Cleveland, Ohio
February 25, 1943

[1] W. T. Anderson, Jr., J. Opt. Soc. Am.
[2] W. Elenbaas, Physica 2, 169–182 (1935).

The Dependence of Intrinsic Sensitivity on Grain Size*

LUDWIK SILBERSTEIN
Kodak Research Laboratories, Eastman Kodak Company, Rochester, New York
(Received December 12, 1942)

THE "intrinsic sensitivity" of a silver halide grain, as applied in several previous publications and denoted by ϵ, is defined as follows:

Let E be the monochromatic exposure expressed in quanta, so that the dimensions of E are those of a reciprocal area. If a be the size (projected area) of a grain, we may say, without committing ourselves to any theory of structure of light, that the grain has been given an exposure of aE quanta. On the continuous theory, this product would be the actual amount of energy thrown upon the grain, and on the discrete or light-dart theory, the mean or the probable amount of energy or number of quanta allotted to the grain. Some part of this energy aE will be reflected or scattered, and the remainder will be absorbed by the grain. Not all the absorbed energy, however, will be photographically efficient, that is, conducive to the developability of the grain. Only some fraction of the absorbed energy will have this property. Now, the meaning of the coefficient ϵ is defined by saying that ϵaE is the photographically efficient part of the energy absorbed by the grain. This (may, but) need not necessarily imply that only a certain fraction ϵ of the total area a of the grain as a target is sensitive to light. The product ϵa stands simply for the efficient absorption coefficient of the *whole* grain, and ϵ itself, for the same absorption coefficient *per unit area* of the grain.

This, of course, does not imply that the intrinsic sensitivity ϵ is, even within a given emulsion, a constant, i.e., independent of the size a, in passing from one grain to another. For the sake of simplicity only, we have previously treated ϵ as a constant for a given emulsion, at a fixed wave-length. There are, however, good reasons for believing that ϵ depends, among other things, on the size a of a grain.

A direct evidence to this effect has been pointed out to me some time ago by Mr. A. P. H. Trivelli. Having plotted the ϵ values determined in our paper[1] for a set of pure AgBr emulsions against the average sizes $\bar{a}$ of these emulsions, all prepared in the same way, only with different precipitation times, Mr. Trivelli has communicated to me that this plot shows a regular dependence of ϵ on $\bar{a}$,† in passing from emulsion to emulsion, and has asked me whether it would be possible to find from this result the dependence of ϵ on grain size a within one and the same (non-uniform) emulsion.

An attempt to answer this question will be made in the present note.

Let $f(a)$ be the size-frequency function of the emulsion normalized so that

$$\int_0^\infty f(a)da = 1.$$

Let us assume, for simplicity, that all grains of the same size a have the same coefficient ϵ, but that ϵ, for any fixed wave-length, varies with the size, say $\epsilon = \epsilon(a)$, where the form of the function $\epsilon(a)$ is to be found from some available experimental results.

The kind of the corresponding mathematical problem will depend, of course, on the nature of such results, that is to say, on the manner in which they have been derived from observations. Two such possibilities seem to deserve special attention.

In the first place, suppose that what has been determined experimentally may be considered, roughly at least, as the simple arithmetical mean of the ϵ values belonging to all grains of the emulsion, i.e.,

$$\bar{\epsilon} = \int_0^\infty \epsilon(a) f(a) da. \tag{1}$$

The mean grain size of the emulsion is

$$\bar{a} = \int_0^\infty a f(a) da. \tag{2}$$

* Communication No. 900 from the Kodak Research Laboratories.

[1] L. Silberstein and A. P. H. Trivelli, J. Opt. Soc. Am. **28**, 441–59 (1938).

† Namely, as will be seen in the sequel, a pronounced, steady decrease of ϵ with increasing $\bar{a}$.

Suppose that $\bar{\epsilon}$ has been found experimentally for a whole set of emulsions with the same form of $f(a)$ and with different mean grain sizes $\bar{a}$ and that, by graphical interpolation, the curve $\bar{\epsilon}$, $\bar{a}$ has been constructed or, virtually, $\bar{\epsilon}$ has been found as a function of $\bar{a}$, $\bar{\epsilon}=\bar{\epsilon}(\bar{a})$. The problem is then reduced to the following question:

Given the relation between $\bar{\epsilon}$, as expressed by (1), and the mean grain size $\bar{a}$, as well as the distribution function $f(a)$, what is the form of the function $\epsilon(a)$?

To simplify matters, suppose that $f(a)$ is of the exponential form, i.e., with the aforesaid normalization,

$$f(a)=(1/\bar{a})\exp(-a/\bar{a}).$$

Then, by (1),

$$\int_0^\infty \epsilon(a)\exp(-a/\bar{a})da=\bar{a}\bar{\epsilon}(\bar{a}),$$

which is an *integral equation* for the unknown function $\epsilon(a)$. Given $\bar{\epsilon}(\bar{a})$ for all values of $\bar{a}$, find the function $\epsilon(a)$.

Write $x=\bar{a}$ and $\bar{\epsilon}(\bar{a})=F(x)$. Then our integral equation is

$$\int_0^\infty \epsilon(a)e^{-a/x}da=xF(x), \tag{3}$$

with $F(x)$ as the empirically given and $\epsilon(a)$ as the unknown function.

It may be safely assumed that both are analytical functions without, from the practical point of view, any loss to generality. If this be granted, then the integral equation is easily solved. In fact, let the expansion of the unknown function be

$$\epsilon(a)=\epsilon_0+\epsilon_1 a+\epsilon_2\frac{a^2}{2!}+\cdots=\sum_{k=0}^{\infty}\epsilon_k\frac{a^k}{k!}, \tag{4}$$

where the coefficients are unknown constants. The contribution of the kth term of this series to the integral in (3) is

$$\frac{\epsilon_k}{k!}\int_0^\infty a^k e^{-a/x}da=\frac{\epsilon_k x^{k+1}}{k!}\int_0^\infty u^k e^{-u}du=\epsilon_k x^{k+1}.$$

Thus, substituting in (3) and removing on both sides the factor x,

$$\sum_{k=0}^{\infty}\epsilon_k x^k=\epsilon_0+\epsilon_1 x+\epsilon_2 x^2+\cdots=F(x).$$

Now, the Taylor expansion of the right-hand member $F(x)=\bar{\epsilon}(x)$ may be written

$$\bar{\epsilon}(x)=\bar{\epsilon}_0+\bar{\epsilon}_1 x+\bar{\epsilon}_2\frac{x^2}{2!}+\cdots=\sum_{k=0}^{\infty}\bar{\epsilon}_k\frac{x^k}{k!},$$

where the $\bar{\epsilon}_k$ are empirically known numerical coefficients. Hence,

$$\sum_{k=0}^{\infty}\epsilon_k x^k=\sum_{k=0}^{\infty}\bar{\epsilon}_k\frac{x^k}{k!},$$

and since this equation has to hold for all values of x, we have the remarkably simple relation between the unknown and the known coefficients,

$$\epsilon_k=\frac{1}{k!}\bar{\epsilon}_k \quad (k=0,\ 1,\ 2,\ \text{etc.}).$$

Thus the required function, (4), becomes

$$\epsilon(a)=\sum_{k=0}^{\infty}\bar{\epsilon}_k\frac{a^k}{k!k!}=\bar{\epsilon}_0+\bar{\epsilon}_1 a+\frac{\bar{\epsilon}_2 a^2}{2!2!}+\frac{\bar{\epsilon}_3 a^3}{3!3!}+\cdots. \tag{5}$$

This, then, is the intrinsic sensitivity in its dependence on size a within the emulsion, as derived from the given average sensitivity

$$\bar{\epsilon}(x)=\bar{\epsilon}(\bar{a})=\sum_{k=0}^{\infty}\bar{\epsilon}_k\frac{\bar{a}^k}{k!}. \tag{6}$$

If the series (6) is convergent, the more so is the series (5), since for the same value of the argument, its first two terms are identical with those of (6) and the following terms are $2!$, $3!$, $\cdots k!$ times smaller than those of (6). That the function (5) solves the problem is readily verified. For, with the assumed form of $f(a)$, the mean of a^k is $k!\bar{a}^k$, so that on averaging (5), term by term, one gets (6) identically.

To pass from the given $\bar{\epsilon}(x)$ to the required sensitivity distribution $\epsilon(a)$, one has only to divide every term of the former by the corresponding factorial $k!$.

Such is the case if the data consist of a set of simple average $\bar{\epsilon}$ values corresponding to different mean sizes $x=\bar{a}$. Some such determina-

tions, in fact, have been made in our previous investigations, but they consisted, each time, of a detached, single $\bar{\epsilon}$ value, from which no conclusions of the kind now contemplated can be derived. The set of sensitivities of the pure AgBr emulsions determined in the paper quoted above has been of a somewhat different character. What we have determined in that connection (cf. Table IV, reference 1), for a sequence of increasing $x=\bar{a}$ values, is not $\bar{\epsilon}$ itself, but the quotient of the mean value of ϵa^2 and the mean square size, i.e.,

$$\langle \epsilon a^2 \rangle_{Av} / \langle a^2 \rangle_{Av} = F(x), \quad \text{say.}$$

With this kind of data, then, the equation for the unknown function $\epsilon(a)$ becomes

$$\int_0^\infty \epsilon(a) a^2 f(a) da = \langle a^2 \rangle_{Av} F(x), \tag{7}$$

where $F(x)$ is to be considered as a given function of $x=\bar{a}$. If we now again assume the simple exponential distribution, $f(a)=(1/x)e^{-a/x}$, then $\langle a^2 \rangle_{Av}=2x^2$, and the integral equation (7) becomes

$$\int_0^\infty \epsilon(a) a^2 e^{-a/x} da = 2x^3 F(x). \tag{8}$$

To solve it, let us again use the expansion

$$\epsilon(a) = \sum_{k=0}^{\infty} \frac{\epsilon_k a^k}{k!},$$

with constant coefficients ϵ_k. The contribution of the kth term to the integral now becomes

$$\frac{\epsilon_k}{k!} \int_0^\infty a^{k+2} e^{-a/x} da = \frac{\epsilon_k x^{k+3}}{k!} \int_0^\infty u^{k+2} e^{-u} du$$

$$= (k+1)(k+2)\epsilon_k x^{k+3}.$$

Hence, if we write again

$$F(x) = \sum \frac{\bar{\epsilon}_k x^k}{k!},$$

$$\sum_{k=0}^{\infty} (k+1)(k+2)\epsilon_k x^k = 2 \sum_{k=0}^{\infty} \frac{\bar{\epsilon}_k x^k}{k!},$$

and since this equation has to be satisfied for every x, we have

$$\epsilon_k = \frac{2}{(k+2)!} \bar{\epsilon}_k.$$

Thus the required sensitivity as function of size becomes

$$\epsilon(a) = 2 \sum_{k=0}^{\infty} \bar{\epsilon}_k \frac{a^k}{k!(k+2)!}, \tag{9}$$

where $\bar{\epsilon}_k$ are the coefficients in the expansion of the empirically given function of $x=\bar{a}$,

$$F(\bar{a}) \equiv \langle \epsilon a^2 \rangle_{Av} / \langle a^2 \rangle_{Av} = \sum_{k=0}^{\infty} \frac{\bar{\epsilon}_k x^k}{k!}. \tag{10}$$

Let us now apply these formulae to the actual experimental findings for the set of seven pure bromide emulsions, Nos. 20 to 26, Table IV of the paper quoted above. What in that paper has been briefly denoted by ϵ is our present $F(\bar{a})$ which, in fact, is some kind of "average" ϵ. Thus the values of $F(\bar{a})$ are the numbers of the last column of Table IV divided by the conversion factor 10^{11} (cf. p. 459, reference 1), and the mean grain size, in μ^2, is given in the third column of that table. Hence our data are as follows:

Em. No.	20	21	22	23	24	25	26
$x=\bar{a}$	0.14	0.50	0.66	1.43	2.30	3.45	5.44
$F(\bar{a})$	1.80	0.58	0.49	0.40	0.35	0.23	0.084×10^{-3}.

The values of F decrease steadily with increasing $\bar{a}$ or x. If the first value is omitted, the remaining six show an almost linear dependence on x. The inclusion of the first datum would call for an elaborate number of terms. Thus, if we are content, in a first attempt, with the size range 0.50 to $5.5\mu^2$, we may represent the function F by the simple form

$$1000F(x) = \alpha - \beta x \tag{10.1}$$

with constant coefficients α, β. In fact, if we take

$$\alpha = 0.572, \quad \beta = 0.0932,$$

this linear form gives, for the six emulsions, Nos. 21 to 26,

$1000F=$	0.53	0.51	0.44	0.36	0.25	0.065
against	0.58	0.49	0.40	0.35	0.23	0.084.

By (9) and (10), the passage from F to $\epsilon(a)$ is accomplished by applying the factor $2/(k+2)!$ to the kth term. In the present case, then, we have only to multiply α by $2/2!=1$ and $-\beta$ by $2/3!=1/3$. Thus the sensitivity as function of size a becomes

$$\epsilon(a) = (0.572 - 0.0311a) \times 10^{-3}, \tag{9.1}$$

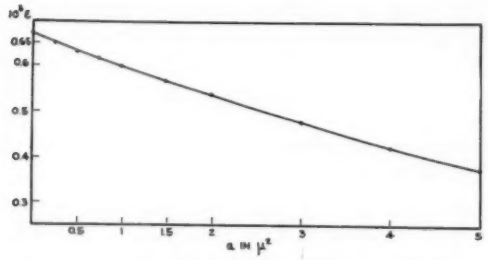

FIG. 1. Graph of formula (9.2). Intrinsic sensitivity ϵ as function of grain size a for emulsion Nos. 20 to 26.

which gives the required dependence, at least, within the range of sizes $a=0.50$ to $5.5\mu^2$, viz., a uniform decrease of intrinsic sensitivity with increasing grain size. The solution (9.1) corresponds to the simple, provisional form (10.1) of $F(x)$.

A more satisfactory representation of $F(x)$, capable of unlimited extension towards increasing sizes, can be achieved by means of an exponential function, to wit,

$$F(x)=Ae^{-cx},\quad A=0.67\times10^{-3},\quad c=0.325, \tag{10.2}$$

which gives for the last six emulsions

$$F=0.57\quad 0.54\quad 0.42\quad 0.32\quad 0.22\quad 0.11,$$

close enough to the quoted values (and $F=0.64$ for the discarded first emulsion).

The expansion of (10.2) is

$$F(x)=A\left\{1-cx+\frac{c^2}{2!}x^2-\frac{c^3}{3!}x^3+\cdots\right\}.$$

Hence, by (9) and (10), the expansion of the required sensitivity as function of the grain size (since $2A=0.00134$),

$$\epsilon(a)=0.00134\left\{\frac{1}{2!}-\frac{ca}{3!}+\frac{c^2a^2}{2!4!}-\frac{c^3a^3}{3!5!}+\frac{c^4a^4}{4!6!}-\cdots\right\}, \tag{9.2}$$

where $c=0.325$. Clearly, this series for $\epsilon(a)$ converges much more rapidly than the (always convergent) exponential series for F. (It converges even more rapidly than the series for the Bessel functions of the zeroth and the first order, but is not reducible to any such or other tabulated functions.) For fractional values of $ca\doteqdot\frac{1}{3}a$, it is enough to take the first two or three terms, and even for $a=5.44$ scarcely more than one or two higher terms need be computed. In this manner one readily finds the following set of ϵ values:

$a=0.10$	0.25	0.50	0.75	1.0	1.5
$10^3\times\epsilon(a)=0.663$	0.652	0.634	0.617	0.600	0.567
$a=2.0$	3.0	4.0	5.0	6.0	
$10^3\times\epsilon(a)=0.536$	0.477	0.421	0.373	0.328	

The corresponding curve, which deviates very little from a straight line, is drawn in Fig. 1. Within the size range of actual interest the intrinsic sensitivity drops steadily to about one-half of its initial value. The product $a\epsilon$ or the total sensitivity of a grain increases with its size. These results hold for each of the set of pure AgBr emulsions specified above. Whether they are extensible to other emulsions may be decided by further measurements.

American Recommended Practice for Dimensions of Photographic Paper (Roll Leaders and Limit Signals)—Z38.1.4–1942*†

This recommendation for leaders for sensitized photographic paper rolls (where leaders are required) refers only to those commonly used for light protective purposes where the length of the leader has no particular bearing on the operation of an exposing machine.

1. Geophysical Recording Roll Leaders

1.1 The width of the leader should never fall below the width of the sensitized paper to which it is attached nor should it exceed that width by more than 1/64 inch (0.4 mm). The length should be approximately 36 inches (915 mm).

2. Photocopy Roll Leaders

2.1 The width of the leader should never fall below the width of the sensitized paper to which it is attached nor should it exceed that width by more than 1/32 inch (0.8 mm). The length should be approximately 54 inches (1370 mm).

3. Limit Signals for Geophysical Recording Rolls

3.1 The term *limit signal* signifies a warning mark near the end of a roll of photographic paper intended to notify the user that the supply is almost exhausted. It should consist of a row of three perforations located parallel to and $\frac{1}{4}$ inch from either edge of the paper and 10 feet from the inside end of the roll. The individual perforations should have a diameter not less than $\frac{1}{8}$ inch nor greater than $\frac{1}{4}$ inch and should be spaced approximately one inch apart.

---

* This document is one of a series of American Standards for Photography (other than Cinematography).
† Approved August 4, 1942 by the American Standards Association. Sponsor: Optical Society of America.

American Standard for Cameras (Tripod Connections for American Cameras)—Z38.4.1–1942*†

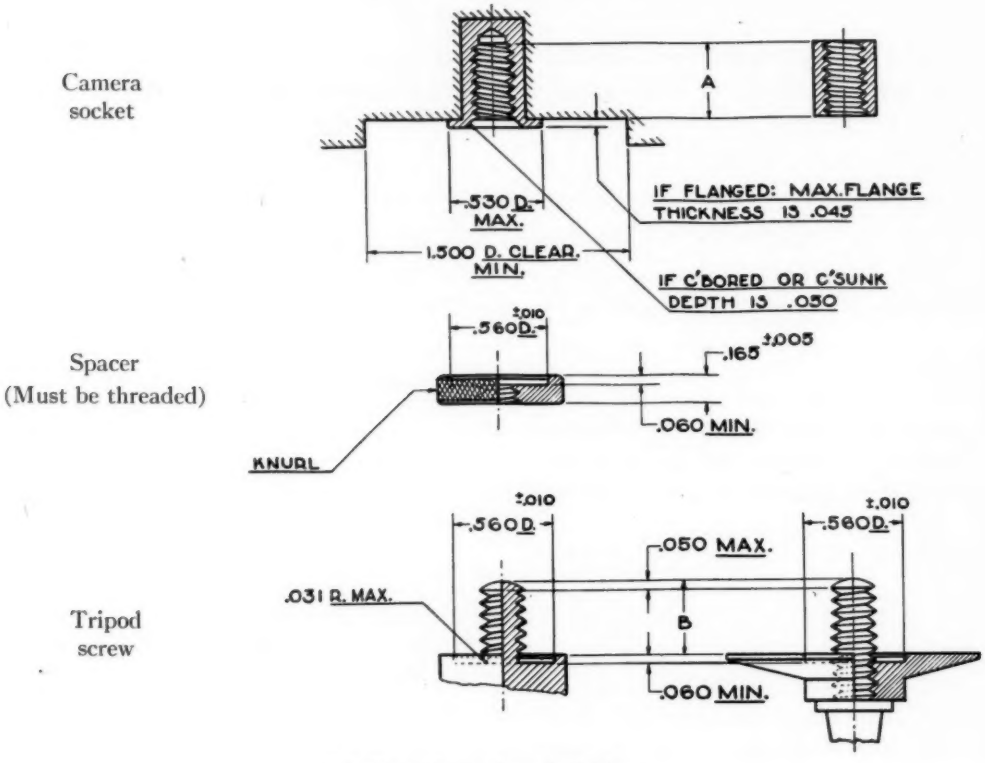

All dimensions given in inches.

Thread specifications: $\frac{1}{4}$ inch–20 N.C.–1 R.H. (These thread specifications are in accordance with American Standard B1.1–1935.)

Am. Std. thread		Major diam. Max.	Major diam. Min.	Pitch diam. Max.	Pitch diam. Min.	Minor diam. Max.	Minor diam. Min.
Screw	in.	0.249	0.238	0.216	0.211	0.187	——
	mm	6.324	6.045	5.486	5.359	4.749	——
Socket	in.	——	0.250	0.223	0.218	0.206	0.196
	mm	——	6.350	5.664	5.537	5.232	4.978

(A) 0.375 inch Socket depth—recommended for heavy cameras.
(A) 0.197 inch Socket depth—recommended for light cameras.
(B) 0.340 inch Screw length—recommended for heavy cameras.
(B) 0.175 inch Screw length—recommended for light cameras.

Spacer diameter should conform to diameter of tripod head. One spacer to be provided for each long tripod screw made.

Design subject to manufacturer's preference.

* This document is one of a series of American Standards for Photography (other than Cinematography).
† Approved August 4, 1942 by the American Standards Association. Sponsor: Optical Society of America.

American Standard for Cameras (Tripod Connections for European Cameras with Adapter for American Tripods)—Z38.4.2–1942*†

Camera socket

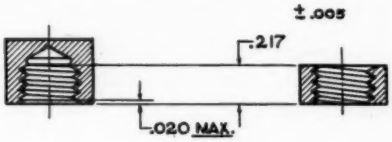

Adapter

($\frac{3}{8}$ inch–16 thread to $\frac{1}{4}$ inch–20 thread)

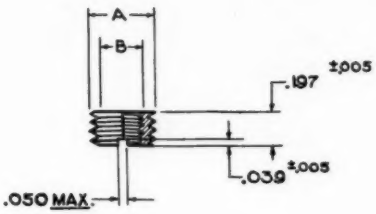

Tripod screw

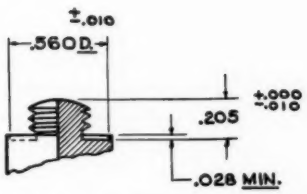

All dimensions given in inches.

Thread specifications: $\frac{3}{8}$ inch–16 N.C.–1 R.H. (These thread specifications are in accordance with American Standard B1.1–1935.)

Am. Std. thread		Major diam. Max.	Major diam. Min.	Pitch diam. Max.	Pitch diam. Min.	Minor diam. Max.	Minor diam. Min.
Screw	in.	0.373	0.361	0.333	0.326	0.297	——
	mm	9.474	9.169	8.458	8.280	7.544	——
Socket	in.	——	0.375	0.341	0.334	0.318	0.307
	mm	——	9.525	8.661	8.484	8.077	7.798

Adapter—From $\frac{3}{8}$ inch–16 N.C.–1 R.H. to $\frac{1}{4}$ inch–20 N.C.–1 R.H.

Am. Std. thread		Major diam. Max.	Major diam. Min.	Pitch diam. Max.	Pitch diam. Min.	Minor diam. Max.	Minor diam. Min.
A Outside thread	in.	0.373	0.361	0.333	0.326	0.297	——
$\frac{3}{8}$″–16 N.C.–1 R.H.	mm	9.474	9.169	8.458	8.280	7.544	——
B Inside thread	in.	——	0.250	0.223	0.218	0.206	0.196
$\frac{1}{4}$″–20 N.C.–1 R.H.	mm	——	6.350	5.664	5.537	5.232	4.978

Design subject to manufacturer's preference.

* This document is one of a series of American Standards for Photography (other than Cinematography).
† Approved August 4, 1942 by the American Standards Association. Sponsor: Optical Society of America.

American Standard for Distance Scales Marked in Feet—Z38.4.3–1942*†

1. Distance scales shall have their markings based on the plane of registration of the sensitized material in the camera to which the lens is fitted, or if the above is impractical, the focusing scale shall be computed from any other clearly marked index.

2. Within the limits of the range or form of the camera and lens fitted thereto distance markings shall be indicated in terms of feet selected from the following: 00, 100, 50, 25, 15, 10, 8, 6, 5, 4, etc.

3. Infinity shall be indicated by the mathematical mark for infinity "∞."

* This document is one of a series of American Standards for Photography (other than Cinematography).
† Approved August 4, 1942 by the American Standards Association. Sponsor: Optical Society of America.

American Standard for Focal Lengths of Lenses: Marking—Z38.4.4–1942*†

Focal lengths of lenses marked on the lens mounts shall be in either mm (millimeters) or cm (centimeters). The actual equivalent focal length of a lens shall be within ± 4 percent of the marked value. The symbol for focal length shall be lower case "*f*."

* This document is one of a series of American Standards for Photography (other than Cinematography).
† Approved August 4, 1942 by the American Standards Association. Sponsor: Optical Society of America.

American Standard for Shutter Cable Release Tip and Socket with Taper Thread—Z38.4.5–1942*†

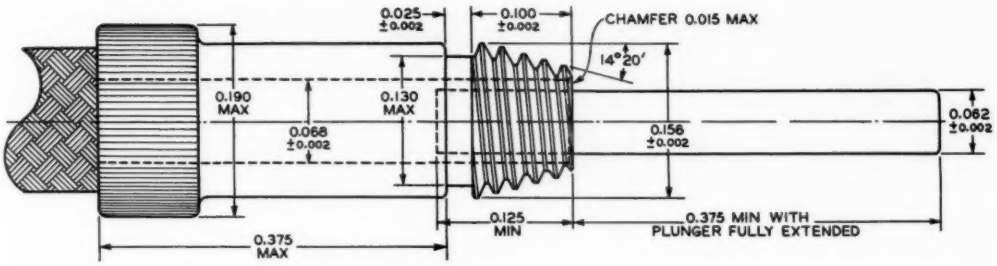

50 threads per inch—R.H. American Standard Form adapted for taper tolerances same as for class 2 fit

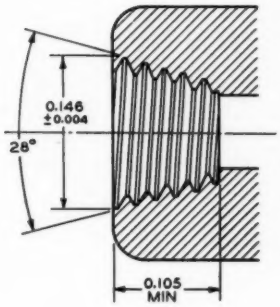

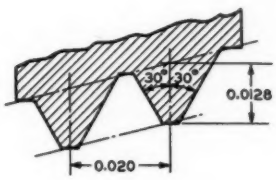

All dimensions given in inches.

Note: For cable release tip and socket with straight thread see American Standard Z38.4.6–1942.

---

* This document is one of a series of American Standards for Photography (other than Cinematography).
† Approved August 4, 1942 by the American Standards Association. Sponsor: Optical Society of America.

American Standard for Shutter Cable Release Tip and Socket with Straight Thread—Z38.4.6–1942*†

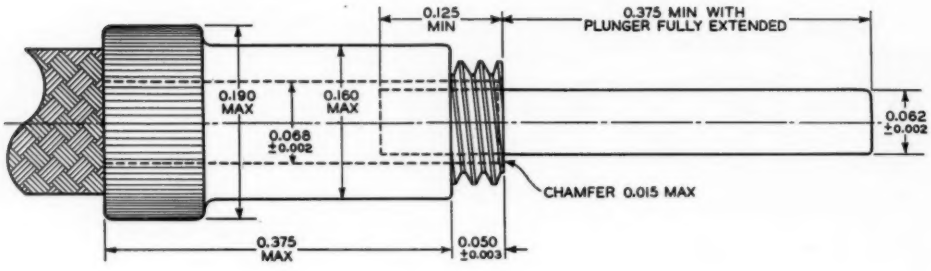

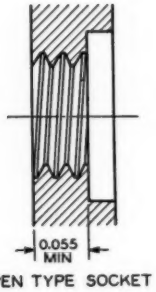

OPEN TYPE SOCKET

All dimensions given in inches.

American Standard Thread No. 5–44 NF–2 (see American Standard for Screw Threads, B1.1–1935)

Note: For cable release tip and socket with taper thread see American Standard Z38.4.5–1942.

---

* This document is one of a series of American Standards for Photography (other than Cinematography).
† Approved August 4, 1942 by the American Standards Association. Sponsor: Optical Society of America.